STUDY OF MASS TRANSFER BEHAVIOR IN A FLUIDIZED BED ELECTROCHEMICAL REACTOR

A THESIS

SUBMITTED TO THE DEPARTMENT OF CHEMICAL ENGINEERING

IN PARTIAL FULFILMENT OF THE REQUIREMENTS

FOR THE DEGREE OF

MASTER OF SCIENCE IN ENGINEERING(CHEMICAL)

BY

EDMOND GOMES

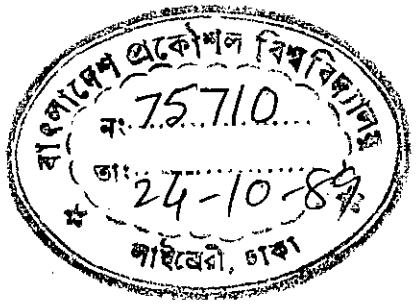

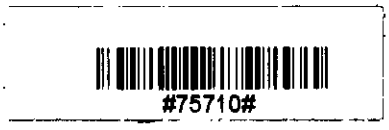

BANGLADESH UNIVERSITY OF ENGINEERING AND TECHNOLOGY, DHAKA

JUNE, 1988.

BANGLADESH UNIVERSITY OF ENGINEERING AND TECHNOLOGY

DEPARTMENT OF CHEMICAL ENGINEERING

CERTIFICATION OF THESIS WORK

We, the undersigned, certify that EDMOND GOMES candidate for the degree of Master of Science in Engineering(Chemical) has presented his thesis on the subject "STUDY OF MASS TRANSFER BEHAVIOR IN A FLUIDIZED BED ELECTROCHEMICAL REACTOR" that the thesis is acceptable in form and content, and that the student demonstrated a satisfactory knowledge of the field covered by this thesis in an oral examination held on the 18th June, 1988.

(Dr. M. Sabder Ali) — Chairman
Associate Professor
Department of Chemical Engineering.

(Dr. A.K.M. Abdul Quader) — Member
Professor and Head,
Department of Chemical Engineering.

(Dr. Iqbal Mahmud) — Member
Professor
Department of Chemical Engineering.

(Dr. Khaliqur Rahman) — Member
Professor
Department of Chemical Engineering.

(Dr. A.M. Azizul Huq) — External Member
Professor
Department of Mechanical Engineering.

ABSTRACT

An experimental investigation into the mass transfer behavior in a fluidized bed, vertical parallel plate electrochemical reactor has been carried out. Dilute copper sulphate solution (0.015 M) acidified with 1.5 M H_2SO_4 has been used as electrolyte and copper electrodes have been used. Spherical glass particles of sizes 3.0 mm, 4.5 mm and 6.0 mm have been used as the bed material. Mass transfer behavior has been studied using the limiting current technique.

The effects of bed voidage, electrolyte velocity and particle size on mass transfer rate have been studied. Optimum bed voidage and velocities for different particle sizes have been found. Mass transfer correlations have been found for different particle sizes. It has been observed that the exponent on the Reynolds number decreases with the increase in particle sizes of the bed materials. The correlations obtained are:

For 3.0 mm particles: $St_I (Sc)^{2/3} = 0.0495\ Re_I^{-0.40}$

For 4.5 mm particles: $St_I (Sc)^{2/3} = 0.0384\ Re_I^{-0.30}$

For 6.0 mm particles: $St_I (Sc)^{2/3} = 0.0195\ Re_I^{-0.25}$

ACKNOWLEDGEMENTS

The author would like to express his gratitude to the following.

Dr. M. Sabder Ali for his constant encouragement, guidance and supervision throughout the work.

Prof. A.K.M. Abdul Quader for making available the necessary research facilities and encouragement.

Prof. Khaliqur Rahman and Dr. Ijaz Hossain for their thoughtful suggestions and encouragement.

Mr. Abdul Mannan and Mr. M. Shahjahan for their sincere cooperation in setting up the experimental rig and carrying out the experiments.

Mr. Md. Hossain Ali, for taking the care and patience in typing this thesis.

His friends and colleagues, Mr. Gopal Chandra Paul and Mr. M.A. Muqeem for their help and encouragement.

CONTENTS

CHAPTER 1

INTRODUCTION

In electrochemical reactors, where one of the reactions is fast, the study of mass transfer is very important. This is especially important to the chemical engineers because it determines the maximum mass transfer rate at which the reactor can be efficiently operated. The maximum practical operating current depends mainly on the hydrodynamic conditions prevalent at the electrodes. Electrodeposition of metal from solutions are generally fast reactions and are important industrially in processes such as electrowinning, electrorefining and electroplating.

Mass transfer studies of electrochemical processes are done in order to ensure good quality deposits, because if the rate of mass transfer is not uniform and intensive over the whole of the electrode then poor or uneven deposition may occur. Generally operation at low current densities gives good quality deposits but the rate of mass transfer is not uniform over the whole of the electrode and locally high rates can cause poor electrodeposition. Well defined and controlled forced convection can give rise to better and uniform rates of deposition.

In order to improve the performance of an electrolytic cell, one can either raise the limiting current density or increase the specific electrode area. Agitation is the most

important means by which the former may be significantly increased. The effects of increased solution concentration may be of comparable magnitude but flexibility may be limited by considerations of solubility and deposit quality. In the past decade there has been considerable effort in the research and development of fluidized bed electrochemical reactors, although inert fluidized beds, in which nonconducting solid particles are fluidized have received limited attention. Quantitative analysis of mass transfer behavior and the optimum conditions for operation have not been studied throughly.

In the present research work, a parallel plate cell is used due to ease of design, construction and maintainance and for the uniformity of current distribution. The chosen shape of the cell also provides a surface area to volume ratio second only to particulate cells. This study utilizes the $Cu-CuSO_4$ system. Since the cathodic reaction for the chosen system is mass transfer controlled, the use of sectioned cathodes enables the current distribution and flow development to be studied by the limiting current technique.

Experimental mass transfer data have mainly been obtained in systems with long hydrodynamic entrance and exit regions thus ensuring that the flow is fully developed. When applied to the design of practical reactors such data result in over design. Moreover, entrance regions of the above kind are not desirable in the working reactors. Keeping the above facts in

view, the present work has been undertaken to investigate the mass transfer rate in the cathodic deposition of copper from acidified solutions of copper sulphate using a fluidized bed cell with sudden expansion at the inlet and contraction at the outlet. Different particle sizes of spherical glass beads have been used to study the effect of particle size on mass transfer. The cell has been operated under different flow conditions and initial bed heights to study the effect of flow rate and bed voidage on the mass transfer. Although in the present system, dilute solutions have been preferred to keep the limiting currents small and to cause slow dissolution of the anode, the experimental results gathered can be adequately used for industrial processes.

Experimental results are presented and correlated for different cell conditions. Comparisons have been made between the present study and the previous relevant works.

CHAPTER 2

LITERATURE REVIEW

2.1 Introduction

A review has been made on mass transfer theories in parallel plate electrochemical reactors, main features of fluidized beds and mass transfer in fluidized bed reactors. Work done by the previous researchers in the relevant areas have also been included. The basic electrochemical principles have been reviewed in Appendix-A.

2.2 Mass Transfer Theories in Electrochemical Cells.

2.2.1 Mass transfer in parallel plate systems for fully developed laminar flow

At steady state and in presence of excess indifferent electrolyte, the flux equation may be written as

$$U_x \frac{\delta C_i}{\delta x} + U_y \frac{\delta C_i}{\delta y} + U_z \frac{\delta C_i}{\delta z} = D_i \left(\frac{\delta^2 C_i}{\delta x^2} + \frac{\delta^2 C_i}{\delta y^2} + \frac{\delta^2 C_i}{\delta z^2}\right) \quad \ldots\ldots \quad (2.1)$$

where,

U is the velocity

D_i is the diffusion coefficient of i

C_i is the concentration of i.

For Parallel plate reactors, considering flow in the x direction, equation (2.1) reduces to

$$U_x \frac{\delta C}{\delta x} = D \frac{\delta^2 C}{\delta y^2} \quad \ldots \qquad (2.2)$$

Leveque [17] obtained an approximate solution of equation (2.2) for analogous heat and mass transfer cases. His solution was

$$Sh = \frac{Kd_e}{D} = 1.85 (Re\ Sc\ \frac{d_e}{L})^{1/3} \qquad (2.3)$$

where,

Sh is the sherwood number

Re is the Reynolds number

Sc is the Schmidt number

K is the average mass transfer coefficient

de is the equivalent diameter of the cell

L is electrode length.

Pickett and Stanmore [20] derived an approximate relationship for mass transfer coefficient in a rectangular duct of finite dimensions, using parabolic velocity distributions in the y direction only, of the form

$$Sh = 1.467\ (Re\ Sc\ de/L)^{1/3}\ (2/1+\gamma)^{1/3} \qquad (2.4)$$

where,

γ is the aspect ratio, b/a

a is the width of the electrode

b is the distance between the electrodes

Tobias and Hickman [28] experimentally verified the Leveque solution. They obtained

$$Sh = 1.85 \ (Re \ Sc \ de/L)^{1/3} \quad \ldots \quad (2.5)$$

for $de/b > 1.85$

which exactly tallied with the theoretical prediction.

Pickett and Stanmore [20] correlated their experimental data for a rectangular duct of aspect ratio of 0.167 and 0.175 as

$$Sh = 2.54 \ Re^{1/3} \ Sc^{0.292} \ (\frac{de}{L}) \quad (2.6)$$

Recently, Ali [1] has correlated his experimental data for a rectangular duct, as

$$Sh = 1.21 \ Re^{0.49} \ Sc^{1/3} \ (de/L)^{0.22} \quad (2.7)$$

which compares very favorably with the Walker and Wragg[31] prediction.

2.2.2 Mass Transfer in Turbulent Flow

The most useful emperical expression available for mass transfer in turbulent flow is the Chilton and Colburn [7] analogy. Chilton and Colburn presented an emperical heat transfer relationship as

$$J_h = St_h (Pr)^{2/3} = 0.023 \ Re^{-0.2} \qquad (2.8)$$

where,

St_h is the Stanton number for heat transfer

Pr is the Prandtl number

J_h is the Colburn J factor for heat transfer

The righthand side of equation (2.8) is equal to half the friction factor(f) defined as $f = 0.046 \ Re^{-0.2}$, and this leads to a general relationship for mass transfer as

$$St(Sc)^{2/3} = f/2 = 0.023 \ Re^{-0.2} \qquad (2.9,a)$$

Or, $$Sh = 0.023 \ Re^{0.8} \ Sc^{1/3} \qquad (2.9)$$

where St is the mass transfer Stanton number

The equation (2.9) is the best known emperical correlation for predicting mass transfer in turbulent flow and has been applied successfully to various flow systems.

Hubbard and Lightfoot [11] found from their experimental studies that mass transfer in turbulent conditions is best represented by the Chilton and Colburn analogy in the ranges of $10^4 < Re < 5X10^4$ and $1 < Sc < 1000$.

Ali [1] also performed some experiments and for length Reynolds number greater than 1700, he represented his data by the relationship

$$Sh = 0.063\ Re^{0.92}\ Sc^{1/3} \qquad (2.10)$$

All the correlations mentioned are for fully developed velocity and concentration profiles and are limited in application because they can not be used for reactors in which the flow is not fully developed.

2.2.3 Simultaneously developing flow and mass transfer

Bird et al. [4] developed an equation for flow in a duct which is suitable for situations when the flow has not fully developed but is laminar. They derived the equation for mass transfer problem with relevant boundary conditions as:

$$Sh = \frac{Kde}{D} = \frac{2}{\sqrt{\pi}} (Re\ Sc\ de/L)^{\frac{1}{2}} \qquad (2.11)$$

Using electrochemical methods to measure mass transfer coefficient entrance region for developing mass transfer boundary

layer, Berger and Hau [3] correlated their experimental data by

$$Sh = 0.0165 \quad Re^{0.86} \quad Sc^{0.35} \qquad (2.12)$$

Pickett and Stanmore [20] obtained an emperical equation

$$Sh = 0.145 \; Re^{0.6} \; Sc^{1/3} (de/L)^{1/4} \qquad (2.13)$$

which is appropriate for parallel plate with $L/de < 7.5$.

2.2.4 Effect of Flow Entrance Shape on Flow Developments and Mass Transfer.

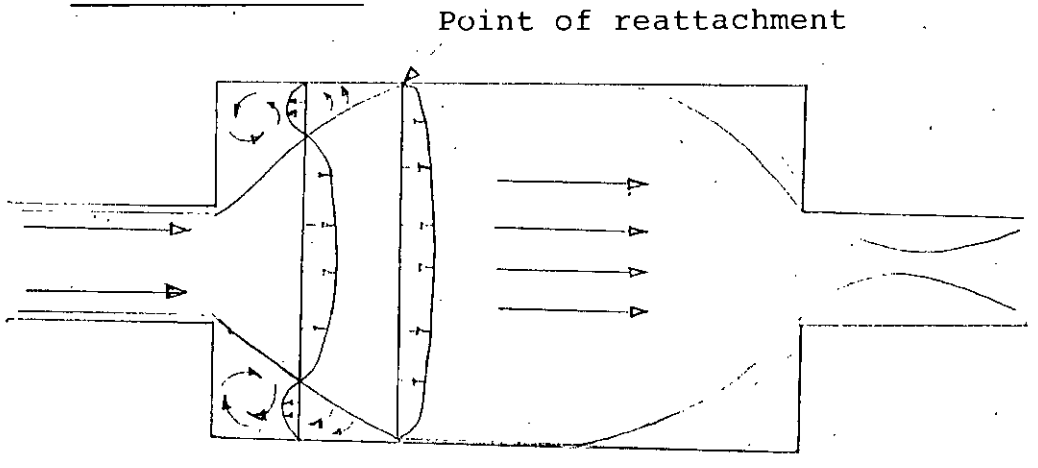

Fig. 2.1: Velocity profile changes due to sudden expansion and contraction.

After sudden expansion, a secondary flow occurs in the boundary layer due to a superimposed external flow field and its direction deviates from that of the external flow. The particles,

near the flow axis have a higher velocity and are acted upon by a larger centrifugal force than the slower particles near the wall and this leads to secondary flow directed out-wards in the centre and in-wards near the wall. Regions of boundary layer separation and backflow are formed due to secondary flows and the backflow in the boundary layer leads to the formation of eddies. These eddies occur in regions where there is an adverse pressure difference.

Krall and Sparrow [15] investigated the heat transfer in the separated, reattached and redeveloped regions in a circular pipe by passing flow through orfices varying from 1/4 to 2/3 of the pipe diameter. They found that the position of the maximum heat transfer coefficient is independent of Reynold's number, although its value is directly proportional to the Reynold's number. They also found that the position of maximum heat transfer occur at of position of 1.25 to 2.25 diameter downstream from the point of entry. In recent times, Runchal [25], Wilson[33], and Wragg, Tagg and Patrick [34] have studied axial local mass transfer distributions immediately downstream of sudden changes in flow cross sectional area using the limiting current technique. Their results were in good agreement with those of Krall and Sparrow. They found the value of mass transfer co-efficient for fully developed turbulent flow to be in agreement with the Dittus Boelter equation.

Their correlation was

$$Sh = 0.023\ Re^{0.88}\ Sc^{0.4} \qquad (2.14)$$

2.3 Liquid-solid Fluidization Systems

2.3.1 Particulate and Aggregate Liquid Fluidization

When the flow of a liquid through a bed of solid particles is gradually increased, a point is reached when effective weight of each particle is just supported by the drag on it. If there is nothing restraining the top surface, the bed at this point transforms itself from a fixed to a fluidised bed. The velocity at incipient fluidisation is called the minimum fluidisation velocity U_{mf}.

If the flow rate of the liquid is increased above the minimum fluidisation velocity to produce a fluidised bed, one of the two things will occur; either the bed will continue to expand so that the average distance between the particles will increase uniformly, or the excess fluid will pass through the bed in the form of bubbles. These two types of fluidization are referred to as particulate fluidisation and aggregate fluidisation respectively.

2.3.2 Pressure Drop Velocity Relationship

If a fluid is passed vertically upwards through a bed of solid particles, the pressure drop, ΔP, will initially rise as the velocity, U, is increased as shown by the AB region in Fig. 2.2. The relation between pressure drop and velocity will be the same as

that of a fixed bed. When the superficial velocity has reached such a value that the frictional pressure drop is equal to the effective weight per unit area of the particles, any further increase in velocity must result in a slight upward movement of the bed. The particles will become rearranged so that the resistance to fluid flow is decreased. In general the voidage of the bed will increase and in an idealised system, the pressure drop will remain constant as shown by the CD region of Fig. 2.2.

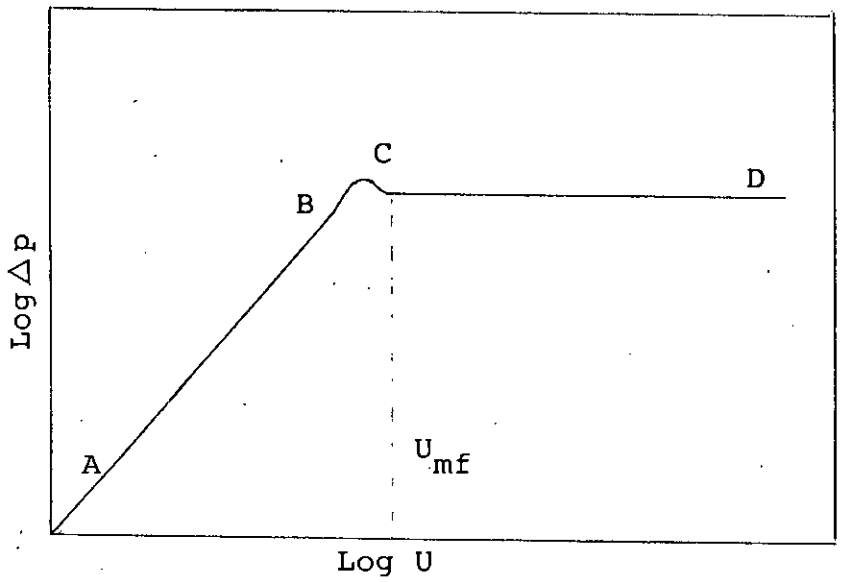

Fig. 2.2: Pressure drop - velocity curve.

At this stage the bed is just fluidised; it is said to be the point of incipient fluidisation and the superficial velocity at this point is known as the minimum fluidising velocity, U_{mf}. As the fluid velocity is further increased, the pressure drop over the bed remains constant.

2.3.3 Bed Expansion Characteristics

A number of workers have suggested that the most convenient way of showing the variation of fluidizing velocity with voidage is on a logarithmic plot since it gives a linear relationship. This can be expressed as:

$$U/U_i = \varepsilon^n \qquad (2.15)$$

where U is the fluidisation velocity and U_i is the fluidization velocity at the voidage (ε) of unity.

The exponent, n, is a function of the ratio of particle diameter to bed diameter (d_p/D_e and Reynolds number Re_t (= $U_t\ d_p.\ \rho_f/\mu$), involving the free- falling velocity of the particles and the size of the particles. The following emperical correlations for uniform spherical particles were obtained experimentally for U_i and n by Richardson and Zaki [24].

For fluidisation relation between U_i and terminal settling velocity is:

$$\log U_i = \log U_t - d_p/D_e \qquad (2.16)$$

$$n = 4.65 + 20\ d_p/D_e \quad (Re_t < 0.2) \qquad (2.17)$$

$$n = (4.4 + 18\ d_p/D_e\ Re_t^{-0.03} \quad (0.2 < Re_t < 1) \qquad (2.18)$$

$$n = (4.4 + 18\ d_p/D_e\ Re_t^{-0.1} \quad (1 < Re_t < 200) \qquad (2.19)$$

$$n = 4.4\ Re_t^{-0.1} \quad (200 < Re_t < 500) \qquad (2.20)$$

$$n = 2.4 \quad (Re_t > 500) \qquad (2.21)$$

Of all correlations, despite its limitations, Richardson and Zaki correlation remains most widely used.

2.3.4 Bubble Formations in Fluidized Beds

It is very important to know the type of fluidization in any practical application of liquid fluidized beds. The mass transfer, heat transfer and mixing properties of the bed may undergo a dramatic change with a particulate aggregate transition.

A fluidized bed is called bubbling when there exists fluid regions devoid of particles. Bubbles form due to the hydrodynamics of the fluid - particle interaction. With an even sintered plate distributor, bubbles form very close to the distributor as particles free small voids.

Transition from particulate to aggregate fluidization has been studied by many investigators and as a result a number of models have been postulated.

The formal classification of fluidized systems as particulate or aggregate is due to the early work of Wilhelm and Kwauk [32] based on the concept of interparticle forces in the vicinity of the bubbles. They suggested a dimensionless group, the Froude number at minimum fluidization, $U_{mf}^2/g\ d_p$, as a criterion. From their experimental results they suggested, for $Fr_{mf} >> 1$, aggregate behavior will be observed. For $Fr_{mf} << 1$, particulate behavior will dominate and for Fr_{mf} of the order of 1, the system is transitional.

2.4 Mass Transfer in a Fluidized Bed Electrode

2.4.1 Mass Transfer Correlation for Fluidized Bed Electrode

Fluidization represents an essentially unstable situation between packed bed operation and hydraulic transport. This implies that relations describing transfer coefficients for the above operations will show much similarity. The segregation of the phases in a fluidized bed leads to a transfer resistance specific for this operation. Experimental studies of mass transfer at a flat plate or cylindrical surface show that mass transfer rate increases with increase in the electrolyte velocity. In fluidized condition, the inert glass beads give additional kinetic energy to disrupt the concentration boundary layer and enhance mass transfer at the wall.

The usual way of correlating mass transfer data is by means of a dimensionless group correlation of the following form:

$$St = \text{constant } Sc^{c} Re^{b} \qquad (2.22)$$

where the Stanton No. St (= K/U) is a mass transport coefficient, the Schmidt No. Sc (= ν/D) describes the transport characteristics of the fluid and the Reynolds number Re (= Ud_p/ν) describes the pattern of fluid flow. Much of the early work on fluidised beds was correlated by means of the particle diameter d_p, but more recently the mean hydraulic diameter of the voids has been

considered to be more appropriate in the case of inert particles. This has been shown in Fig. 2.3 in which the bed is represented as a series of N hydraulic channels and (N+1) columns of particles. For simplicity it is assumed that all channels are of equal width. It is also assumed that the velocity in this channel is proportional to the interstitial velocity, U, in the bed and that the hydraulic diameter of this channel is proportions to the mean hydraulic diameter of the voids between the particles. For the two dimensional section, the area of particles present can be expressed as:

$$(N+1)L_f\, d_p = A(1-\varepsilon) \quad \ldots \quad (2.23)$$

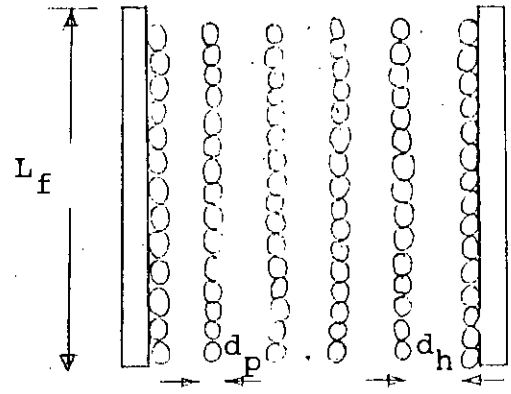

Fig. 2.3: Model for fluidized bed.

where A is the total area of section and ε is the bed voidage. The area of hydraulic voids is then given by:

$$N\, L_f\, d_h = A\, \varepsilon \quad (2.24)$$

where d_h is the hydraulic diameter. Eliminating L_f from equation (2.23) and (2.24)

$$d_p = \left(\frac{N}{N+1}\right) \left(\frac{1-\varepsilon}{\varepsilon}\right) d_h \qquad (2.25)$$

Equation (2.25) can be further simplified by assuming that $(N/N+1) \longrightarrow 1$ where N is very large.

$$d_p = \left(\frac{1-\varepsilon}{\varepsilon}\right) d_h \qquad (2.26)$$

Hence a modified Reynolds number can be defined using the hydraulic diameter;

$$Re_I = \frac{U_o d_p \varepsilon}{\nu(1-\varepsilon)} \qquad (2.27)$$

where U_o is the actual velocity of fluid within the voids. This is related to the superficial velocity U by:

$$U_o \varepsilon = U \qquad (2.28)$$

Then by substitution;

$$Re_I = \frac{U d_p}{\nu(1-\varepsilon)} \qquad (2.29)$$

Defining Stanton Number in terms of superficial velocity as:

$$St_I = K\varepsilon / U \qquad (2.30)$$

Hence the modified dimensionless correlation becomes:

$$St_I = \text{Constant } (Sc)^c \ (Re_I)^b \qquad (2.31)$$

The mean hydraulic diameter may also be defined in terms of the effective cross sectional area of flow i.e., the volume of voids and the surface area of the solid particles, A_p as:

$$d_h = \frac{k_c \ V_v}{A_p} \qquad (2.32)$$

where k_c is a constant. But as the volume of voids is given by $V_v = V_b \varepsilon$, where V_b is the total volume of the bed. The surface/volume ratio of the solid spherical particles is $6/d_p$, it may be written as:

$$d_h = \frac{k_c d_p}{6} \cdot \left(\frac{\varepsilon}{1 - \varepsilon}\right) \qquad (2.33)$$

If the value of k_c is 6, equation (2.26) and (2.33) become identical.

2.5 Review of Previous Works on Mass Transfer in Fluidized beds

Krishna et al. [16] used a system for the oxidation of ferrocyanide ion and the reduction of ferricyanide ion. They used equimolar solution of potassium ferrocyanide and potassium ferricyanide (0.01M) with excess of indifferent electrolyte

(0.5N sodium hydroxide) was used as the fluidizing medium. They used rockwood shot and glass spheres of different sizes (1 mm to 5 mm) with annular electrodes. They obtained a correlation as:

$$J_{D\varepsilon} = 0.43\ (Re_I)^{-0.43} \qquad (2.34)$$

Rama Rao and Venkata Rao [22] used a square channel packed bed instead of annular channel and they suggested the correlation as:

$$J_{D\varepsilon} = 0.79\ (Re_I)^{-0.404} \qquad (2.35)$$

Carbin and Gabe [6] studied the mass transfer behavior using cylindrical test electrode in a cylindrical bed. They used ballotini glass beads (0.1 mm $\sim$ 0.3 mm) such that $D_e/d_p \geqslant 80{:}1$. They found the maximum value of limiting current density at a voidage $\varepsilon = 0.59$. With their experimental results, they suggested the correlation to be

$$St_I\ (Sc)^{2/3} = 1.24\ Re_I^{-0.57} \qquad (2.36)$$

Smith and King [27] studied the ionic mass transfer coefficients between the wall of a tube (2") and liquid fluidized beds of lead glass, soda glass and lucite spheres using diffusion controlled reduction of ferricyanide ion at a nickel cathode for porosites 0.90 to 0.45 and Schmidt numbers 580 to 2100. The developed flui-

dization mass transfer coefficient for $41 < D_e/d_p < 105$ were:

$$J_D\varepsilon = 0.274\ Re_I^{-0.38} \quad \text{for } 10 < Re_I < 1600 \tag{2.37}$$

and by

$$J_D\varepsilon = 0.455\ Re_I^{-0.44} \quad \text{for } 16.7 < D_e/d_p < 27 \tag{2.38}$$

$$50 < Re_I < 3500$$

The distinct effect of D_e/d_p ratio is attributed to the wall effects and non particulate behavior of the fluidized bed for large size particles.

Coeuret and Goff [9] reviewed the problem of mass transfer in an immersed cylindrical surface and the liquid in a fluidized bed of non conducting spherical particles. Their electrolyte solution consisted of equimolar solution (0.005 M) of Potassium ferrocianide and ferricyanide with excess of indefferent electrolyte (0.5 NaOH). Their data exibited a maximum mass transfer coefficient (K) at a voidage of $0.55 < \varepsilon < 0.6$. They found the correlation to be:

$$J_D = 1.20\ Re_I^{-0.52} \tag{2.39}$$

Walker and Wragg [31] performed electrochemical mass experiments involving the cathodic deposition of copper from aqueous solutions containing H_2SO_4 in a rectangular channel.

They determined mass transfer rates at a plane wall electrode in the presence of a fluidized bed of glass beads. They found the correlation as:

$$J_{D\,\varepsilon} = 0.138\ Re_I^{-0.39} \quad \text{for} \quad \text{for } 0.936 < Re_I < 67 \qquad \ldots\ldots \qquad (2.40)$$

They also found maximum mass transfer rate to occur at a voidage of $0.7 \sim 0.75$.

TABLE 2.1

Comparison of mass transfer correlations according to:

$$St_I . Sc^{2/3} = a\ Re_I^{\ b}$$

Author(s)	a	b	D_e/d_p	System	Re_I	Sc	Particle size ((mm)
Smith and King [27]	0.32	0.38	41-105	Cylindrical wall mass transfer	0.7-1067	580-2100	-
	0.54	0.44	17-27		34-2334	-	-
Jattrand and Grunchare[14]	0.45	0.375	93-36	Planar test electrode in cylindrical bed	6-200	1250	0.220-0.780
Jagannadharaju and Venkata Rao [13]	0.43	0.38	8-27	Inner anode of annular bed	200-3800	1300	1.54-6.00
Coeuret et al. [9]	1.20	0.52	93-290	Various cylindrical probes	6-200	1250	0.35-1.07
Carbin and Gabe [6]	1.24	0.57	80-150	Cylindrical test electrode in cylindrical bed	0.1-70	787-1777	0.185-0.355
Walker and Wragg[31]	0.138	0.39	43	Rectangular Channel wall Mass Transfer	0.936-67	2675	0.274-0.548

CHAPTER 3

EQUIPMENT AND EXPERIMENTAL PROCEDURE

3.1 Introduction

A number of experiments were performed with a vertical parallel plate cell having copper electrodes in fluidized conditions. The electrolyte consisted of 0.015 M copper sulphate in 1.5 M sulphuric acid as the electrolyte. The copper - copper sulphate system was chosen because unlike other systems it is stable and remains uncatalysed by light. The cathodic reaction is mass transfer controlled, has been used by previous workers and has direct bearing on existing electrochemical processes. The cathode was sectioned to allow current measurements to be made at various sections and this enabled to determine the mass transfer rates at different positions in the cell to be determined. For fluidization spherical glass beads of average sizes 6.00 mm, 4.5 mm and 3.00 mm were used to examine the effect of size and voidage on mass transfer. The diameters of the particles were experimentally determined by measuring the diameter of fifty particles of each size and then taking the average.

3.2 Main Experimental System

3.2.1 The electrolytic cell

The cell used in this study was simple in construction with five main sections, the inlet section, the anode side, the

cathode side, the side plates and the exit section. The inlet and exit sections were provided to connect the cell to ½" PVC tubing. All the five parts were detachable. The electrolyte entered at the bottom and flowed upwards. There was no entrance length so that the mass transfer boundary layer and hydrodynamic boundary layer started at the leading edge of the electrode. Figures 3.1, 3.2 and 3.3 shows the five main units of the cell with detailed dimensions. Figure 3.4 is a sketch of the assembled cell with relevant dimensions as seen from the cathode side.

The cell was constructed by perspex sheet of 1.2 cm thickness except the side walls. Both the anode and cathode sides had the dimensions of 38.3 cm X 10.4 cm. The anode and cathode sides were kept at a distance of 2 cm from one another by side plates (38.3 cm X 2 cm and 2.0 cm thickness). Thus the total effective cross-sectional flow area of the cell was 5 cmX 2 cm (=10 cm^2). The anode was a piece of 3.2mm thick copper plate (30 cm X 6 cm) glued with Araldite into a groove of the same size and depth of 3.2mm made into the perspex wall. The side perspex plates were fitted along the long edges of the exposed anode and overlapped 0.5 cm from both sides of the anode and as such the total exposed anode area was 30 cm X 5 cm (=150 cm^2). The electrical connectrions were made with two 1.6mm diameter copper wires soldered to the back of the anode through two 3.2mm holes drilled at two positions.

The cathode was 30 cm long and 6 cm wide and made of 3.2mmthick copper plate, but the width of the electrode exposed in the cell was 5 cm due to ovcerlapping of the side plates in

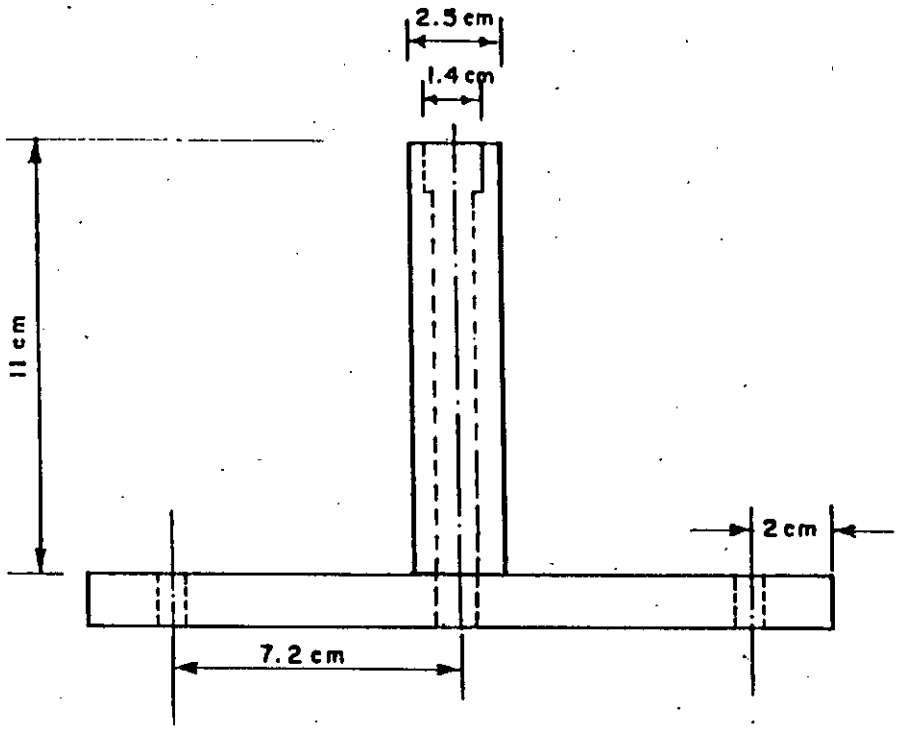

FRONT VIEW

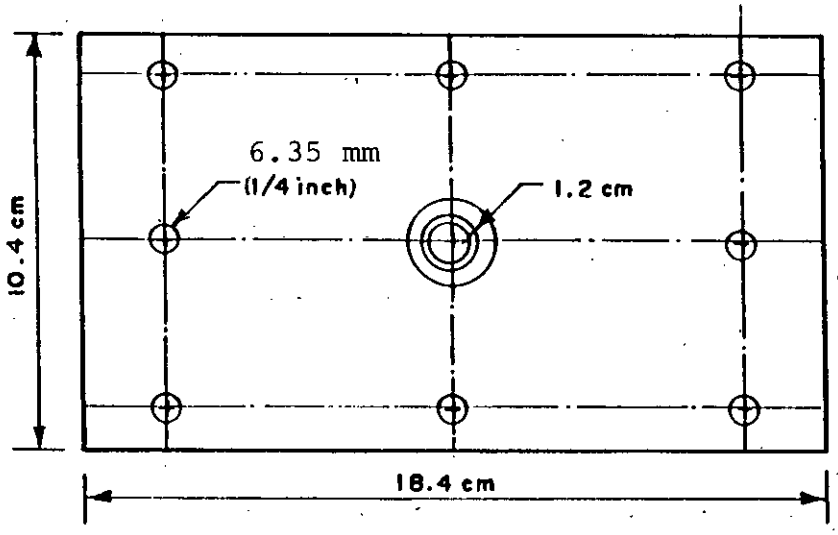

TOP VIEW

FIG. 3.1 THE INLET AND EXIT SECTION.

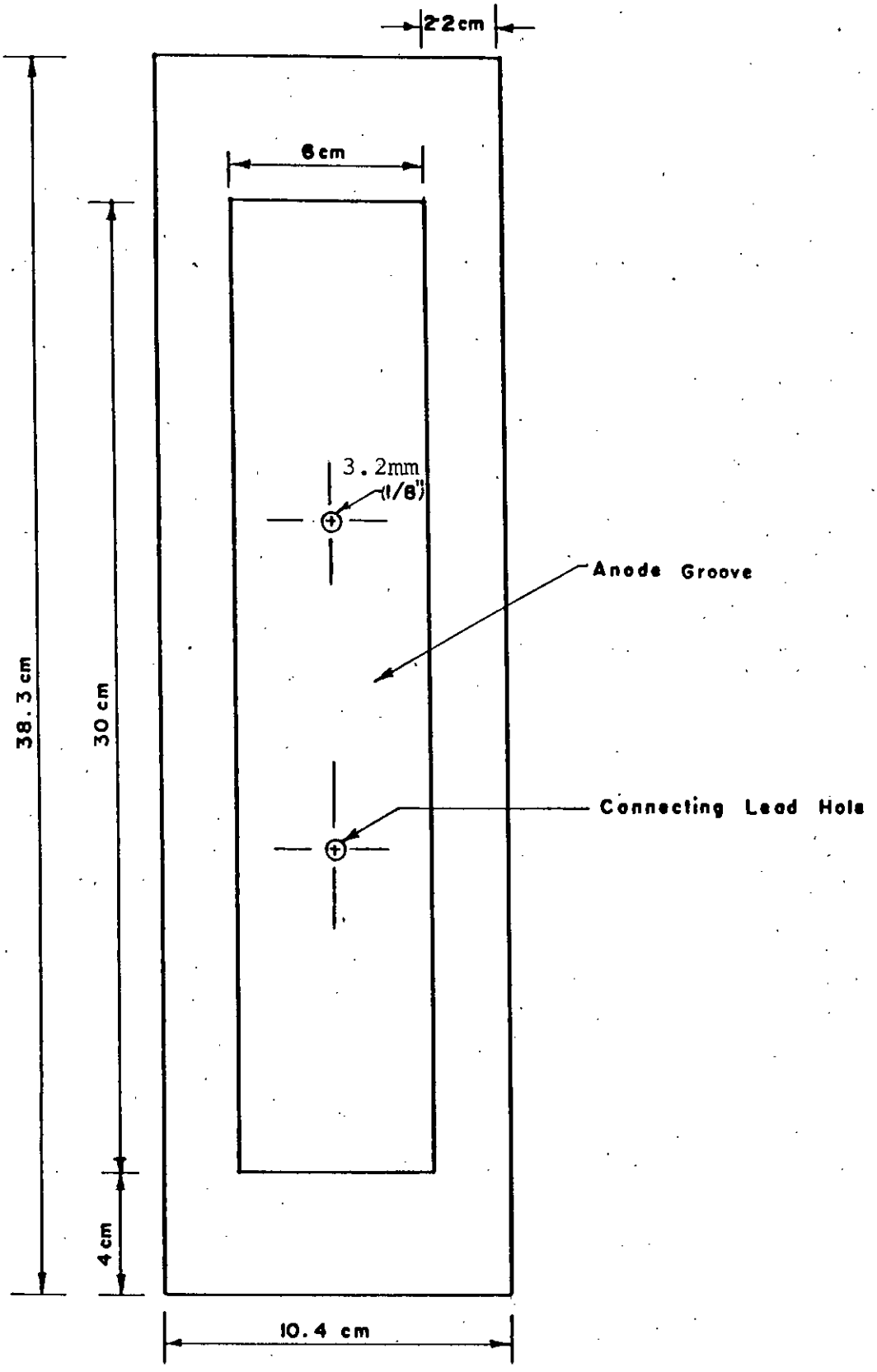

FIG. 3.2 THE ANODE SIDE OF THE CELL.

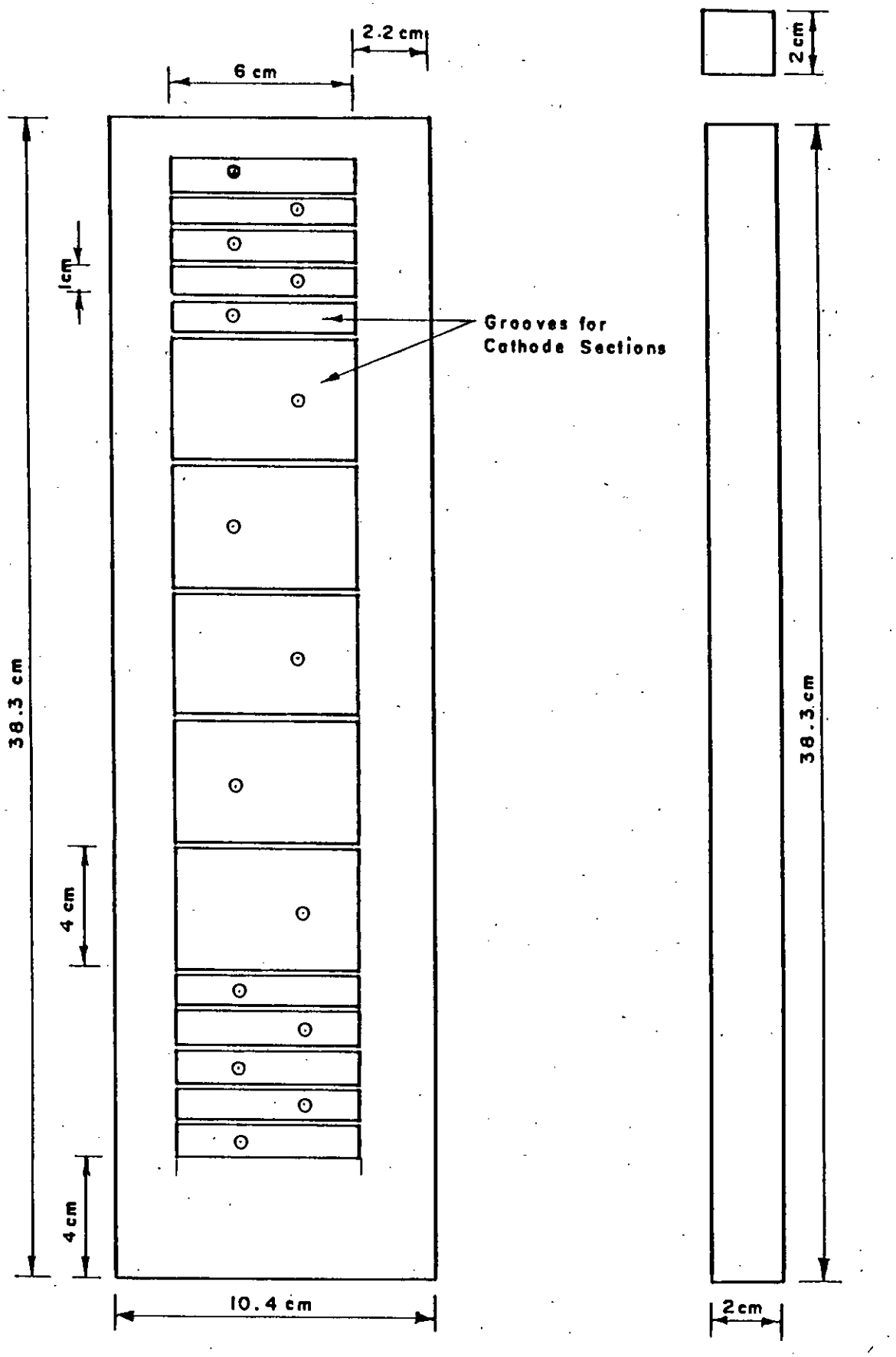

(a) THE CATHODE SIDE (b) THE SIDE PLATE

FIG. 3.3 THE CATHODE SIDE AND THE SIDE PLATE

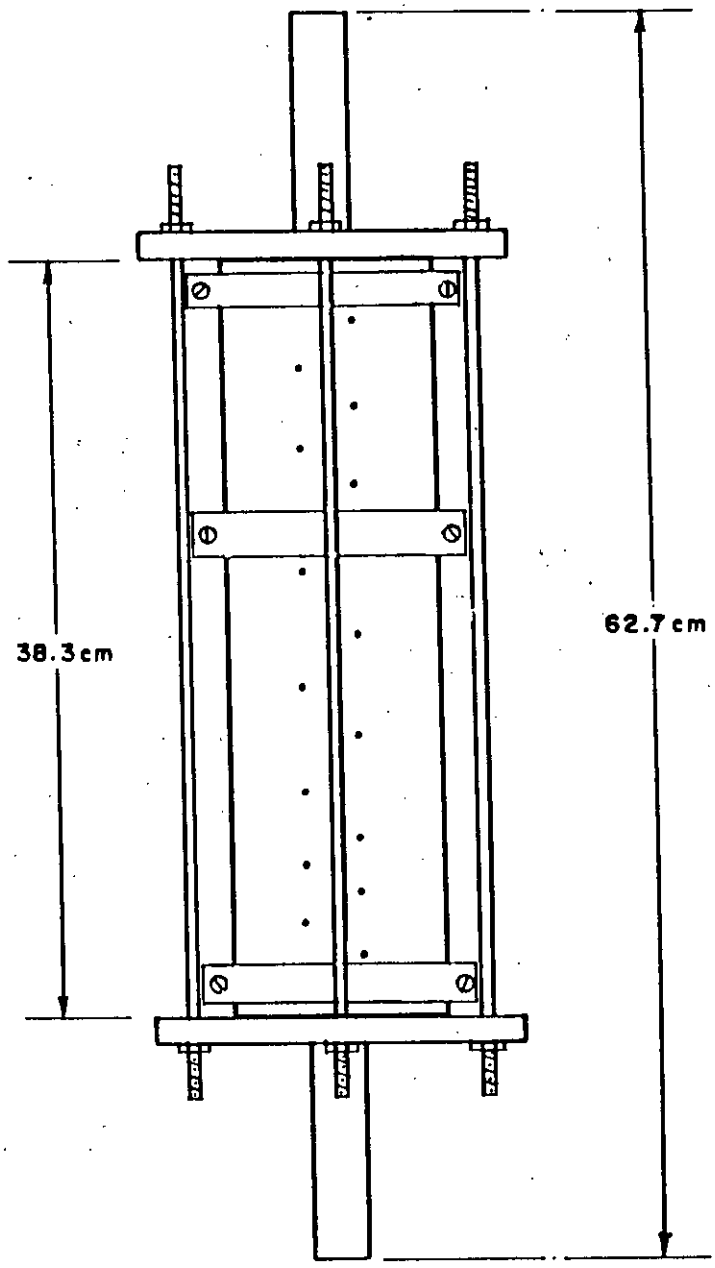

FIG. 3.4 SKETCH OF ASSEMBLED CELL.

keeping coformity with the anode.

The cathode was divided into fifteen sections from the leading edge of the electrode, the lengths of the sections were 1.0 cm for the first five (inlet) sections, 4.0 cm for the next five sections and 1.0 cm for the last five (exit) sections.

This is shown in Figure 3.3a. The cathode sections were arranged in this manner as it was anticipated that the current and hence the mass transfer rates would vary significantly at the inlet and exit regions of the cathode.Smaller sections in these portions enabled more accurate measurements of the variations in current distribution. Each cathode section was fixed with Araldite to a groove of corresponding size cut into the perspex sheet and separated from the adjacent electrode by thin strip of perspex of 0.2 cm thickness. This facilitated the measurement of the current in each section without interference from the neighbouring sections. Electrical connections to each cathode sections were made with fifteen 1.6mm diameter copper wires soldered to the back of each cathode section through fifteen 3.2 mm holes in the cathode side perspex plate.

The anode plate and side plates were joined together with the help of ethylene dichloride solvent. The anode and the cathode plates were joined together with three clamps at top, middle and bottom regions. Two rubber gaskets were used between cathode plate and side walls to minimise the leakage. The main cell body and the inlet and outlet sections were joined together together with 6.4 m.m diameter brass tie rods through siz6.4mm holes in the inlet

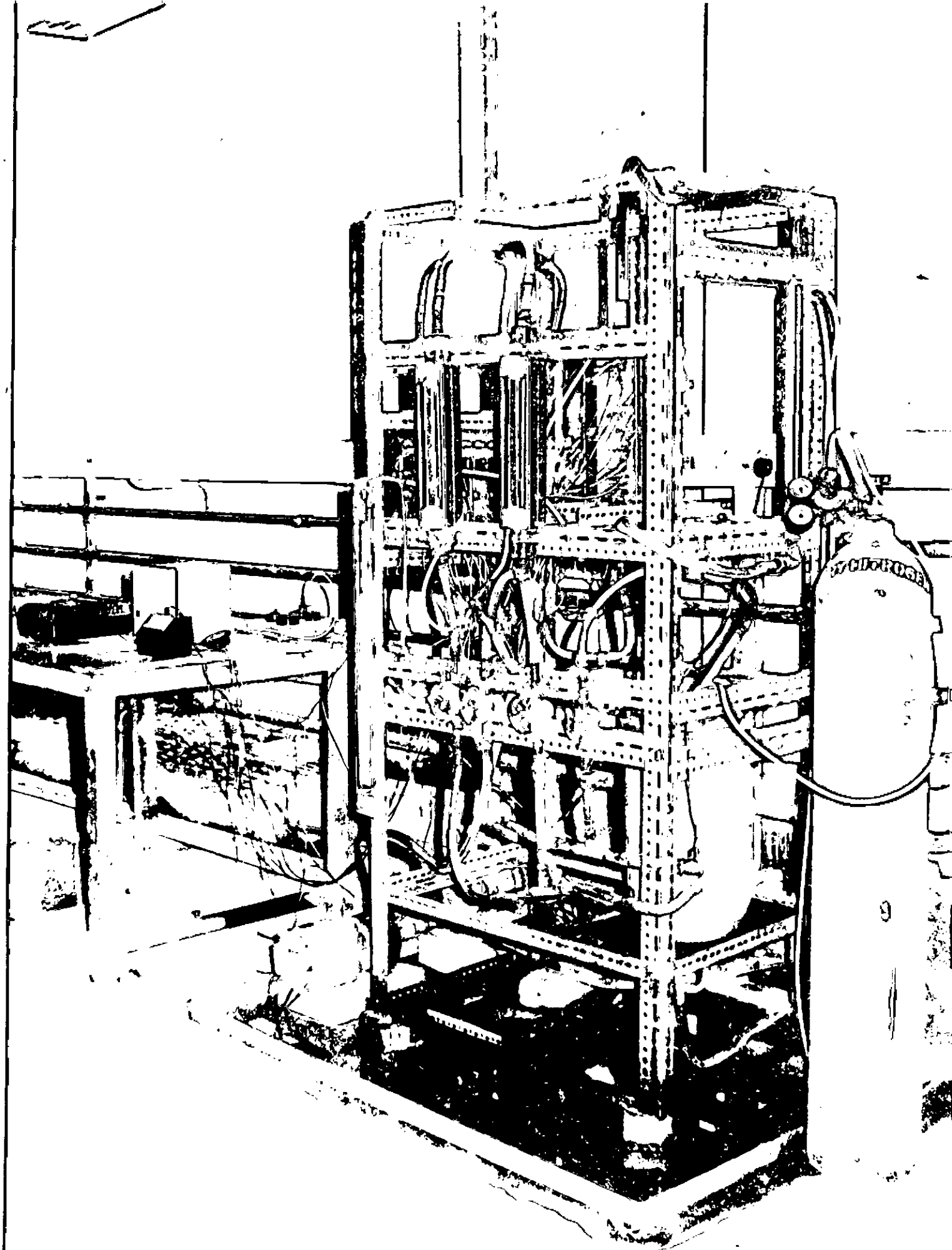

Fig. 3.5: The Experimental setup.

and exit section flanges. Rubber gaskets were used between the main cell body and inlet, exit sections to prevent leakage. Finally a thin layer of Araldite was applied to all the sides to make the cell completely leakproof.

The inlet and outlet portions of the cell were of indentical shape and dimensions. The diameter of the inlet and exit piping adjacent to the main cell body was 1.2 cm and this diameter was flared to 1.5 cm at the connection point to the ½" PVC tubing for easy pressure fit. The size of the inlet and exit section plates were such that (18.4 cm X 10.4 cm) they served as flanges to provide adequate space for the tie rods. Two copper wire meshes were used to support the bed particles and prevent them from escaping in the flow pipings and pump.

3.2.2 The flow system

The whole flow system consisted of a pump, a cooler, two rotameters, the electrochemical cell, a storage tank four two way glass valves and PVC pipes and tubes. Except the pump, all the major units were mounted on the experimental rig as shown in Figure 3.5. Figure 3.6 gives a detailed schematic diagram of the entire flow circuit.

An Electronidioren Werke - Kaiser pump (220 V, 2.15 A, 0.25 KW and 50 Hz) with corrosion resistant plastic impeller and casing was used to circulate the acidified copper sulphate solution from a 25 Kg capacity plastic tank through the whole system.

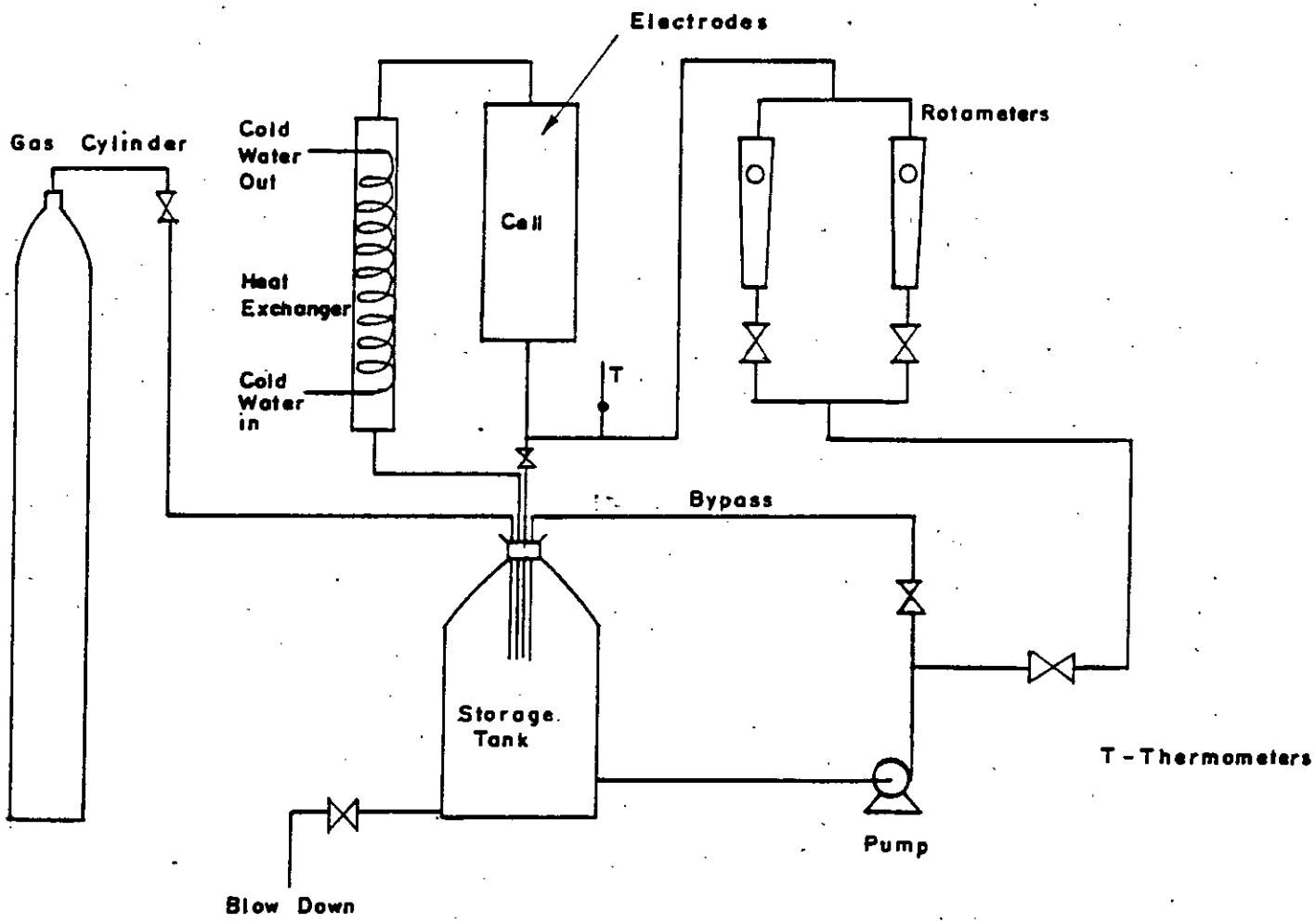

FIG. 3.6 FLOW CIRCUIT DIAGRAM.

The flow line consisted of ½" PVC pipes and tubes and the flow rate was measured by two rotameters of different ranges. The calibration curve for each rotameter for 0.015 M copper sulphate in 1.5 M sulphuric acid are presented in Appendix B. The flow through the cell was adjusted by using the flow bypass and the two way Pyrex ½" glass valves fitted before each rotameter. The flow direction in the cell was always vertically upwords. A cooler was used to prevent the increase of the electrolyte temperature although the temperature increased by several degrees after sufficient period of time. Two two way control valves were used to control the flow direction as necessary. Dry nitrogen gas was used to deoxygenate the solution before each experiment.

3.2.3 The electrical circuit

An electrical circuit was designed for the electrochemical reactor which would allow the measurement of current on each section of the cathode separately without interferring with the main electrolytic process or changing the total current passing through the electrode. The electrical circuit is shown in fig. 3.7.

An d.c. power supply type (PHYWE, 0-20V,12A) connected with 220 V line was used as the power source. The total cell voltage was measured by a voltmeter placed across the cell. The total current passing through the cell was measured by an d.c. ammeter (Weston Instruments Company, 0-3A). The individual sectional currents were measured with miliammeters (Philip Harris Ltd. 0-100 mA, 0-250 mA).

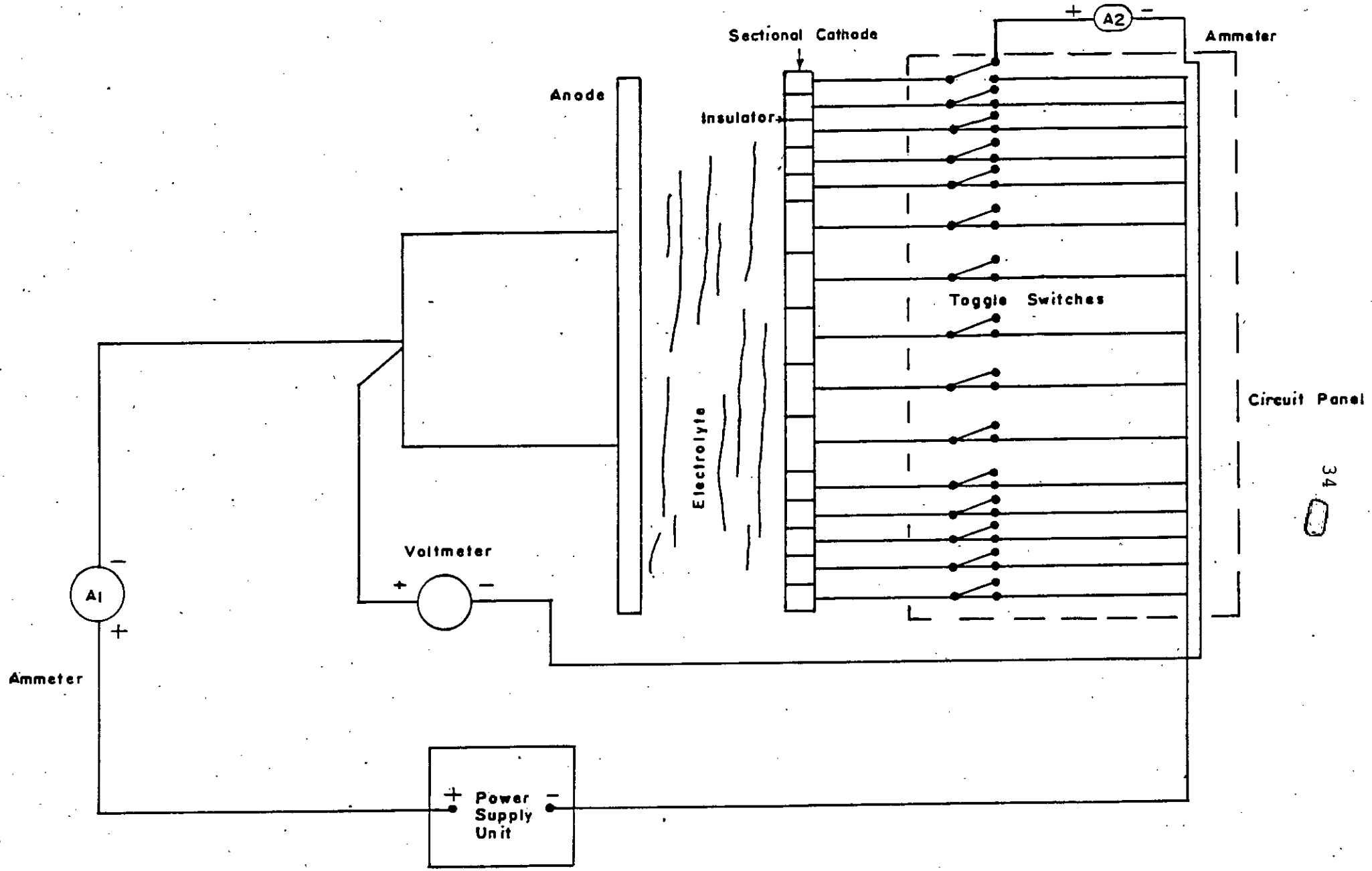

FIG. 3.7 ELECTRICAL CIRCUIT FOR MEASURING CURRENT.

Toggle switches of current rating 10A were used to switch away any section of the cathode from the main circuit, through the ammeter A2 the cathode current of that section was measured. In this way the cathode current in all the sections were measured in turn.

3.2.4 Experimental procedure

The concentration of coppersulphate solutions used in the experiments were approximately 0.015 M in 1.5 M sulphuric acid. Analytical grade anhydrous copper sulphate ($CuSO_4$) was dissolved in distilled water and sulphuric acid to make the electrolyte solution (.015 M $CuSO_4$ in 1.5 M H_2SO_4 solution). The solution concentrations were determined volumatrically. The method used for the computation of the concentrations of copper sulphate is outlined by Jabbar et al. [12] and Vogel [30] involving precipitation of the copper as cuprous iodide with excess potassium iodide and titration of iodine formed with standard sodium thiosulphate solution. Analysis of the copper sulphate content was done after a series of runs. Dilute solutions of copper sulphate were used to ensure small limiting currents with correspondingly low rates of dissolution of the anode and deposition on the cathode and for minimum natural convection. Since the activation overpotential of an electrode is greatly dependent on electrode surface, both the electrodes were throughly cleaned before assembling the cell prior to each run. The cleaning was done by rubbing the

electrode surface with successively finer grades of 'emery' paper and eventually finishing with ultra fine (number '0') 'emery' paper. The electrodes were then rinsed with distilled water and degreased with an organic solvent (acetone). The smoothened electrode surface was finally washed with distilled water and left to dry in air.

The electrical connections to each cathode sections and the anode were cleaned and their electrical connections were checked by a multimeter before assembling the cell. The main body of the cell (i.e. anode plate, cathode plate and the sidewalls) was assembled first by three clamps. Then holding the main body on the inlet section, glass particles of a particular size (6.0 mm, 4.5 mm and 3.0 mm) were put into the cell upto a certain bed height. It may be mentioned here that for each particle size, three initial bed heights, such as 8 cm, 12.0 cm and 16 cm were used to make different voidages in the cell at different flow conditions.

At the start of each run nitrogen from a gas cylinder was used to pass nitrogen through the solution in the storage tank for about 1-2 hours in order to deoxygenate the solution because an extra current density of approximately 0.25 mA/cm^2 is needed due to the reduction of oxygen at the cathode [34].

After deoxygenating the electrolyte, the pump was started and the electrolyte was recirculated through the system with flow rate adjusted by means of valves and the flow rate was measured from the rotameter. Before taking the readings, the cell

was operated at low current densities (about 0.2 mA/cm²) for about 15-20 minutes to get an even deposit of copper at the cathode. This was done by applying a small voltage across the cell from the power supply.

To investigate the limitting current at a given flow rate the applied voltage was set to a definite value with the help of the power source. Two to three minutes were allowed for the system to reach steady state before the current readings were taken. The bed height at fluidized condition was measured to find the voidage of the cell. The sectional current on the cathodes and the total cell currents were measured by two ammeters. The applied voltage was then increased in steps with intervals of 50 mV and the measurements were repeated untils the individual currents in the sections exceeded their limiting values. This shows the start of the secondary reaction (i.e. hydrogen evolution at the cathode) and a sharprise in current occurs. Between each run, the cell was dismantled, cleaned and reassembled. The experiment was repeated for different flowrate and different bed heights with different particle sizes.

The concentration of the solution was checked after taking readings for each size of particles, and negligible difference was found with the original value. In any case, the solution was replaced after taking readings for each particle size.

The problem with the cell was the continued cleaning of the electrodes required, since, repeated runs without cleaning

did not reproduce the original results which is due to oxide formation on the anode surface. At the end of each run the anode was always coated with a thin layer of black powder (copper oxide) which was formed by the reaction [8]

$$Cu + H_2O \longrightarrow CuO + 2H^+ + 2e \qquad ..$$

Moreover, difficulty was encountered due to the deposition of copper on the unexposed sides of the cathode as a result of leakage of electrolyte between cathode section and perspex plate. Again, at higher current densities, there was deposition of copper sulphate on the anode surface.

CHAPTER 4

RESULTS AND DISCUSSIONS

4.1 Introduction

In the electrolysis of copper sulphate - sulphuric acid solution, the rate of copper deposition at the cathode is controlled by the rate of mass transfer across a hypothetical diffusional layer near it. To increase the mass transfer rate and to make it uniform, fluidized bed of inert glass particles was used. The cathode was sectioned to allow the measurement of the current at different segment and hence the mass transfer rate along its length. In the present research work, dilute solutions of copper sulphate (0.015 M) in an excess of indifferent ions (1.5 M H_2SO_4) have been used to keep the limiting current low and to reduce the transport number of copper ions.

Experimental work was carried out to study the effect of the following parameters of the fluidized bed electrolyte on the mass transfer rate in the electrochemical reactor.

(a) Effect of particle size of the fluidized bed on the mass transfer rate.

(b) Effect of bed voidage on the mass transfer rate at fluidized conditions.

(c) Effect of electrolyte velocity on the mass transfer rate.

To study the effect of the above parameters on the mass transfer rates, total and sectional currents along the length of the cathode were measured against different applied voltages at different flowrates and bed conditions.

The flow rate of the electrolyte in the system varied from 5.7 litres/min to 10.8 litres/min. Below 5.7 litres/min fluidization does not occur and beyond 10.5 litres/min particles are carried away with the liquid and accumulated at the top of the cell. Glass particles of 3.00 mm 4.50 mm and 6.00 mm sizes were used as the bed materials and the bed voidage varied from 0.45 to 0.90. The temperature of the system varied from 22°C to 32°C

4.2 Analysis and Presentation of the Results

The experimental procedure for the measurement of total current, as well as the individual current on different section elements of the cathode has been described in Chapter 3. The individual current on the sections of the cathode and the total currents were measured at different flow rates and at different bed voidages by progressive increases in the applied voltage until all the sectioned elements attained and exceeded their limiting currents. This procedure was repeated for each particle size. The reproducibility of the results was tested by making repeated runs which showed reasonably good agreement (about $\pm$ 5%).

All the experimental and calculated results for different particle sizes have been presented in Appendix C and some of the

summaries of the results are presented in this chapter.

Both individual sectional current and total current are plotted against different flowrates and cell conditions. Since the current measurement at an electrode section is not a point value but covers the entire area of that electrode section element, it is most useful to represent the variation of the current flowing at different sections in the form of a histogram.

From the total current-voltage curve, the overall limiting current will be used to obtain overall mass transfer coefficient. The average mass transfer coefficient over an electrode section will be calculated from the individual limiting current on that section and the variation of the average mass transfer coefficient along the length of the electrode will also be calculated by progressively averaging the individual mass transfer coefficients over the length of the electrode (cumulitive average mass transfer coefficient, K_{cav}). The overall mass transfer coefficients were plotted against the superficial velocity and bed voidages for different particles sizes. The product of Stanton number St_I ($=K\,\varepsilon/U$) and $Sc^{2/3}$ were plotted against modified Reynolds number ($Re_I = d_p U/\nu\,(1-\varepsilon)$) to obtain a correlation for different particle sizes. These correlations will then be compared with those of other workers.

The physical properties of acidified copper sulphate solution which will be used for the calculations, have been taken from reference [26]. The data in this reference were collected from several sources and are presented in Appendix B. For dilute

solutions the diffusion coefficient of the copper ion can be taken as that of copper sulphate without any appreciable error.

4.3 The Current-Voltage Curve

Investigations were carried out to determine the influence of electrolyte flow rate on the current-voltage curves at different fluidizing condition and the measurement of currents against applied voltage was conducted. The total cell current, as well the individual currents on the sections of the cathode were measured. The total current obtained by summation of individual section currents and the measured total current were compared and were found to agree within $\pm 10\%$. This discrepancy could be explained by the fact that two different types of ammeters were used to monitor the total and sectional currents respectively and the readings from the two might not have tallied exactly due to different resistances.

Figure 4.1 shows typical individual current - voltage curves. Figure 4.2 shows total current-voltage curves at different flow rates. There is a sharp increase in current with increase in potential till the process approaches the limiting current conditions. At limiting current region the rate of increase of current is slowed down significantly and becomes constant in most cases. After this region, the current increases rapidly again. It is evident from Figure 4.1 that there is a distinct limiting current plateau on each curve for each flowrate of the electrolyte

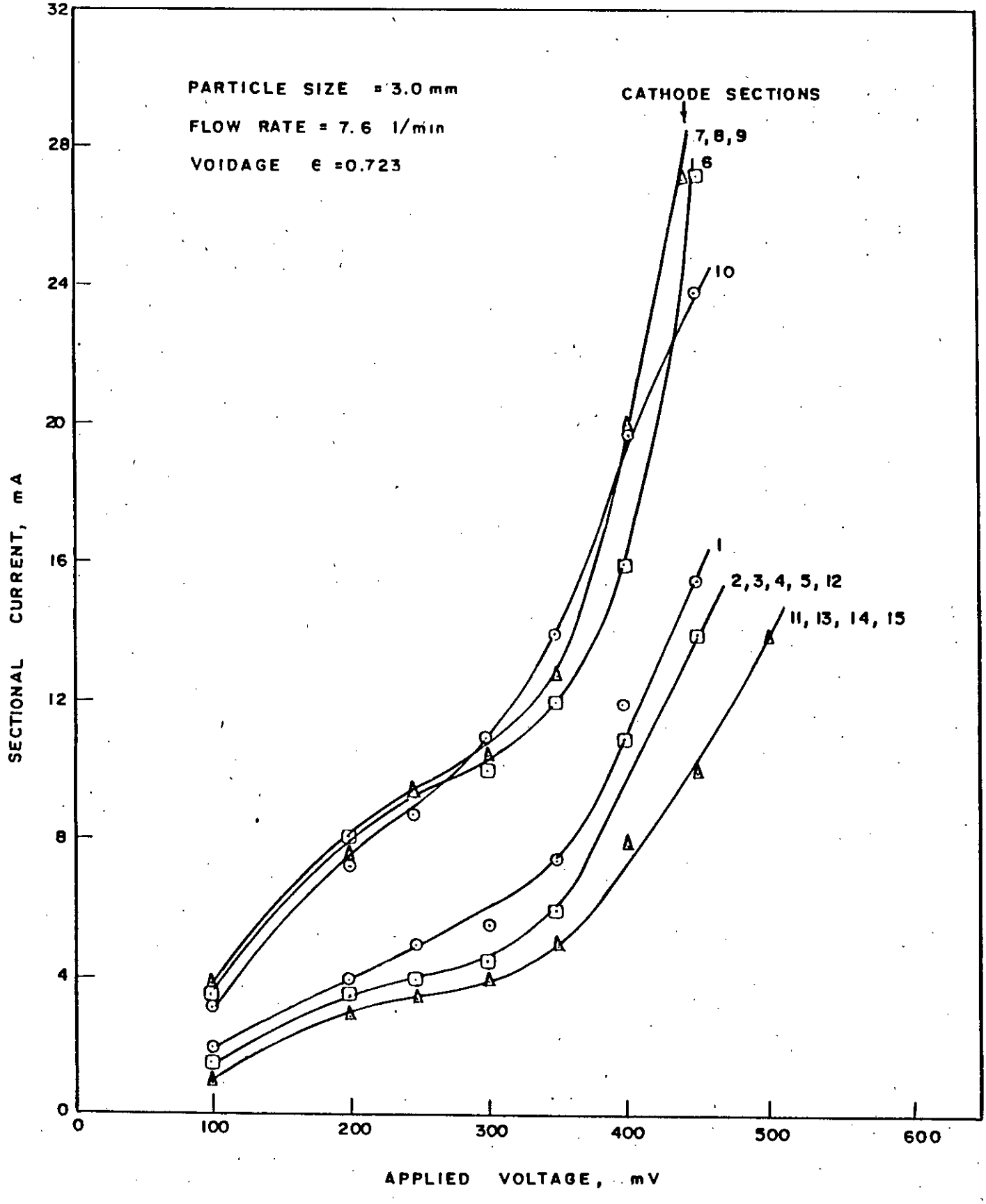

FIG. 4.1 CURRENT VOLTAGE CURVES FOR INDIVIDUAL CATHODE SECTIONS.

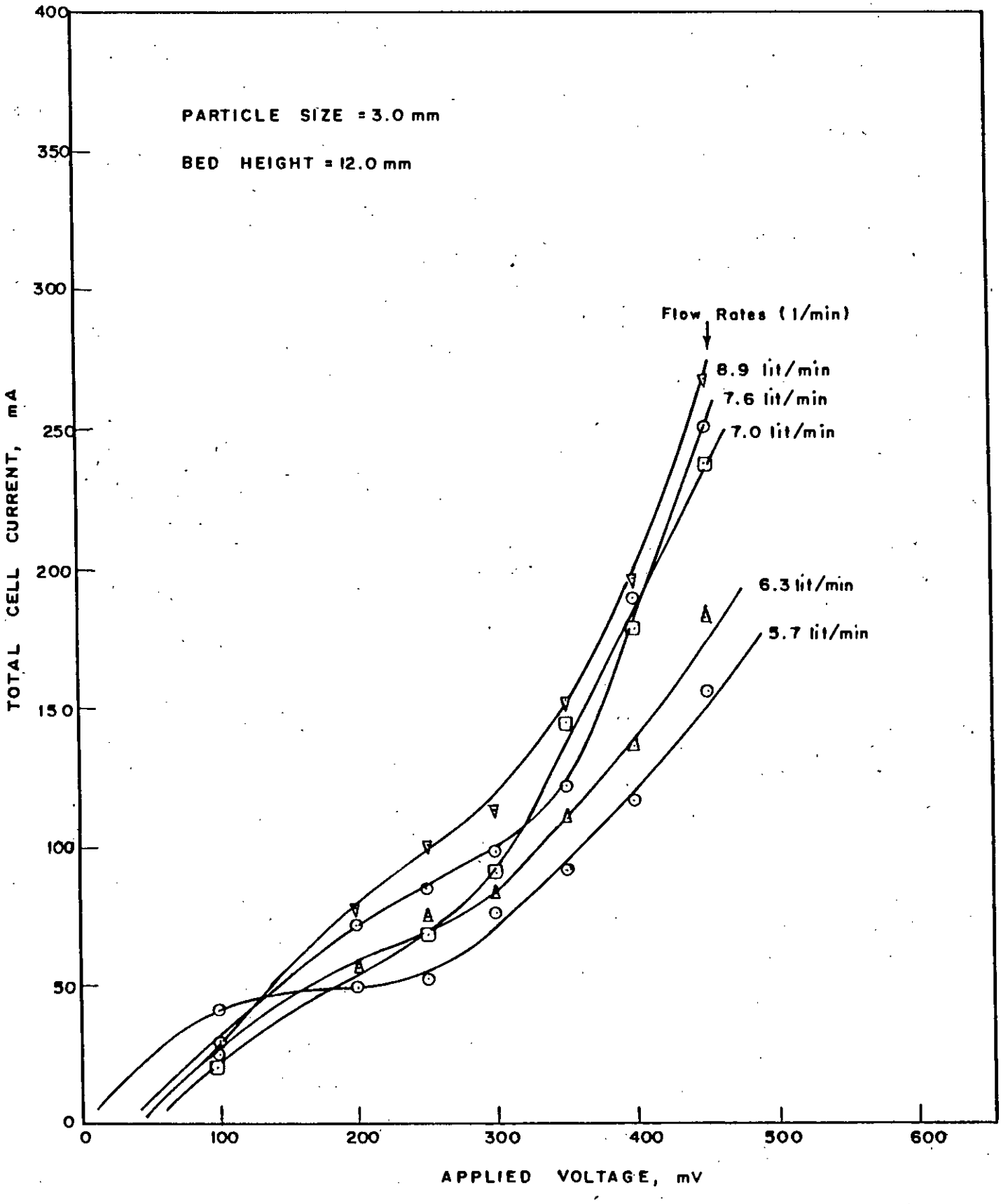

FIG. 4.2 TOTAL CURRENT VOLTAGE CURVES AT DIFFERENT FLOW RATES.

and these plateaus are well defined and wider for lower flow rates and less defined and less wider for higher flowrates. At higher flowrates the limiting current plateau reduces to an inflection point only. It is also seen that the overall limiting current plateau starts at 250 mv lower flow rates (5.7 l/min) and 300 mv for medium flow rates (8.0 l/min) and 400 mv for high flowrates (10.0 l/min). For further high flow rates the limiting current shifts to lower voltage region again. The shrinkage and the shift of limiting current plateau in the higher voltage region occurs with increased flowrates. With increased flowrates, the limiting current densities increase. This may be due to the reason that with increased agitation at these conditions higher local current densities may result which form a very crystalline or porous electrodeposits. This increases the effective electrode area and hence the current density. From the expression of actual voltage requirement as mentioned in Chapter 2.

$$V = V_a - V_c + \Sigma n_a + \Sigma n_c + V_s \qquad (2.11)$$

It can be seen that with increase of limiting current density, n_a increases since n_a= a+b logi and the total cell voltage increases. For very high flow rates however, the limiting current plateau shifts to the lower voltage region again. This may be due to the reason that the rough deposits are able to catalyze the formation of gas at lower potential giving rise to early current plateaus And also with every high flowrates, the particles becomes

so dispersed that the fluidization effect tend to decrease.

The limiting currents on the segments start and end more or less at the same potential. It can also be observed the variation of the currents in some sections e.g., sections 11 to 14, and section 2 to 3 are similar.

4.4 Current Distribution Along the Electrode

Figure 4.3 shows a typical example of variation of current density along the length of the electrode. From the figure it can be seen that the peak value of current density and hence the mass transfer rate occur at one of the cathode sections of 1,2 and 3 from the leading edge of the electrode. After the initial increase the mass transfer rate shows a downward trend as the distance from the entrance is increased. In the middle rigion, the current density remains essentially constant and ultimately near the exit region, it rises again. So three different regions of mass transfer emerge namely the inlet, the midsection and the exit. Since local average mass transfer co-efficient of the cathode sections have been calculated from the current densities of the respective sections they will obviously show similar behavior. The rise in mass transfer coefficient at the inlet sections is due to the entrance effects, the change in shape and size of the flow area and the complexity of hydrodynamic conditions such as secondary flow and back mixing, eddying effect, separation and reattachment of the flow after sudden expansion. This agrees with the study of Krall and Sparrow [15] , Runchal [25] and Wragg, Tagg and Patrick [31] who had obtained a region of maximum mass

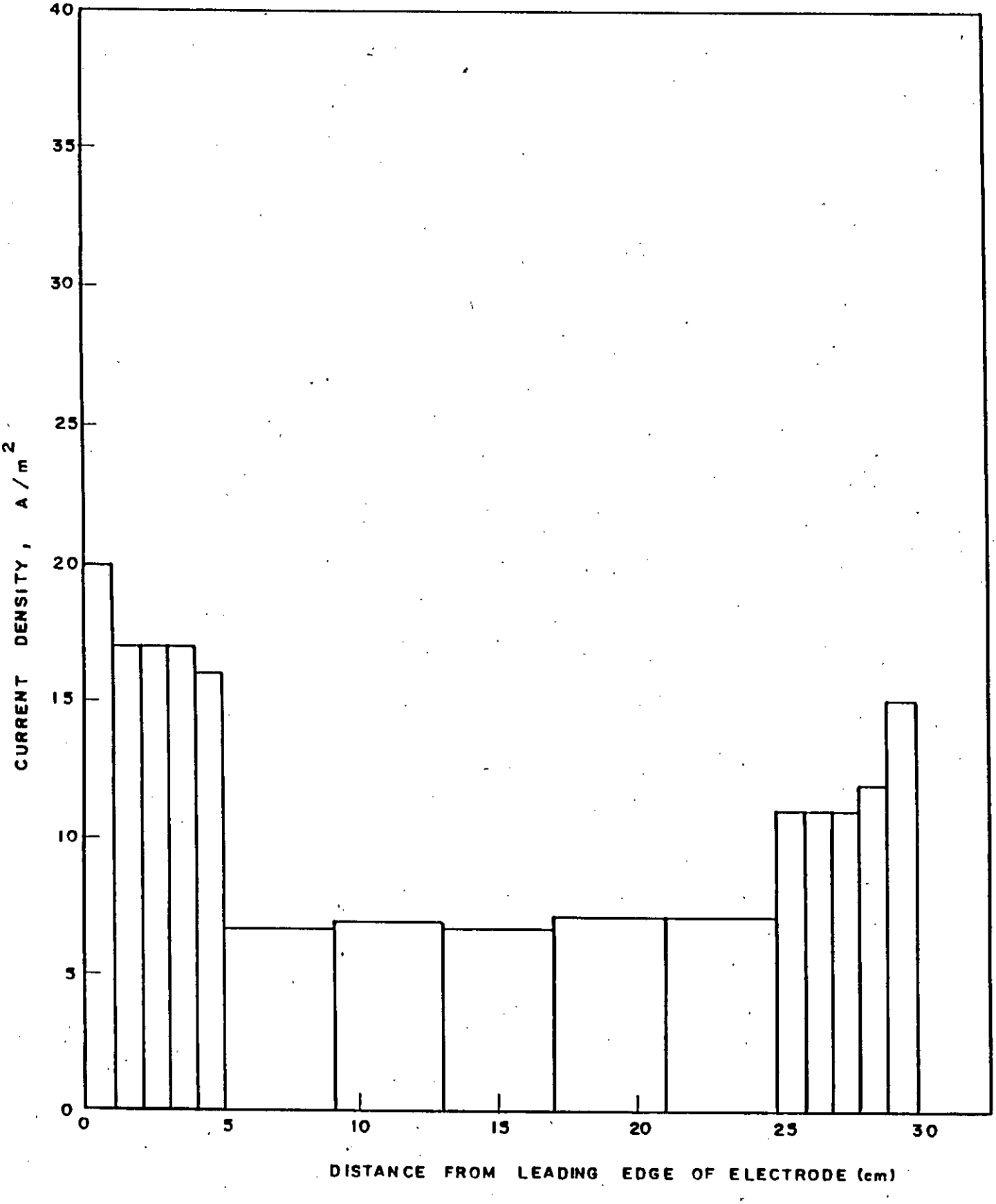

FIG. 4.3 CURRENT DENSITY IN DIFFERENT SECTIONS AT A FLOW RATE OF 7.0 lit/min, PARTICLE SIZE = 6.0 mm, INITIAL BED HEIGHT = 12.0 cm

transfer rate at a distance of 1.5 to 2.5 times the equivalent diameter of the large duct downstream from the leading edge of the electrode. The point of maximum mass transfer co-efficient has been taken as the point of reattachemnt. The current density in the middle section of the reactor is approximately constant. This may be due to the agitational effects of the fluidized bed. The current density increases again in the exit section. This is caused by the turbulence generated by the sudden decrease in flow channel area at the exit.

4.4.1 Variation of the current distribution with different electrolyte flowrates

From the experimental data it has been observed that the current density increases with the increase of electrolyte flow rates. With the increase of flow rates, turbulence increases and as a result the current density as well as the mass transfer rates increases.

4.4.2 Variation of the current distribution with different initial bed height

Variation of the current distribution along the electrode length have been observed for different initial bed height. The initial bed heights were 8.0 cm, 12.0 cm and 16.0 cm. It has been seen that there is slight increase in current density with the increase of initial bed height. The fluctuation of current den-

sity along the electrode length decreases with increase of initial bed height, because uniform agitation can be obtained with the increase in bed height. Hence the fluctuation in the current density as well as mass transfer rate decreased along the cathode length.

4.4.3 Variation of the current distribution with different particle size.

Figures 4.4, 4.5 and 4.6 show the variation of the current distribution with different particle sizes. From the figures, it can be observed that the current density is lowest for smallest particle size (3.0 mm) and for particles sizes of 6.0 mm and 4.5 mm the current density is almost same, but is slightly higher for 4.5 mm particle size. With the increase of particle size, the agitation caused by the particle movement in the cell become more vigorous and hence current density as well as mass transfer rate increases. Further increase in particle size, the particles become heavier and the agitation to the electrode decreases and hence current density as well as mass transfer rate decreases. Also with 6.0 mm particle size, vigorous bubbling ocurs in the cell and pockets of liquids passes through the cell without proper mixing and this may contribute to the decrease of the current densities.

4.5 Variation of Mass Transfer Co-efficient Along the Electrode Length

In Fig. 4.7, cumulative average mass transfer co-efficient (K_{cav}) has been plotted against L/D_e at different flowrate in

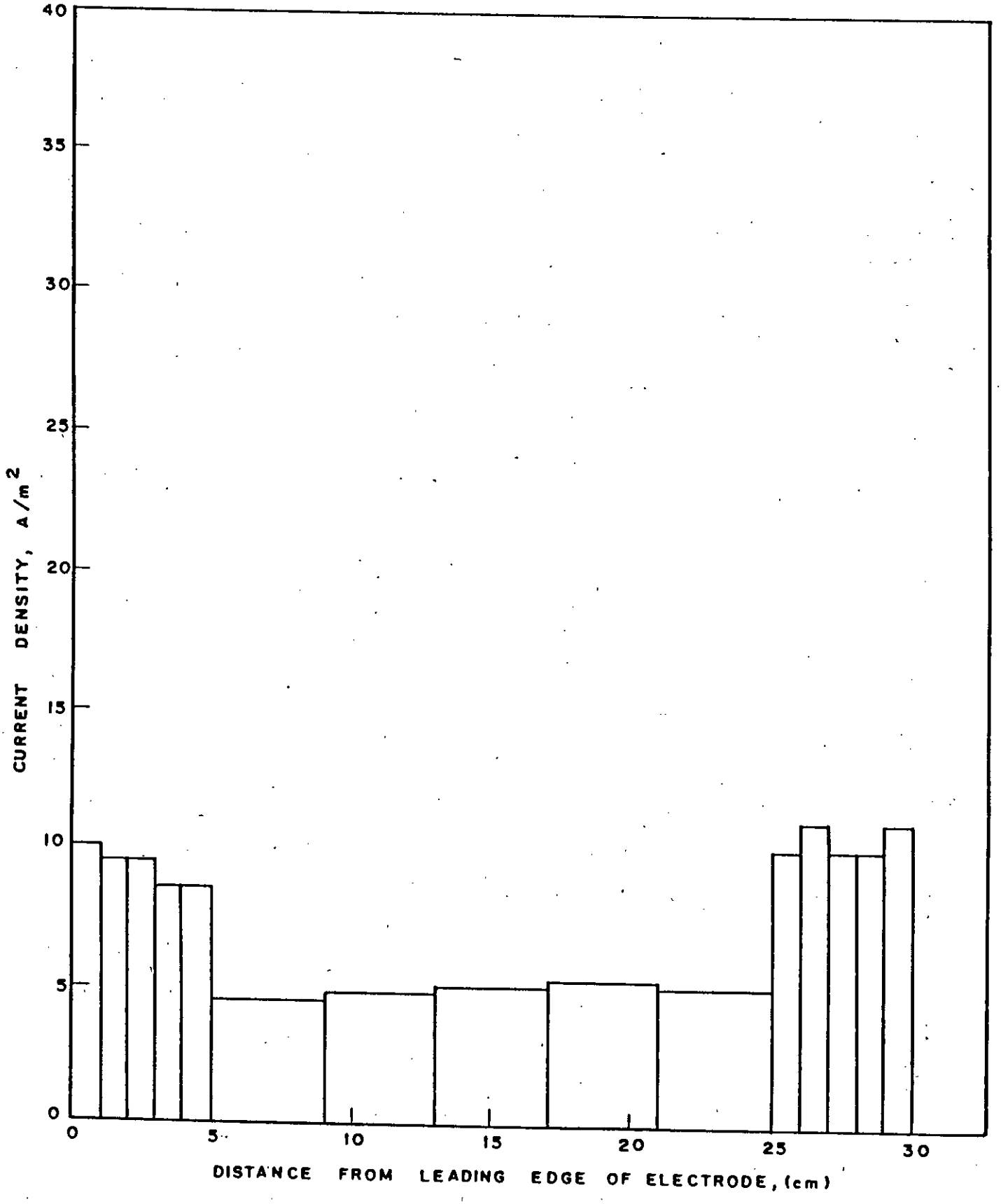

FIG. 4.4 CURRENT DENSITY AT A FLOW RATE OF 7.0 lit/min
PARTICLE SIZE = 3.0 mm
INITIAL BED HEIGHT = 12 cm

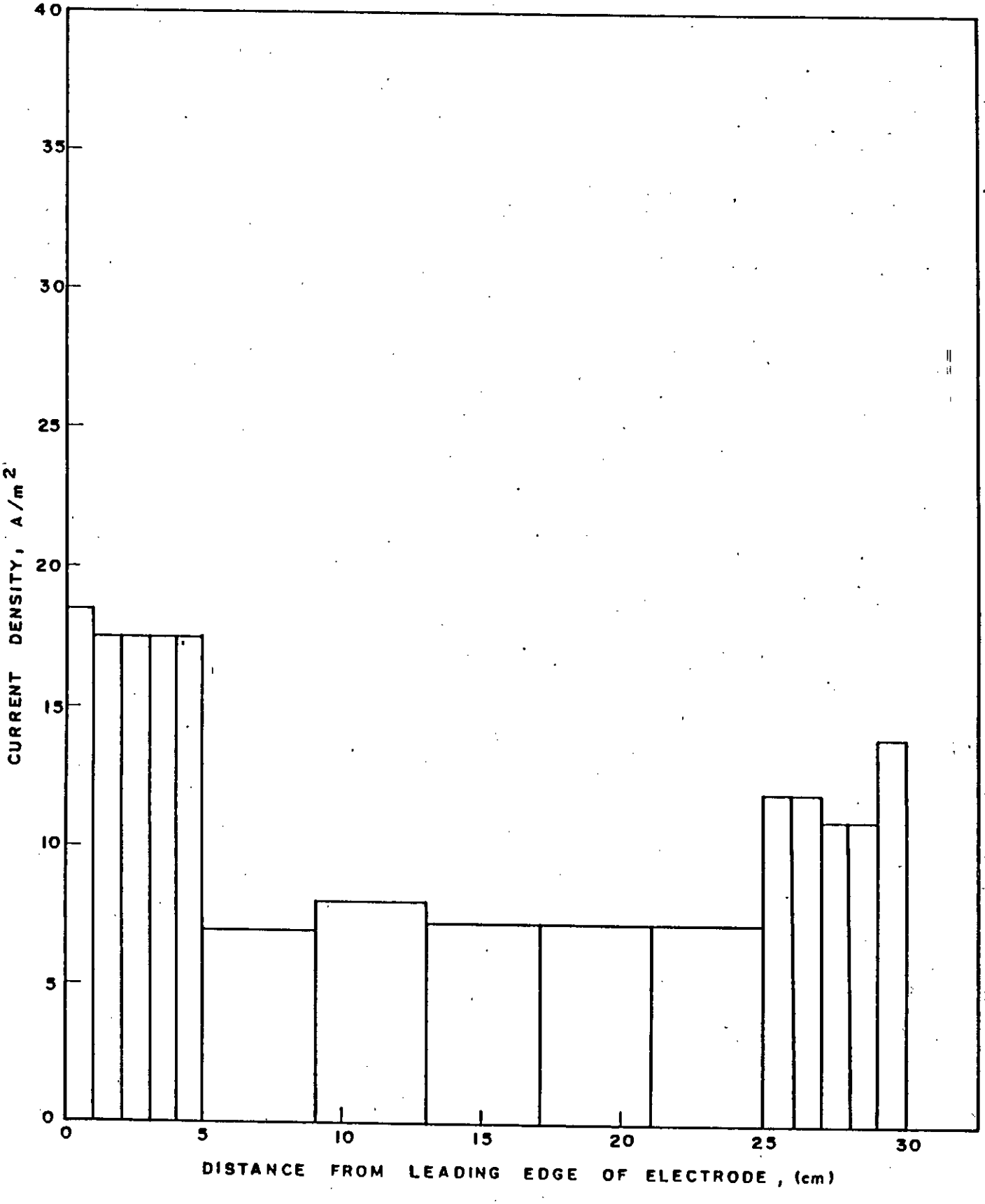

FIG. 4.5 CURRENT DENSITY AT A FLOW RATE OF 7.0 lit/min

PARTICLE SIZE = 4.5 mm
INITIAL BED HEIGHT = 12 cm

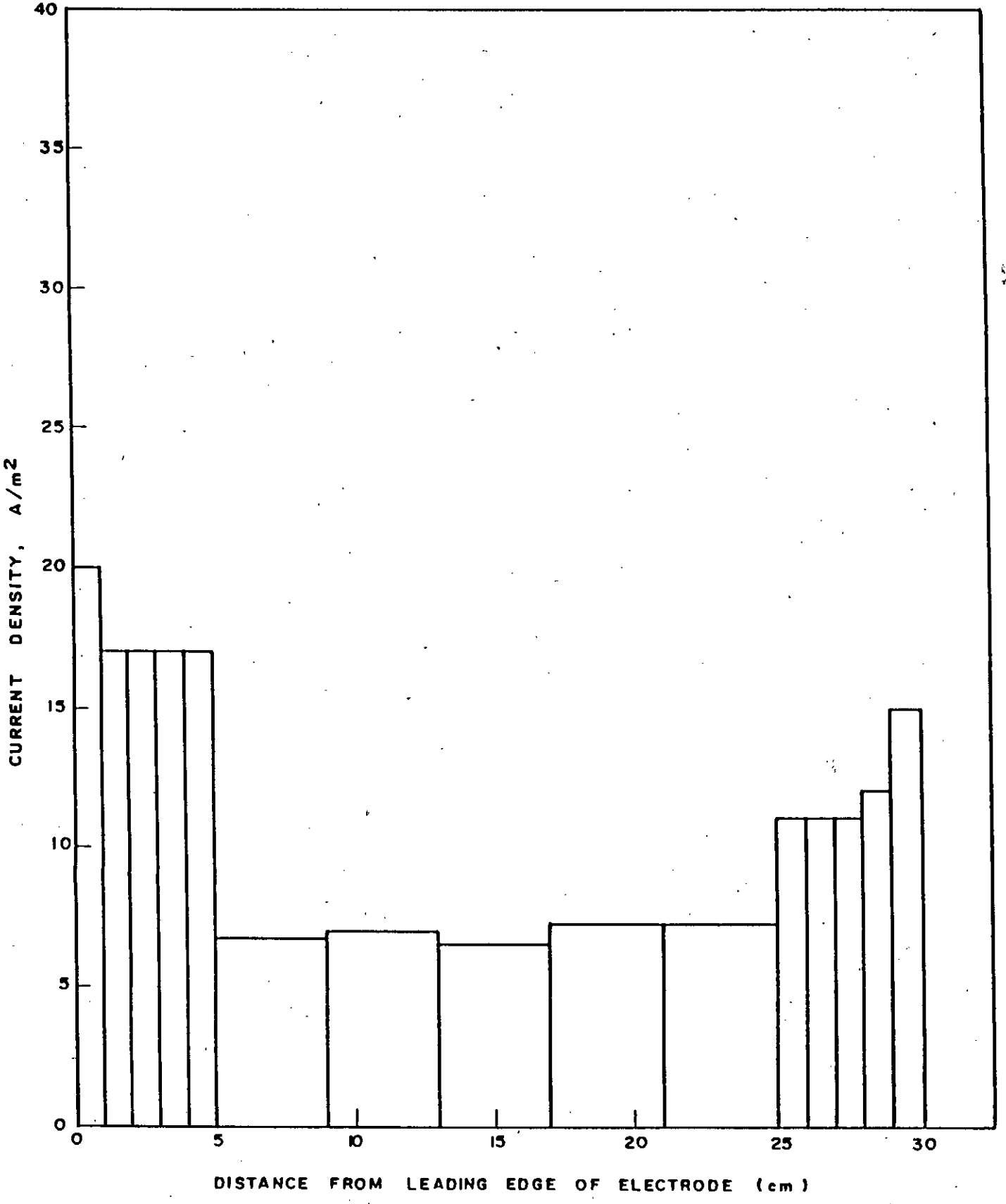

FIG. 4.6 CURRENT DENSITY AT A FLOW RATE OF 7.0 lit/min.
PARTICLE SIZE = 6.0 mm
INITIAL BED HEIGHT = 12.0 cm

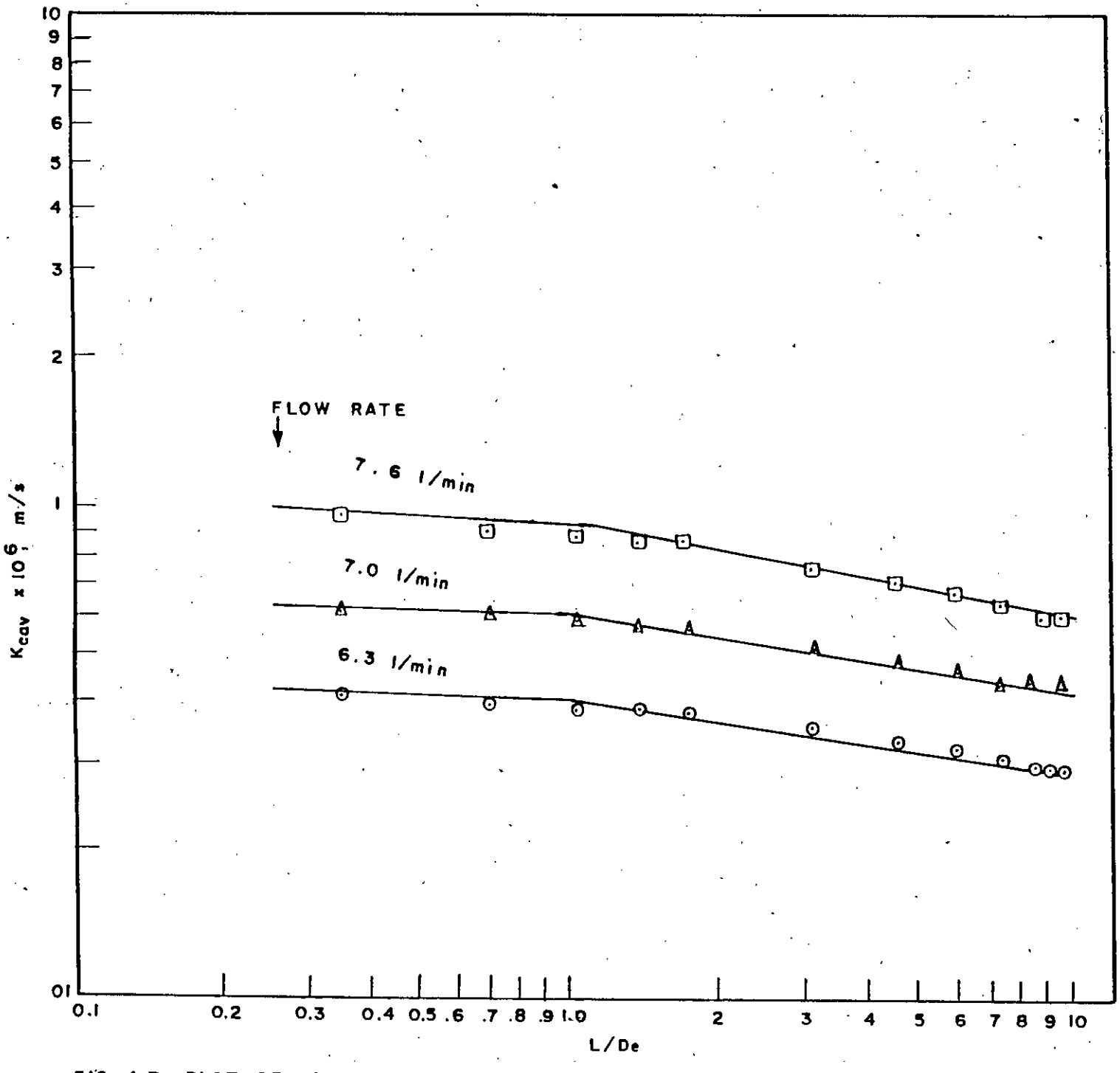

FIG. 4.7 PLOT OF CUMULATIVE AVERAGE MASS TRANSFER COEFFICIENT, K_{cav} vs. L/De
PARTICLE SIZE = 4.5mm
INITIAL BED HEIGHT = 12.0 cm

logarithmic scale. Although it has been shown by histograms in the previous sections that current densities and hence mass transfer co-efficients remain almost constatant in the middle regions of the cell, but current density varies at the inlet and exit sections. This means that rate of deposition at middle section are uniform and due to sudden expansion at the inlet and contraction at the exit there is entrance and exit effect. If a continuous cathode is used, mass transfer along the cathode length will be influenced by the inlet and the exit effects.

Figure 4.7 shows that the cumulative average mass transfer coefficient is related to $L/D_e \leqslant 10.0$ by the equation of the form

$$K_{cav} \propto (L/D_e)^{-0.19} \qquad (4.1)$$

The above findings can be compared with the correlation for rectangular duct obtained by Pickett and Ong [19] upto $L/D_e \leqslant 12.5$ as

$$K_{cav} \propto (L/D_e)^{-0.2} \qquad (4.2)$$

The exponent on the L/D_e term was obtained by Van Shaw et al. [29] as -0.3 for the turbulent flow. Ali M.S. [1] found the value of the exponent in the range of -0.33 to -.16. The lower value of the exponent in the present study is probably due to fluidization which imparts increased agitation and thereby ensures better mixing. Up to $L/D_e = 1$ the variation of mass transfer coefficient is less due to entrance effects.

4.6 Variation of mass transfer coefficients with bed voidage

Figure 4.8 shows the variation of the mass transfer co-efficient with bed voidages for different particle sizes. For all the three particle sizes, it is observed that the maximum values of mass transfer coefficient occurs in the range of $\varepsilon = 0.7 \sim 0.8$. Walker and Wragg [31] studied mass transfer rate with much smaller glass particles (.274~.548 mm) and their data exibited a maximum value of mass transfer coefficient at $\varepsilon = 0.7 \sim 0.75$. The maximum value of mass transfer coefficient in the voidage range of 0.7 to 0.81 occur because the kinetic energy imparted by the particles are maximum in the above voidage range. Maximum kinetic energy imparted by the particles to the electrode and maximum mass transfer rate are closely related [5].

From figure 4.8 it can be observed that maximum value of K for particle size of 6.0 mm occurs at $\varepsilon = 0.74$ and that for particle sizes of 4.5 mm and 3.0 mm occur at $\varepsilon = 0.80$ and $\varepsilon = 0.81$ respectively.

The value of voidage at which the maximum mass transfer occurs decreases with the increase in particle size. This was also observed by Smith and King [27] from their experimental resuts. They also observed that for larger glass particles (above 2.0 mm) the maximum coefficients are not as well defined as for the smaller particles.

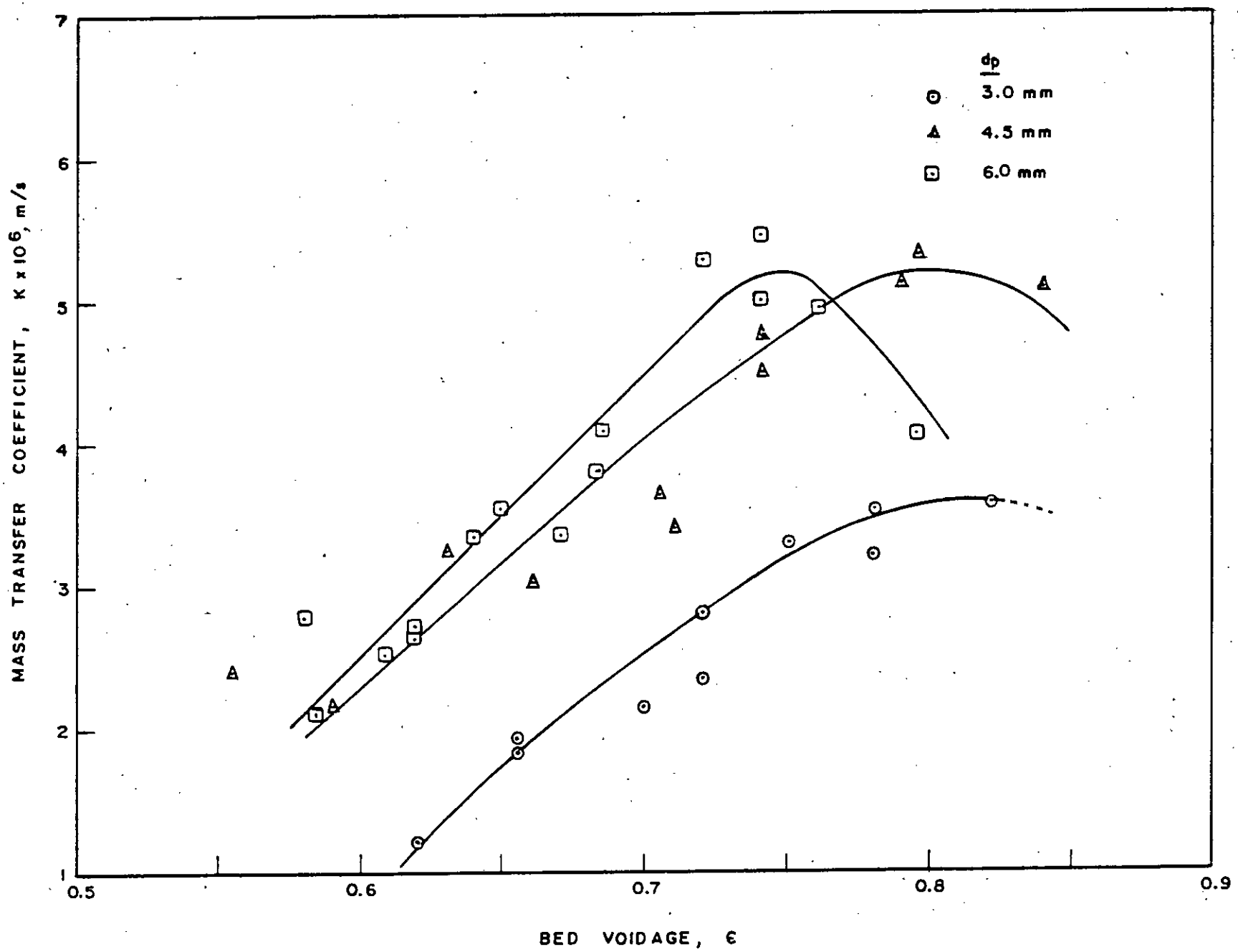

FIG. 4.8 PLOT OF MASS TRANSFER COEFFICIENT AGAINST FLUIDIZED BED VOIDAGE.

4.7 Variation of mass transfer coefficients with velocity

Figure 4.9 shows the variation of mass transfer coefficient with superficial cell velocity for different particle sizes. From the figures it can be observed that the maximum mass transfer coefficient occurs in the range of U = 13.5 ~ 15.5 cm/s. For 6.0 mm particle size, the maximum valve of K ocurs at U = 15.5 cm/s and for 4.5 mm and 3.0 mm particle sizes the maximum value of K occur at U = 14 cm/s and 13.5 cm/sec respectively. The velocity at which the maximum value of mass transfer occurs, increases with the increase in particle size. For the same amount of agitation larger particles require higher superficial velocity. Further increase in velocities, the fluidizing particles become so dispersed that the fluidizing effect start to disappear and the two effects super–impose each other. As a result mass transfer coefficient decreases.

Walker and Wragg [31] studied this aspect of the fluidized bed electrochemical reactor and they found the maximum value of K at a superficial velocity of U = 1~3 cm/s for particle sizes of .275 to .548 mm. F. Coeuret and Le Goff [9] also found maximum value of K for the superficial velocity of U = 4 ~ 8 cm/s for the particle sizes of 0.6 ~ 2.0 mm.

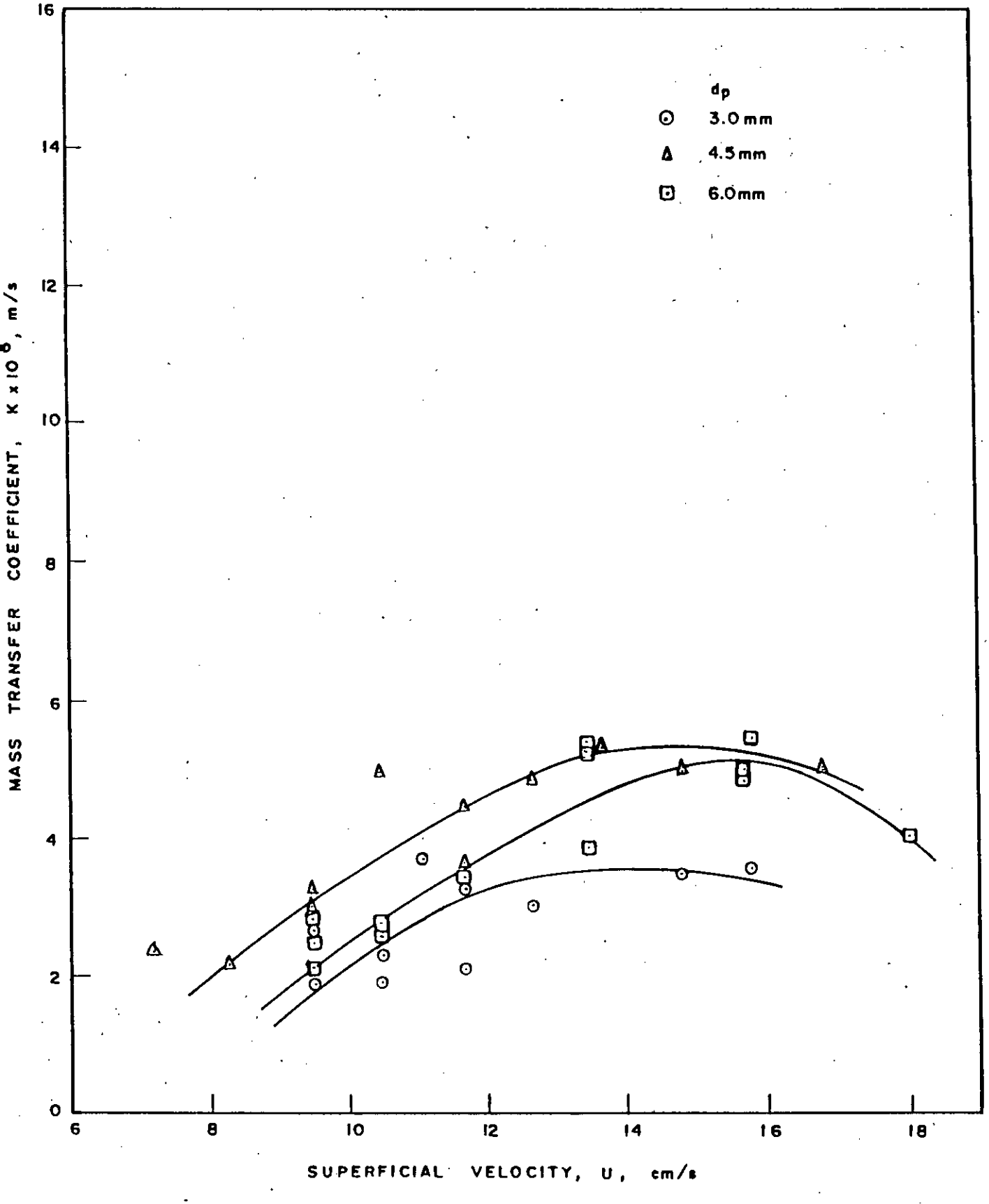

FIG. 4.9 PLOT OF MASS TRANSFER COEFFICIENT AGAINST SUPERFICIAL VELOCITY.

TABLE 4.1

Comparison of Maximum Mass Transfer Velocity and Particle Sizes

Author(s)	Maximum mass transfer velocity U cm/s	Particle size (mm)
Walker and Wragg [31]	1 ~ 3	0.275 ~ 0.548
Coeuret and Goff [9]	4 ~ 8	0.6 ~ 2.0
Present Study	13.5 ~ 15.5	3.0 ~ 6.0

4.8 Effect of particle size on the mass transfer coefficient

Figure 4.9 also shows the effect of particle size on the mass transfer coefficient. Mass transfer coefficient is smallest for the 3.0 mm particle size and it is almost same for the 4.5 mm and 6.0 mm particle sizes, although mass transfer coefficient is slightly higher in the case of 4.5 mm particle than that of 6.0 mm particles. The increase in the mass transfer coefficient with the increase of particle sizes may be due to the bubble formation in the fluidized bed for the larger particles. In the present study three different sizes of particles (3.0 mm, 4.5 mm and 6.0 mm) are used and Froude number, Fr ($= \frac{U^2_{mf}}{gd}$), calculated for the three particle sizes are 0.33, 1.1 and 2.66 repectively. As mentioned earlier, Wilhelm and Kwauk [32] suggested

the Froude number as a criterion for the bubble formation. According to them, for 4.5 mm and 6.0 mm particles, bubbles should be observed. In fact bubbles are observed for these two particles sizes. With 6.0 mm particles vigorous bubbles are observed with pockets of liquids passing through the bed without proper mixing. Although 4.5 mm particles fall in the transition regions ($Fr \gtrsim 1$), considerable amount of bubbles are also observed for this particle size. No bubbles are visually observed for the 3.0 mm particles. With the formation of bubbles agitation in the cell increases vigerously and hence the mass transfer coefficient increases.

4.9 Mass Transfer Correlations

Mass transfer correlations are obtained for each particle size. In the present study Reynolds number is varied from 675 to 5933 and Schmidt number (Sc) is varied from 1200 to 1700. Correlations are obtained for each particle size using the data of that particle. The form of the correlation is assumed as $St_I (Sc)^c = a\ Re_I^b$. No attempt has been made to find the exponent of the Schmidt number which is an established fact and whose value is 2/3. The correlations have been obtained by regressional analysis of the data by computer which is equivalent of plotting $St_I (Sc)^{2/3}$ against Re_I in a log-log graph paper.

Plots are shown in Figure 4.10, 4.11 and 4.12. The correlations obtained are:

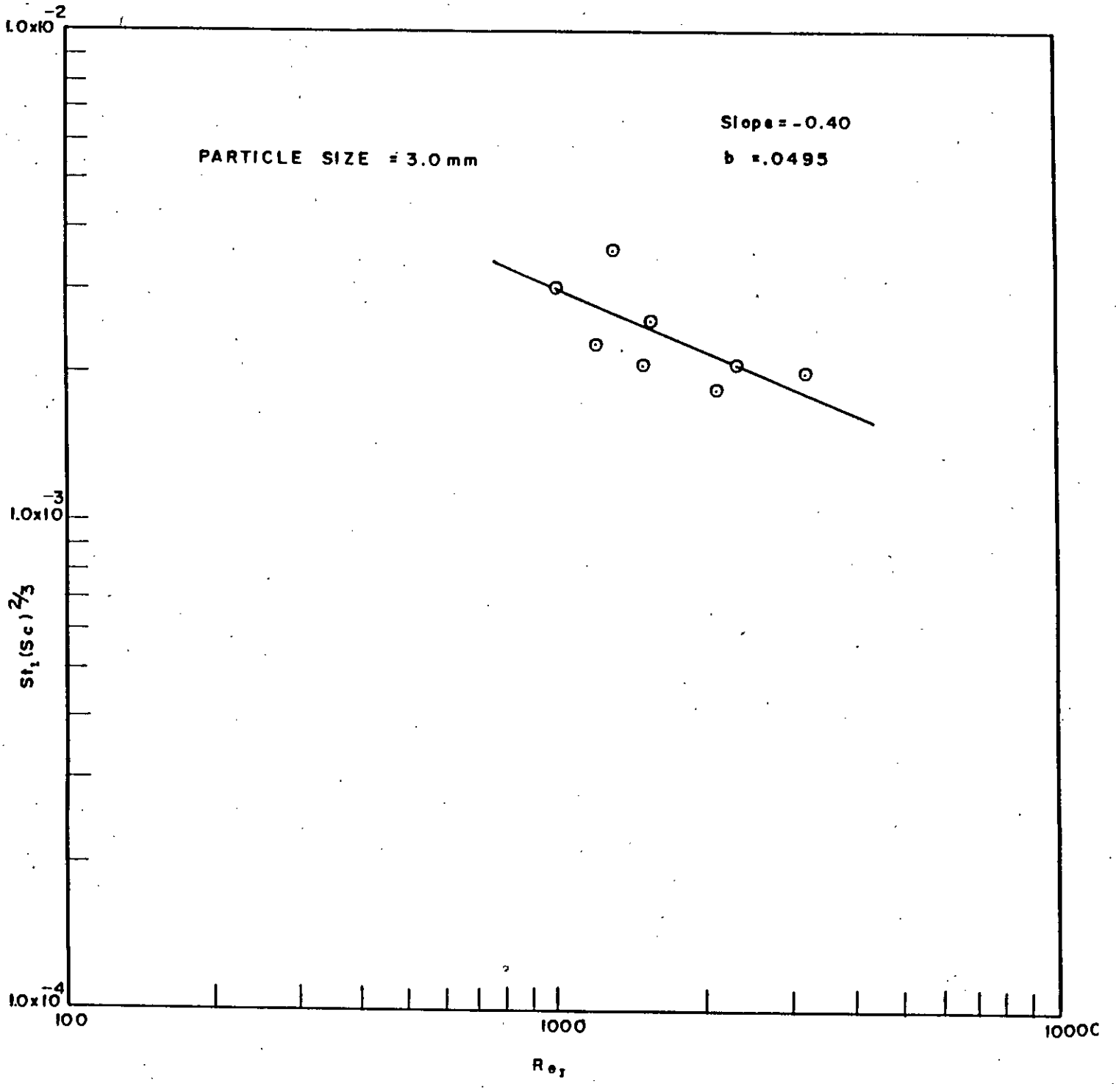

FIG. 4.10 PLOT OF $St_1 (Sc)^{2/3}$ AGAINST Re_1

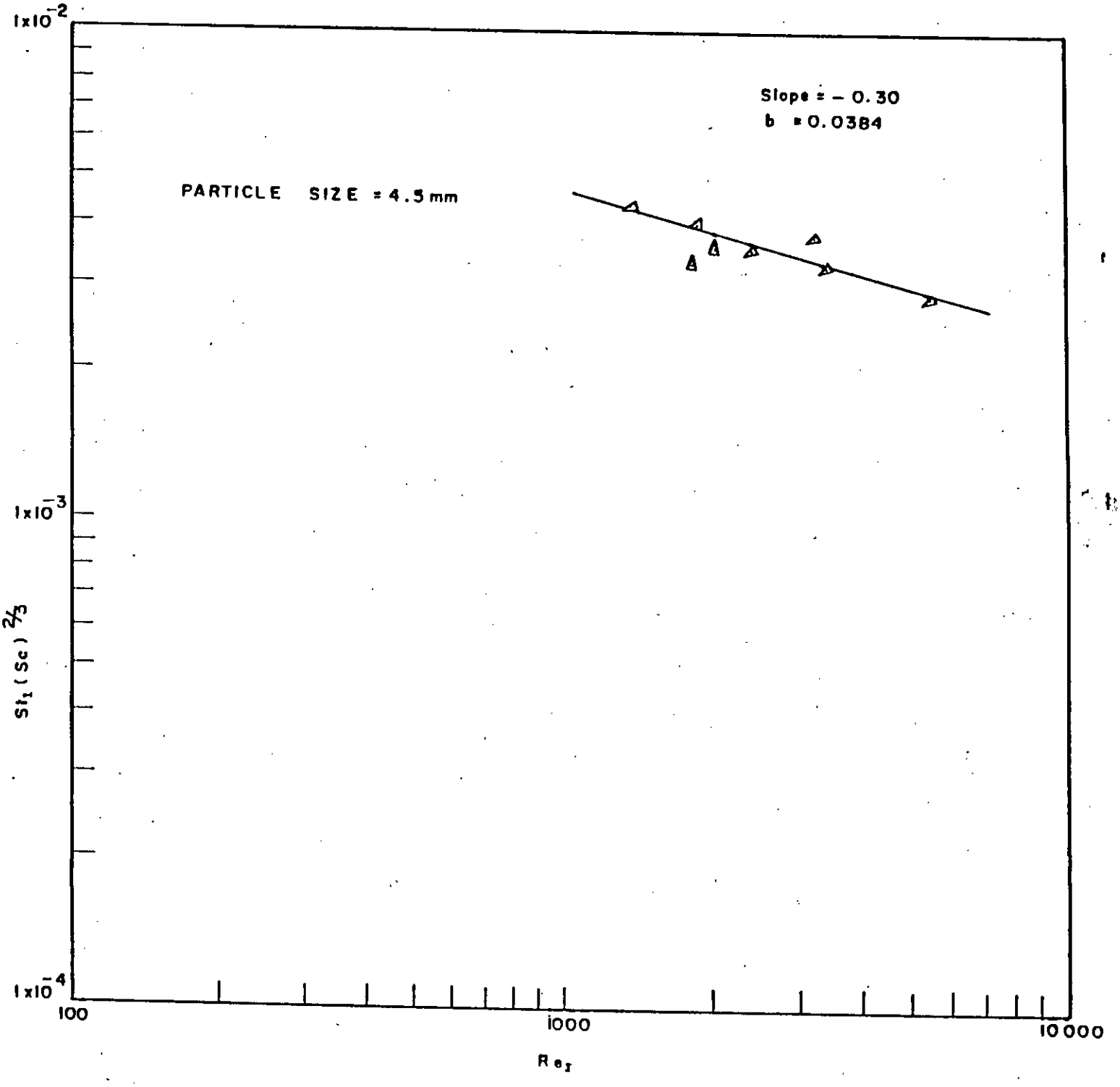

FIG. 4.11 PLOT OF $St_1 (Sc)^{2/3}$ AGAINST Re_1

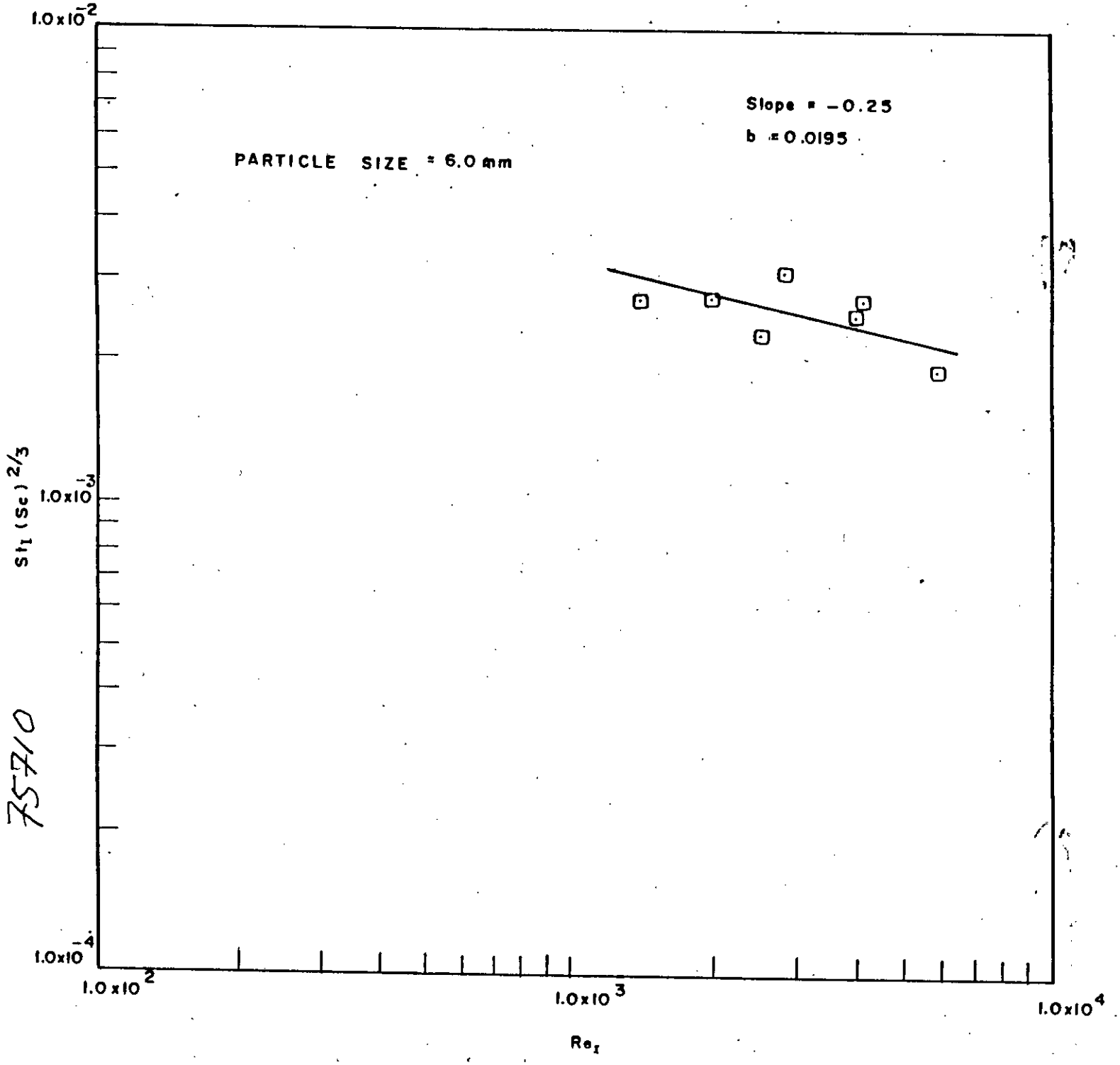

FIG. 4.12 PLOT OF $St_I (Sc)^{2/3}$ AGAINST Re_I

$$St_I (Sc)^{2/3} = 0.0494\ Re_I^{-0.40} \qquad (4.3)$$

for 3.0 mm particles

$$St_I (Sc)^{2/3} = 0.0383\ Re^{-0.30} \qquad (4.4)$$

for 4.5 mm particles

$$St_I (Sc)^{2/3} = 0.0195\ Re_I^{-0.25} \qquad (4.5)$$

for 6.0 mm particles

It is observed from the correlations that the exponent on Reynolds number decreases with the increase of the particle size. It has been shown earlier that both 4.5 mm and 6.0 mm particles fall in the range of aggregate fluidization where bubbles form in the bed. Experimentally bubbles have been observed for these two particle sizes and the intensity of bubbles has been observed to be higher for the 6.0 mm particles than that of 4.5 mm particles. No bubbles have been visually observed for 3.0 mm particles. In the presence of bubbles in the fluidizing bed, the influence of the flow rate and hence Reynolds number on the mass transfer coefficient becomes more prominent. It happens because once bubbling starts in the cell, agitation in the cell becomes very high and it increases with the increase of flow rates and since agitation in the cell and mass transfer rate are closely related, the mass transfer rate also increases. This might be the possible reason for the decrease of the exponent of Reynolds number with the increase of the particle sizes of the bed.

4.10 Comparision with previous studies

A number of workers have investigated the mass transfer behavior in fluidized systems. Their results together with the results of the present study have been summerised in Table 4.2.

TABLE 4.2

Comparison of mass transfer correlations according to

$$St_I \, Sc^{2/3} = a \, Re_I^{-b}$$

Author(s)	a	b	D_e/d_p	System	Re_I	Sc	Particle size((mm)
Smith and King [27]	0.32	0.38	41-105	Cylindrical wall mass transfer	0.7-1067	580-2100	-
	0.54	0.44	17-27		34-2334	-	-
Jattrand and Grunchare[14]	0.45	0.375	93-36	Planar test electrode in cylindrical bed	6-200	1250	0.220-0.780
Jagannadharaju and Venkata Rao [13]	0.43	0.38	8-27	Inner anode of annular bed	200-3800	1300	1.54-6.00
Coeuret et al. [9]	1.20	0.52	93-290	Various cylindrical probes	6-200	1250	0.35-1.07
Carbin and Gabe [6]	1.24	0.57	80-150	Cylindrical test electrode in cylindrical bed	0.1-70	787-1777	0.185-0.355
Walker and Wragg[31]	0.138	0.39	43	Rectangular Channel wall Mass Transfer	0.936-67	2675	0.274-0.548
Present study	0.049	0.40	9.5	Rectangular channel wall mass transfer	675-3238	1150-1710	3.0
	0.038	0.30	6.3		1473-5300	1300-1760	4.5
	0.0195	0.25	4.8		2015-5934	1100-1760	6.0

From table 4.2 it can be seen that the exponent of Reynodlds number obtained in the present study is smaller (for 4.5 mm and 6.0 mm) than any other previous works. Reynolds number range of the present study is also much higher than the other works. Particle sizes of the present study is also different. Only comparable sizes of particles were used by Jagonnadharaju and Venkata Rao [13]. But the effect of particle size on the exponent of Reynolds number is not known. Moreover, they used annular bed which is completely different from the system of the present study. The lower value of the exponent of Reynolds number signifies the increase of the effect of Reynolds number on the mass transfer coefficient. The sizes of the glass particles (4.5 mm and 6.0 mm) which have been used in the present study fall in the bubble formation region. It has been found [23] that glass particles greater than 2.0 mm size form bubbles in the liquid fluidized beds. The agitation in the bed increases significantly with the formation of bubbles and with the increase of flow rate it increases further. Since the intensity of bubbles increases with the increase of particle sizes, influence of flow rate and hence Reynolds number also increases accordingly.

The value of mass transfer coefficient at the electrode with fluidized bed has been compared with that of non fluidized bed studied by Chowdhury [8]. It has been found that mass transfer coefficient has increased by 25% for 4.5 mm and 6.0 mm particle size for the same flow conditions.

CHAPTER 5

CONCLUSIONS AND SUGGESTIONS FOR FUTURE WORK

5.1 Conclusions

1. In fluidized bed electrochemical reactors, mass transfer coefficients increases with the increase of particle size when the particle size is less than 4.5 mm.
2. Mass transfer coefficient undergoes a maximum value in the voidage range of $\varepsilon = 0.7 \sim 0.8$.
3. Mass transfer coefficient undergoes a maximum values for a certain superficial velocity of the electrolyte which is a function of particle size and cell geometry.
4. In fluidized bed reactors, mass transfer rate becomes more uniform along the electrode length.
5. In mass transfer correlations, the value of the exponent of Reynolds number decreases with the increase of particle sizes of the bed materials.

5.2 Suggestions for future works

1. More experimental investigations should be carried out with different sizes of particles, especially with smaller (< 3.0 mm) particles.
2. Mass transfer behavior with conducting bed materials can be studied.
3. An alternative way of interpreting the results may be by assuming mass transfer occuring between flat plate and liquid and considering fluidization as a means to increase the agitation only. This view point may be explored in future.

NOMENCLATURE

C_B	Bulk concentration, gm mole/cm³
C_s	Surface concentration, gm mole/cm³
D	Diffusivity of the ions, cm²/sec.
D_e	Equivalent diameter
d_p	Particle diameter.
F	One Faraday (96500 Coulombs).
Fr_{mf}	Froude number at minimum fluidization velocity.
$\triangle G$	Free energy change.
$\triangle G°$	Standard free energy change.
I	Amount of current passed, Ampere.
i	Current density, Amp/m².
i_L	Limiting current density, Amp./m².
i_o	Exchange current density, Amp./m².
J_D	Mass transfer j-factor.
K	Overall mass transfer coefficient, m/sec.
K_{lav}	Local everage mass transfer coefficient.
K_{cav}	Cumulitive average mass transfer coefficient. m/sec.

L	Length of the electrode.
n_a	Activation overpotential, volts.
n_c	Concentration overpotential, volts.
Pr	Prandtl number.
Re	Reynolds number.
Re_I	Modified Reynolds number, $\frac{d_p U \rho}{\mu(1-\varepsilon)}$
Sc	Schmidt Number.
Sh	Sherwood number.
St	Stanton number, K/U.
St_I	Modified Stanton number, $K \varepsilon / U$.
T	Absolute temperature, °K.
t	Time of passage of current, sec.
U	Superficial Electrolyte Velocity, cm/sec.
U_{mf}	Minimum fluidization velocity, cm/sec.
V	Voltage applied across the cell volts
V_{min}	Minimum electrolysing voltage
z	Number of electrons involved in the reaction.

Greek letters:

ε	Bed voidage.
μ	Viscosity of the solution, cp.
ν	Kinamatic viscosity, cm^2/sec.
δ_n	Thickness of the diffusion layer, cm.

REFERENCES

1. Ali, M.S., Ph.D. Thesis, University of Manchester, 1982.

2. Beek W.J., "Fluidization" (Edited by Davidson and Harrison), P.431, Academic Press, London (1971).

3. Berger F.P. and Hau K.F., Int. J. Heat and Mass Transfer, 20, 1185(1977).

4. Bird R.B., Stewart W.E., Lightfoot E.N. and Chapman T. W., A.I.Ch.E., Continuing Education Services, 4, 42, (1969).

5. Bordet J., Borlai O., Vergnes F. and Goff P.Le, Instn. Chem. Engnns Symp. Series 30, 165, (1958).

6. Carbin D.C and Gabe D.R., Electrochemica Acta, 19, 64 (1974).

7. Chilton T.H. and Colburn A.P., Ind. Engg. Chem., 26, 1183, (1934).

8. Chowdhury M.A., M.Sc. Thesis, Bangladesh University of Engg. and Tech. (BUET), 1982.

9. Coeuret F. and Goff P.Le, Electrochemica Acta, 21, 195 (1976).

10. Davidson J.F. and Harrison D., "Fluidized Particles" Cambridge University Press (1963).

11. Hubbard D.W. and Lightfoot F.N., I. and C.E. Fundementals 5, 370, (1966).

12. Jabbar A. M. and Hoque M.M., "Practical Chemistry", 2nd Edition, Student ways, Bangladesh, 1972.

13. Jagannadharaju and Rao C.V., Ind. J. of Technol., 3, 201 (1965).

14. Jottrand P.R. and Grunchard F., Symp. Interaction between Fluids and Particles, Instn. Chem. Engns (1962).

15. Krall K.M. and Sparrow E.M., J. Heat and Mass Transfer, 14, 781 (1971).

16. Krishna M.S., Jagannadha Raju G.J.V. and Rao C.V. Ind. J. Technol., 4, 8, (1966).

17. Leveque J., J. Ann. Mines, 13, 201, (1928).

18. Pickett, D.J., "Electrochemical Reactor Design", 2nd Edition, Elsenier Scientific Publishing Company, 1979.

19. Pickett D.J. and Ong K.L., Electrochimica Acta, 19, 875, (1974).

20. Pickett D.J. and Stainmore B.P., J. Applied Electrochemistry, 2, 151 (1972).

21. Rahman K. and Streat M., Chemical Engg. Sci., 36, 293 (1981).

22. Rao M.V.R. and Rao C.V., Ind. J. Technol., 8, 44, (1970).

23. Richardson J.F., "Fluidization" (Edited by Davidson and Harrison), P.26, Academic Press, London (1971).

24. Richardson J.F. and Zaki W.N., Trans. Instn. Chem. Engrs, 32, 35, (1954).

25. Runchal A.K., Int. J. Heat and Mass Transfer 12, 781, (1971).

26. Stanmore, B.R., M.Sc. Thesis, University of Manchester, (1970).

27. Smith J.M. and King D.H., Can. J. Chem. Engg., 53, 41, (1975).

28. Tobias C.W. and Hickman, J. Phys. Chem. (Leipzig), 229, 145, (1965).

29. Vanshaw P., Reiss L.P. and Hanratty T.J., A.I. Ch.E. J., 9, 132, (1963).

30. Vogel A.I., "A Textbook of Quantitative Inorganic Analysis", 3rd Edition, Longmons, (1961).

31. Walker A.T.S. and Wragg A.A., Electrochimica Acta, 25, 523, (1980).

32. Wilhelm R.H. and Kwauk M., Chem. Engg. Prog., 44, 201(1948).

33. Wilson, C.J., Ph.D. Thesis, University of Manchester, (1974).

34. Wragg A.A., Ph.D. Thesis, University of Manchester, (1965).

APPENDICES

APPENDIX-A

REVIEW OF ELECTROCHEMICAL PRINCIPLES

A.1 Introduction

A review has been made of relavant literature together with a study of the theoretical principles governing the electrodeposition of copper in the electrodeposition of copper in the electrochemical reactor. The main aspects that have been considered here are electrode kinetics, mass transfer principles and current distribution in a parallel plate electrochemical reactor.

A.2 Basic Electrochemical Factors

A.2.1 Faraday's Law of Electrochemistry

Faraday's Law of Electrochemistry states that the passage of 96500 coulombs through an electrochemical reactor produces in total one gram - equivalent of products at each electrode.

$$\text{i.e. Mole produced } (n) = It/zF \quad .. \quad (A.1)$$

where,

I is the amount of current passed, Ampere,

t is the time of passage of current, sec.

z is the number of electrons involved in the reaction.

F is the one Faraday (96500 Coulombs).

Very often more than one reaction occurs at an electrode. In the deposition of metal, there is evolution of hydrogen or codeposition of another metal with that of desired metal. To achieve a good product purity without any side reaction, the reactor must be operated in a range of electrode potentials which ensures only the desired reaction to take place.

A.2.2 Minimum Electrolysing Voltage

In an electrochemical reactor, electrical energy is supplied to increases the free energy of the reacting species which changes the free energy defference to a negative value and consequently promotes the reaction. The electrical energy is supplied by applying a certain voltage to the reactor. Minimum electrolysing voltage for a given process can be defined as the applied voltage necessary to keep the system at equilibrium when no current flows. The minimum electrolysing voltage, V_{min}, is related to the free energy change for a cell reaction at a certain temperature and pressure under thermodynamic equilibrium and it can be written as,

$$\Delta G = zF\, V_{min} \quad .. \quad (A.2)$$

where,

ΔG is the free energy change

z is the number of electrons required for either electrode reactions to produce 1 molecule of product.

F is the Faraday Constant

The free energy change for an overall reaction

$$aA + bB \longrightarrow cC + dD$$

can be written as

$$\Delta G = \Delta G^\circ + RT \ln \frac{a_C^c \; a_D^d}{a_A^a \; a_B^b} \qquad (A.3)$$

where,

R is the universal gas constant

T is the absolute temperature

ΔG° is the standard free energy change

a,b,c and d are the stoichiometric coefficients of the reactants and the products

a_A, a_B, a_C, a_D are the activities of the species involved.

If all the constituents are at standard states, the minimum electrolysing voltage will be standard minimum electrolysing voltage and it can be written as:

$$\Delta G^\circ = zF \; V^\circ_{min} \qquad (A.4)$$

where V°_{min} is the standard minimum electrolysing voltage corresponding to unit activity of A,B,C and D.

Combining equations (2.2), (2.3) and (2.4), minimum voltage can be found as,

$$zF \; V_{min} = zF \; V^\circ_{min} + RT \ln \frac{a_C^c \; a_D^d}{a_A^a \; a_B^b} \qquad (A.5a)$$

$$V_{min} = V^\circ_{min} + \frac{RT}{zF} \ln \frac{a_C^c \; a_D^d}{a_A^a \; a_B^b} \qquad (A.5)$$

This leads to the Nernst equation:

$$V_{min} = V^{\circ}_{min} - \frac{RT}{zF} \ln \left[\frac{\text{Product of the activities of reduced species}}{\text{Product of the activities of oxidized species}}\right] \quad \ldots\ldots \quad (A.6)$$

The minimum electrolysing voltage of an electrochemical cell is the difference between the equilibrium or reversible anode (V_a) and cathode (V_c) potentials which can be expressed as:

$$V_{min} = V_a - V_c \quad (A.7)$$

The equilibrium anode and cathode potentials are those electrode potentials which are just sufficient to allow the cathodic deposition and anodic dessolution reactions to proceed at an electrode surface at equal rates so that no net change occurs.

A.2.3 Reactions in Copper Deposition Systems

In the electrorefining processes, the copper deposition takes place in an electrochemical reactor which consists of impure copper anode and a thin sheet of pure copper cathode immersed in an acidified copper sulphate solution. At the soluble anode, metal is oxidized and dissolved as copper ions as follows:

$$Cu \longrightarrow Cu^{2+} + .2e \qquad V^{\circ}_a = 0.34V \quad (A.8)$$

where V°_a is the standard equilibrium potential for the reaction at the anode when all the species or ions present are at unit activity. As previously stated, the equilibrium potential depends on the activities of the species present in the system, as well as the temperature and pressure, but for a rough estimation the standard equilibrium potentials will be used.

At the cathode the reduction of ion takes place to deposit copper,

$$Cu^{2+} + 2e \longrightarrow Cu \qquad V^\circ_C = 0.34 \text{ V} \qquad (A.9)$$

Thus, the theoretical minimum electrolysing voltage for the overall reaction is (0.34 - 0.34) = 0.0 volts.

At high current densities and a sufficiently more negative cathode potential, a secondary reaction occurs, namely hydrogen evolution, as

$$2H^+ + 2e \longrightarrow H_2 \qquad V^\circ_C = 0.0 \text{ V} \qquad (A.10)$$

The cathode potential should be controlled so that the hydrogen evolution reaction does not occur because it will reduce the current efficiency of copper deposition in the reactor.

A.3 Practical Voltage Requirements

A.3.1 Operating Voltage

In actual operation of an electrochemical reactor, the cell operating voltage is larger than the equilibrium value given by the Nernst equation and can be expressed by considering only one reaction at each electrode as

$$V = V_a - V_c + \Sigma n_a + \Sigma n_c + V_s \qquad (A.11)$$

where,

V is the cell operating voltage

Σn_a is the combined activation overpotential for both processes

Σn_c is the combined concentration overpotential for both processes.

V_s is the potential drop across the electrolyte.

An overpotential can be defined as the extra energy necessary to reduce the energy barrier of the rate determining step to a value that enables the electrode reaction to proceed at the desired rate.

A.3.2 Activation Overpotential

Activation overpotential is basically an electrokinetic phenomena and associated with the charge transfer mechanism. It

is caused by the irreversibility of the electrode process. The irreversibility of an electrode process increases as the voltage applied to the cell is increased, altering the potential of each electrode.

A theoretical expression can be obtained for the activation overpotential by considering the kinetics of a reversible electrode reaction

$$O + 2e \rightleftharpoons R \qquad \ldots \qquad (A.12)$$

The current density of deposition, i, is related to the overpotential by Arrhenius type rate constant/activation energy relationship. Thus an equation for the cathodic current density can be expressed (for small concentration changes between the surface and bulk concentration) as:

$$i = i_o[\{\exp\{\frac{-\alpha zF\ n_a}{RT}\} - \exp\{\frac{(1-\alpha)zF\ n_a}{RT}\}\}] \qquad (A.13)$$

where,

- i is cathodic current density
- i_o is the exchange current density
- α is the fraction of overpotential assisting the discharge process.

For appereciable overpotential, when n_a is greater than 0.05 volts, the second term in equation (A.13) which represents

the reaction rate in the reverse direction can be ignored.

Consequently,

$$i = i_o \exp \{ \frac{- \alpha z F \, n_a}{RT} \} \qquad \text{(A.14)}$$

Rearranging in a more convenient form we have,

$$n_a = \frac{RT}{\alpha z F} \ln i_o - \frac{RT}{\alpha z F} \ln i \qquad \text{(A.15a)}$$

or, $n_a = a + b \log i \quad \ldots \qquad \text{(A.15)}$

where $a = \frac{RT}{\alpha z F} \ln i_o$ and $b = -2.303 \frac{RT}{\alpha z F}$

Equation (A.15) is the "Tafel Equation" which relates overpotential to the net anodic or cathodic current. Tafel equation is most widely used especially for engineering purposes since it has a practical form and it satisfactorily represents the conditions in industrial electrochemical reactors.

A.3.3 Concentration Overpotential

As metal deposition proceeds in the electrochemical reactor, the concentration of the reacting species or ions close to the electrode surface decreases in the absence of adequate supply of ions from the bulk of the solution. This is associated with a rise in electrode potential as given by the Nernst equation (A.6)

and is known as concentration overpotential. The movement of ions is controlled by three processes:

(a) Molecular deffusion

(b) Reactant transported by macroscopic hydrodynamic flow known as "convection".

(c) Movement of ions under the influence of an electric field called "ionic migration".

The effect of ionic migration is usually very small in practical electrochemical reactors, including the copper deposition systems. As the solutions contain excess of an indefferent electrolyte normally acid, the hydrogen ion being the main species that carry the electricity through the solution rather than the Cu^{+2} ions. Convection effected by stirring or flow helps to keep a uniform concentration of the electrolyte in the cell as well as near to the electrode wall.

A relationship between current density and the mass transfer coefficient can be written as

$$\frac{i}{zF} = K(C_B - C_s) \quad .. \quad (A.16)$$

where,

K is the mass transfer coefficient

C_B is the bulk concentration of solution

C_s is the surface concentration.

This expression is an alternative approach to that of Nernst

and Merrium's diffusion layer theory for flow systems. The molar flux across the diffusion layer can be expressed by using Fick's law of diffusion as

$$\frac{i}{zF} = \frac{D}{\delta_n} (C_B - C_s) \qquad (A.17)$$

where,

D is the diffusivity of the ions

δ_n is the thickness of the diffusion layer

Considering Nernst equation (A.6) applied to ionic concentration for a cathodic deposition reaction of the form

$$M^{z+} + ze \longrightarrow M \qquad (A.18)$$

The value of concentration overpotential is given by

$$n_c = V_c^* - V_c = \frac{RT}{zF} \ln \frac{C_s}{C_B} \qquad (A.19)$$

where,

V_c^* is the cathode potential during operation

V_c is the equilibrium cathode potential

C_s, C_B is the surface and bulk concentration of the reacting species.

The simplification made for the derivation of equation (A.19) is based on the consideration of perfectly reversible process and it neglects any kinetic effect. In practice most of the processes are irreversible for the deposition of metal or any other reactions to occur.

A.3.4 Concept of Limiting Current Density

As the current in the electrodeposition of a metal increases, the concentration in the vicinity of the cathode decreases until it becomes so small that a substantially constant current density is reached, giving the largest concentration gradient and the highest diffusion rate. This constant current density is referred to as the limiting current density. The limiting current density may also be defined as the maximum operating current that can be generated by a given electrochemical reaction, at a given reactant concentration, under well established hydrodynamic conditions under steady states.

According to the defination of limiting current, C_s becomes negligibly small so that equation (A.16) becomes

$$\frac{i_L}{zF} = K\, C_B \qquad .. \qquad (A.20)$$

where,

i_L is the limiting current density.

For a real process C_s is not zero and it has a finite value for an electrochemical reaction to occur, otherwise the concentration overpotential will increase to an infinite value. By eliminating K and zF between equations (A.16) and (A.20) the ratio of concentration becomes

$$i/i_L = \frac{C_B - C_s}{C_B} = 1 - C_s/C_B \quad \ldots \quad (A.21a)$$

or,

$$\frac{C_s}{C_B} = 1 - i/i_L \quad \ldots \quad (A.21)$$

Combining equations (A.19) and (A.21) the value of concentration overpotential is given by

$$n_c = \frac{RT}{zF} \ln (1 - i/i_L) \quad \ldots \quad (A.22)$$

The effect of concentration overpotential in an electrochemical reactor can be reduced by increasing the mass transfer rate (i.e., decreasing the thickness of diffusion layer), resulting in an increase in the limiting current. The mass transfer co-efficient depends on the shape and entrance condition of the cell, the electrolyte and the reaction taking place. The limiting current can be increased by increasing the temperature of the electrolyte causing an increase in diffusivities.

Figure A.1 shows a typical polarization curve characterized

by the occurence of a limitting current plateau and this is terminated by the onset of a secondary reaction, usually a gas evalution.

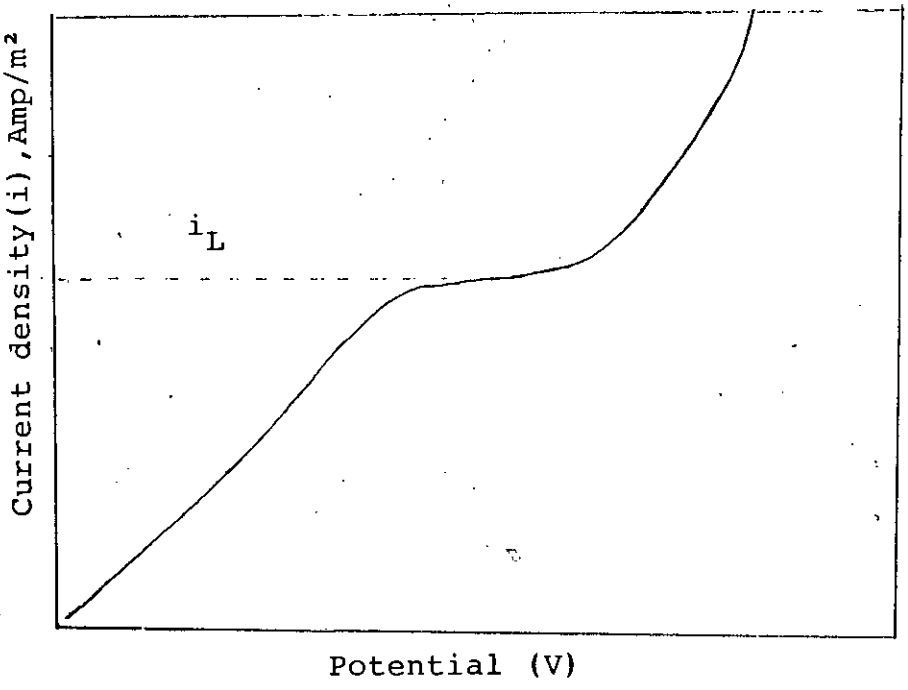

Fig. A.1: Typical polarization curve.

For the systems where secondary reaction affects the operation of the reactor, most of the reactors are operated below the limiting current. Practical operation of electrochemical reactors are carried out well below the limiting current, because the application of increased voltage at this stage does not improve the reaction rate and decreases the current efficiency. Nevertheless, limiting current measurements provide a very convenient technique for mass transfer studies because mass transfer coefficients (K) can be readily and accurately calculated from the experimentally obtained current plateau on a current density - potential plot as shown in Figure A.1.

A.3.5 Potential Drop in Solution

This added energy is caused by a change in solution conductivity and by the formation of poorly conducting films on electrodes. This has also been designated as 'IR' drop. The conductivity of an electrolyte can be related to the solution voltage drop by the following equation

$$V_s = \frac{iS}{k} \qquad (A.23)$$

where,

S is the distance between the electrode, m.

k is the electrolyte conductivity, mho/m.

The conductivity of the solution can be increased by the addition of excess indifferent electrolyte which is normally acid or alkali and the presence of indifferent electrolyte reduces the migration flux of the reacting species.

A.4 Current Distribution in an Electrochemical Reactor

A desirable electrochemical reactor is one in which the current is uniformly distributed. Irregularities from the average current densities and uneven potential distribution can lead to a loss in product selectivity and local corrosion problems. For a parallel plate reactor, having an electrode of equal area on the entire opposite side of the reactor one would expect uniform current distribution due to

symmetry. When the electrodes are polarised, the current distribution in a reactor not only depends on the geometry of the reactor and electrodes but also on the reaction occuring at the electrode surface, the electrolyte composition, the effect of ionic migration and concentration gradient and voltage drop within an electrode. These effects are very important for systems where reactions are slow, reactions occur in a narrow potential range, electrolyte conductivity is low and where the cell is operating much below the limiting current.

APPENDIX-B1

CELL DIMENSIONS, PHYSICAL PROPERTIES OF COPPER SULPHATE IN SULPHURIC ACID SOLUTION AND OTHER RELEVANT DATA OF FLUIDIZED BED.

The physical properties of 0.015 M Copper sulphate solution in 1.5 sulphuric acid has been taken from stanmore [26] and Wilson [32]. They collected the data from several sources. For dilute sulutions, the diffusivity of the copper ion can be taken equal to that of copper sulphate without any apreciable error.

TABLE B.1

Solution Characteristics for 0.015 M $CuSO_4$ in 1.5 M H_2SO_4

Temperature °C	Diffusivity D(cm^2/sec) X 10^{+6}	Kinamatic Viscosity cm^2/sec	Schmidt No. Sc = ν/D.
21.5	6.15	1.035	1682.9
40.0	9.50	0.718	754.0

The Cell Dimensions

Length of the electrode (L) = 0.3 m

Width of the electrodes (w) = 0.05 m

Spacing between the electrodes (S) = 0.02 m

Equivalent diameter (D_e) = 0.0286 m

Aspect ratio (S/w) = 0.4

Total Electrode area = 0.015 m^2

Cross sectional area for flow = 0.001 m^2

The Data for the Fluidized Bed

Average diameters of the glass particles = 6.0 mm, 4.5 mm and 3.0 mm.

Density of the glass particles = 2550 Kg/m^3

TABLE B.2

Static bed voidage and Froude number for the glass particle.

Particle size, mm	Density ρ_s, Kg/m^3	Static bed Voidages (ε_o)	Froude number (U^2_{mf}/gd_p)
6.0	-	0.437	2.66
4.5	2550	0.413	1.10
3.0	-	0.405	0.33

Minimum fluidization velocity, U_{mf} has been calculated theoretically [23].

APPENDIX-B2

FLOW CALIBRATION CURVES FOR ROTAMETERS USED IN THE EXPERIMENT

Appendix-B2 presents the rotameter calibration curves for the electrolyte solution (0.015 M copper sulphate solution in 1.5 M sulphuric acid). The calibration curves were drawn from experimentally obtained data.

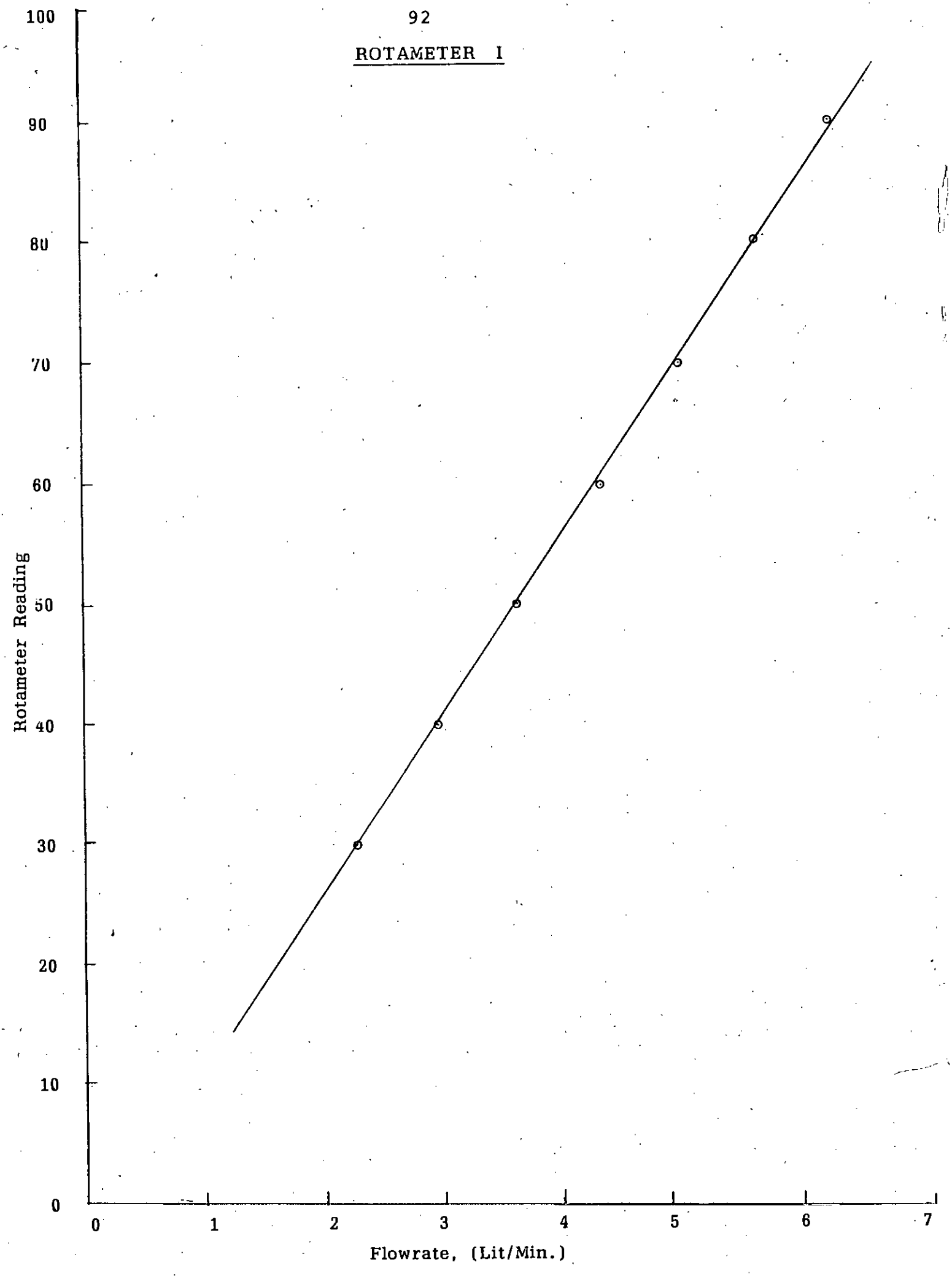

Fig. B-1: Plot of rotameter reading Vs. flowrate (Lit/min.)

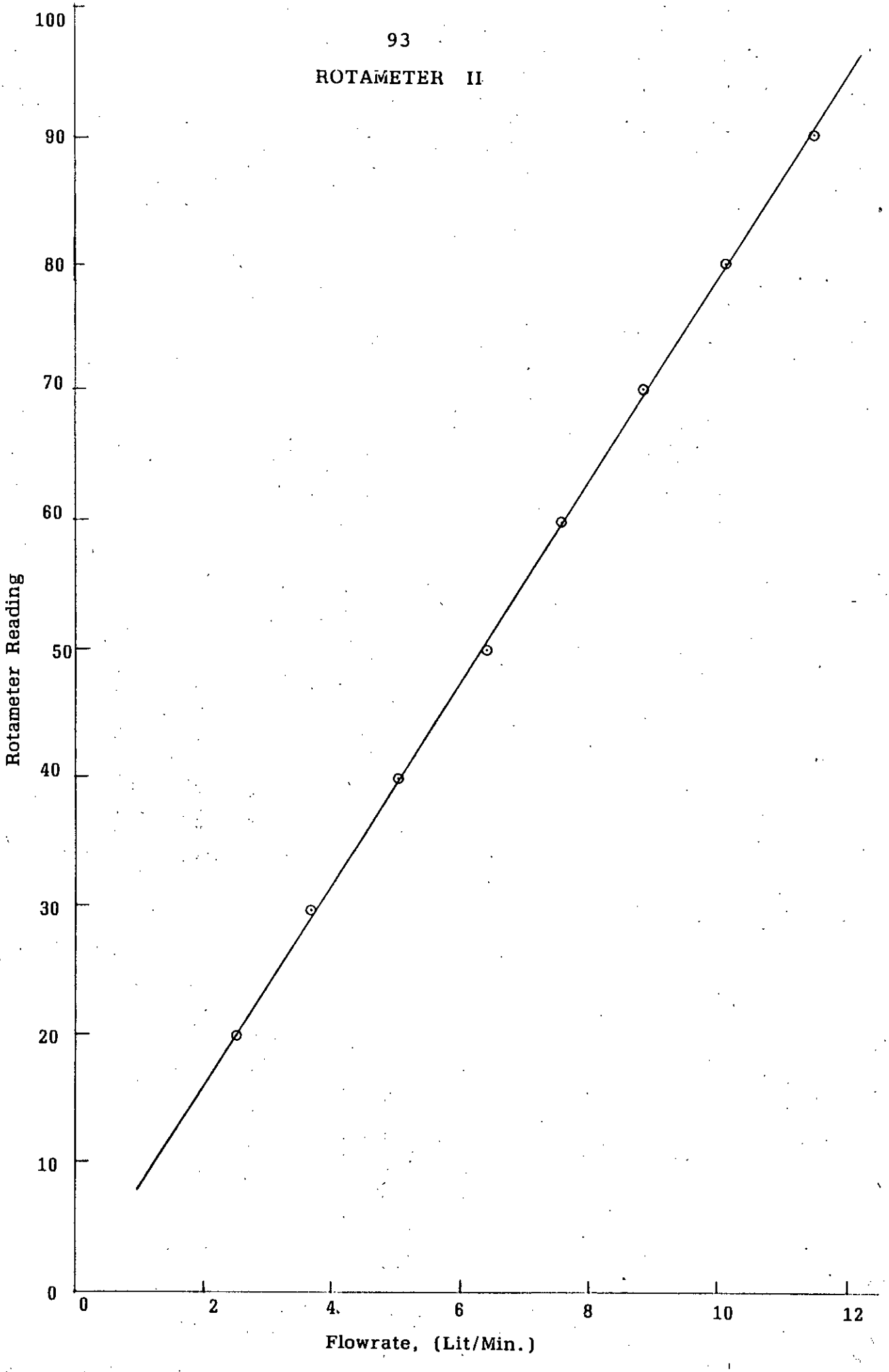

Fig. B-2: Plot of rotameter reading Vs. flowrate (Lit/min.)

APPENDIX-C

Experimental current-voltage data and calculated results.

APPENDIX-C.1

Particle size = 6.0 mm Initial bed height: 16 Temp.: 22°C

Flow rate: 5.7 Lit/min. Voidage: 0.585

Applied volt / mV Catho-de section	100	200	250	300	350	400	500	600
	Current mA							
1	1.5	4.0	4.5	4.0	7.0	10.0	15.0	23.0
2	1.0	3.0	3.5	4.5	6.0	8.5	14.0	21.5
3	1.0	2.5	3.0	4.5	6.0	8.5	13.5	21.0
4	1.5	2.5	3.0	5.5	6.0	8.0	14.5	21.0
5	1.5	2.5	3.0	4.0	8.0	8.0	18.5	21.0
6	3.0	6.5	7.0	8.0	11.0	16.0	22.0	38.0
7	4.0	7.0	8.0	9.0	9.5	17.0	23.0	40.0
8	4.0	7.0	8.0	9.0	9.5	17.0	23.0	40.0
9	3.0	6.5	9.0	9.5	13.0	17.0	24.0	35.0
10	3.5	6.0	8.0	9.5	11.5	15.5	22.0	30.0
11	1.0	2.5	4.0	4.0	5.0	6.0	7.0	8.5
12	1.0	2.5	4.0	4.5	5.5	6.0	8.0	9.5
13	1.0	2.5	4.0	4.0	5.0	5.5	7.0	8.0
14	1.0	3.0	4.0	4.0	5.0	6.0	7.0	8.5
15	1.5	5.0	5.0	5.5	8.0	9.0	12.0	14.0
Total:	29.5	63.0	77.5	90.5	116.5	158.0	227.5	339.5

APPENDIX-C.2

Particle size = 6.0 .Initial bed height: 16 cm. Temp.: 22°C.

Flow rate: 6.3 Lit/min. Voidage: 0.62

Applied volt.,mV	100	200	250	300	350	400	500	600
Cathode section	Current mA							
1	2.0	4.0	4.5	5.0	8.0	10.5	16.0	22.0
2	1.0	3.5	4.0	4.5	7.0	9.5	15.0	20.0
3	1.0	3.0	4.0	4.5	7.0	9.5	15.0	20.0
4	1.0	3.0	4.0	4.5	7.5	10.0	15.0	20.0
5	1.0	3.0	4.0	5.0	8.0	10.5	16.0	21.0
6	3.0	6.0	7.0	9.5	11.0	14.0	20.0	34.0
7	3.5	6.5	8.0	10.5	14.5	17.0	25.0	43.0
8	3.5	6.5	8.0	10.5	14.5	17.0	25.0	43.0
9	3.5	6.5	9.0	11.0	14.5	17.0	25.0	43.0
10	3.5	6.5	8.0	9.5	12.5	16.0	21.0	35.0
11	1.0	2.5	4.0	4.5	5.5	7.0	8.5	10.0
12	1.0	3.0	4.0	4.5	6.0	7.0	9.0	10.5
13	1.0	3.0	4.0	4.5	5.5	6.0	8.5	9.5
14	1.0	3.0	4.0	4.5	5.5	6.0	8.0	9.5
15	2.0	4.5	5.0	5.5	7.0	8.5	10.0	12.0
TOTAL:	29.0	64.5	81.5	98.0	134.0	165.8	237.0	352.5

APPENDIX -C.3

Particle size = 6.0 mm. Initial bed height: 16 cm. Temp.: 24°C

Flow rate: 7.0 Lit/min. Voidage: 0.649

Applied volt.,mV	100	200	250	300	350	400	500	600
Cathode section	Current, mA							
1	1.5	4.5	5.5	7.0	9.0	12.0	20.0	26.0
2	1.0	4.0	5.0	6.0	8.0	11.0	19.0	25.0
3	1.0	3.5	5.0	6.0	8.0	11.0	19.0	25.0
4	1.0	4.0	5.0	6.0	10.0	11.0	19.0	25.0
5	1.0	4.5	5.5	7.0	8.5	12.0	20.0	25.0
6	2.5	6.0	8.0	10.0	15.5	16.0	21.0	43.0
7	3.0	7.0	9.5	12.5	16.0	21.0	35.0	48.0
8	3.0	7.0	9.5	12.0	16.0	21.0	35.0	48.0
9	3.0	7.5	10.5	13.0	17.0	21.0	34.0	48.0
10	3.0	7.0	9.5	12.5	15.0	20.0	27.0	38.0
11	1.0	3.5	4.0	5.5	7.0	8.5	11.0	12.0
12	1.0	4.0	4.5	5.5	7.0	8.5	11.0	13.0
13	1.0	3.5	4.0	5.0	6.0	8.0	10.0	12.0
14	1.0	3.5	4.0	5.0	6.0	8.0	10.0	12.0
15	1.5	4.0	5.0	6.0	7.0	8.5	11.0	14.0
TOTAL;	25.5	73.5	94.5	119.5	154.0	198.0	302.0	414.0

APPENDIX -C.4

Particle size = 6.0 mm. Initial bed height: 16 cm. Temp.: 30°C

Flow rate: 8.2 Lit/min. Voidage: 0.685

Applied volt.,mV	100	200	250	300	350	400	500	600
Cathode section	Current, mA							
1	1.5	4.5	5.5	7.5	9.5	14.0	22.5	28.0
2	1.0	4.0	4.5	6.5	9.0	13.0	21.0	26.0
3	1.0	4.0	4.5	6.0	9.0	12.5	20.5	26.0
4	1.0	4.0	4.5	6.0	9.0	13.0	22.0	27.0
5	1.0	4.5	5.0	7.0	9.5	13.0	22.0	27.0
6	2.5	6.5	8.5	9.5	18.5	21.0	30.0	49.0
7	3.0	8.0	10.0	14.5	18.0	23.0	38.0	50.0
8	3.0	8.0	10.0	14.5	18.0	23.0	38.0	50.0
9	3.0	8.0	10.0	15.0	19.0	24.0	38.0	55.0
10	3.0	7.5	9.5	12.0	16.0	23.0	36.0	52.0
11	1.0	4.0	5.0	7.0	9.0	10.5	16.0	22.0
12	1.0	4.5	5.5	7.0	9.0	10.5	16.0	20.0
13	1.0	4.5	5.0	6.0	8.0	9.5	12.0	14.0
14	1.0	4.5	5.0	6.0	7.5	9.5	12.0	14.0
15	1.5	5.0	5.5	6.5	8.0	10.0	12.5	15.0
TOTAL;	25.5	81.5	103.0	131.0	177.0	229.5	356.0	475.0

APPENDIX -C. 5

Particle size = 6.0 mm. Initial bed height: 16 cm. Temp.: 31.°C

Flow rate: 9.5 Lit/min. Voidage: 0.739

Applied volt.,mV	100	200	250	300	350	400	500	600
Cathode section	Current, mA							
1	1.5	5.0	6.5	8.0	11.0	14.0	22.0	30.0
2	1.0	4.5	6.0	7.5	10.5	12.5	20.0	29.0
3	1.0	4.5	5.5	7.5	10.0	12.5	20.0	28.0
4	1.0	4.5	6.0	7.5	10.0	13.0	20.0	28.0
5	1.0	5.0	6.0	8.0	10.5	14.0	20.0	29.0
6	2.5	8.0	11.0	15.0	18.0	24.0	35.0	40.0
7	3.0	9.0	11.5	15.0	19.0	25.0	40.0	55.0
8	3.0	9.0	11.0	15.0	19.0	25.0	40.0	55.0
9	3.0	9.0	11.5	15.0	19.0	25.0	41.0	55.0
10	2.5	8.5	11.0	14.0	17.5	21.0	39.0	48.0
11	1.0	4.5	5.5	7.0	9.0	13.0	22.0	28.0
12	1.0	5.0	5.5	7.5	10.0	13.0	22.0	28.0
13	1.0	4.5	5.0	7.0	9.0	11.0	18.0	22.0
14	1.0	4.0	5.0	6.5	9.0	10.0	14.0	18.0
15	1.0	4.5	5.5	7.0	9.0	11.0	15.0	18.0
TOTAL;	24.5	89.5	118.5	145.5	188.5	238.0	388.0	571.0

15.

APPENDIX -C. 6

Particle size = 6.0 mm. Initial bed height: 12.0cm. Temp.: 22°C

Flow rate: 5.7 Lit/min. Voidage: 0.577

Applied volt.,mV	100	200	250	300	350	400	500	600
Cathode section	Current, mA							
1	2.5	4.0	4.5	6.0	10.0	13.0	20.0	27.0
2	1.5	3.5	4.0	5.5	8.0	11.0	18.0	24.0
3	1.0	3.5	4.0	5.5	8.0	11.0	18.0	24.0
4	1.0	3.5	4.0	5.5	8.0	11.0	18.0	24.0
5	1.0	3.5	4.0	6.0	8.5	11.0	18.0	24.0
6	4.0	8.0	10.0	15.0	15.5	20.0	24.0	45.0
7	4.5	8.0	10.5	16.0	20.0	22.0	32.0	48.0
8	4.0	7.5	10.0	12.0	15.0	22.0	24.0	35.0
9	4.0	8.0	10.5	14.0	16.0	18.0	21.0	30.0
10	4.0	8.0	10.0	13.0	14.0	15.0	19.0	20.0
11	1.0	2.5	2.5	4.0	5.0	5.5	5.5	7.0
12	1.0	3.0	3.0	4.5	5.0	5.5	5.5	7.5
13	1.0	3.5	3.5	4.5	5.0	5.5	5.5	7.0
14	1.5	3.5	4.0	4.5	5.5	6.0	6.5	7.5
15	2.5	5.0	6.0	7.5	9.0	11.0	13.0	15.0
TOTAL;	34.5	75.0	90.5	121.8	152.5	175.5	247.0	344.5

APPENDIX -C.7

Particle size = 6.0 mm. Initial bed height: 12 cm. Temp.: 22°C

Flow rate: 6.3 Lit/min. Voidage: 0.61

Applied volt.,mV	100	200	250	300	350	400	500	600
Cathode section	Current, mA							
1	2.5	4.5	5.0	6.5	10.0	13.0	20.0	30.0
2	1.5	4.0	4.5	5.5	8.5	11.5	18.0	27.5
3	1.0	4.0	4.5	5.5	8.5	11.5	17.5	27.0
4	1.0	4.0	4.5	5.5	8.5	11.5	17.5	27.5
5	1.0	4.0	4.5	6.0	9.0	12.0	17.0	28.0
6	3.0	7.5	9.0	11.0	14.0	19.0	34.0	42.0
7	3.0	7.5	9.5	12.5	17.0	21.0	35.0	45.0
8	3.0	7.0	9.5	10.0	14.0	22.0	27.0	40.0
9	3.0	8.0	10.0	12.0	15.0	19.0	25.0	30.0
10	3.0	8.0	10.0	11.0	14.0	17.0	22.0	24.0
11	1.0	3.0	3.5	4.0	5.0	5.5	6.0	6.5
12	1.0	3.5	4.0	4.5	5.5	6.0	6.5	7.0
13	1.0	3.5	4.0	4.5	5.0	5.5	6.0	7.0
14	1.0	4.0	4.0	4.5	5.5	6.0	7.0	7.5
15	1.5	5.5	6.5	7.0	8.5	9.5	12.0	14.0
TOTAL;	27.5	78.0	93.0	110.0	148.0	190.0	272.0	362.5

APPENDIX -C.8

Particle size = 6.0 mm. Initial bed height: 12 cm. Temp.: 26°C

Flow rate: 7.0 Lit/min. Voidage: 0.638

Applied volt.,mV	100	200	250	300	350	400	500	600
Cathode section	Current, mA							
1	2.0	5.0	6.0	7.5	10.0	13.0	22.0	34.0
2	1.5	4.5	5.0	6.0	8.5	12.0	20.0	30.0
3	1.0	4.5	5.0	6.0	8.5	12.0	20.0	30.0
4	1.0	4.5	5.0	6.0	8.5	12.0	20.0	30.0
5	1.0	4.5	5.5	6.5	8.0	12.5	20.0	32.0
6	3.0	7.5	9.5	12.0	13.5	20.0	38.0	43.0
7	3.5	8.0	10.0	13.0	14.0	22.5	28.0	48.0
8	3.5	7.5	9.5	12.5	13.5	21.0	35.0	45.0
9	3.5	8.0	10.0	12.5	14.5	20.0	28.0	35.0
10	3.5	8.0	10.0	11.5	14.5	18.0	25.0	30.0
11	1.0	2.5	3.5	4.5	5.5	7.5	8.0	9.0
12	1.0	3.0	4.0	5.0	5.5	7.5	9.0	10.0
13	1.0	3.0	4.0	5.0	5.5	7.0	9.0	9.5
14	1.0	3.0	4.0	5.0	9.0	7.0	9.0	10.0
15	1.0	4.5	5.5	5.5	7.0	9.5	12.0	14.0
TOTAL;	28.5	78.0	96.0	118.5	144.5	183.5	313.0	409.5

APPENDIX -C.9

Particle size = 6.0 mm. Initial bed height: 12 cm. Temp.: 28°C

Flow rate: 8.2 Lit/min. Voidage: 0.678

Applied volt.,mV	100	200	250	300	350	400	500	600
Cathode section	Current, mA							
1	2.5	5.0	6.5	8.0	10.5	15.5	23.0	33.0
2	1.5	4.5	5.5	7.0	9.5	13.0	21.0	28.0
3	1.0	4.5	5.0	6.5	9.5	13.0	21.0	27.0
4	1.0	4.0	5.0	6.5	9.5	13.0	21.0	28.0
5	1.0	4.5	5.5	7.0	9.5	13.0	22.0	28.0
6	3.0	7.5	9.0	14.0	16.5	19.0	27.0	38.0
7	3.5	8.0	10.0	14.5	18.0	23.0	28.0	48.0
8	3.0	7.5	9.5	14.0	16.0	19.0	28.0	45.0
9	3.0	7.5	10.0	14.5	18.0	22.0	27.5	44.0
10	3.0	7.5	10.0	13.5	16.0	19.0	27.0	35.0
11	1.0	2.5	4.0	5.0	6.5	8.0	10.0	11.0
12	1.0	3.0	4.5	5.5	6.5	8.5	11.0	12.0
13	1.0	3.0	4.5	5.0	6.0	8.0	9.5	10.0
14	1.0	3.0	4.0	5.0	6.0	8.0	10.0	12.0
15	1.5	4.0	5.5	6.5	8.0	10.0	12.0	14.0
TOTAL;	28.0	76.0	98.5	132.5	164.0	211.5	298.0	408.0

--

APPENDIX -C. 10

Particle size = 6.0 mm. Initial bed height: 12 cm. Temp.: 31°C

Flow rate: 9.5 Lit/min. Voidage: 0.74

Applied volt.,mV	100	200	250	300	350	400	500	600
Cathode section	Current, mA							
1	2.5	5.5	7.5	9.0	11.0	15.0	25.0	35.0
2	2.0	4.5	6.0	7.5	10.0	12.0	22.0	21.0
3	1.0	4.5	5.5	7.0	10.0	12.0	22.0	29.0
4	1.0	4.5	5.5	7.0	10.0	12.5	21.0	29.0
5	1.5	4.5	6.0	7.5	10.5	13.0	22.0	32.0
6	3.5	7.5	9.5	14.0	16.0	20.0	32.0	40.0
7	3.5	8.0	10.5	15.0	18.0	22.0	35.0	45.0
8	3.5	7.5	9.5	14.0	16.0	20.0	32.0	41.0
9	3.5	8.0	10.0	14.5	18.0	21.5	34.5	42.0
10	3.5	8.0	10.0	14.0	17.0	21.0	31.0	40.0
11	1.0	3.5	4.0	5.5	7.0	10.0	14.0	17.0
12	1.0	4.0	5.0	6.0	7.5	10.0	14.0	17.0
13	1.0	4.0	4.5	5.5	7.0	9.0	11.0	13.0
14	1.0	4.0	4.5	5.0	6.5	9.0	11.0	13.0
15	2.0	5.0	5.5	5.5	8.0	10.0	13.0	16.0
TOTAL:	31.5	83.0	103.0	137.0	172.5	217.0	339.0	440.0

APPENDIX -C.11

Particle size = 6.0 mm. Initial bed height: 8 cm. Temp.: 22°C

Flow rate: 5.7 Lit/min. Voidage: 0.62

Applied volt.,mV	100	200	250	300	350	400	500	600
Cathode section	Current, mA							
1	4.0	4.5	6.0	7.5	9.0	13.5	20.0	
2	2.5	4.0	5.5	6.5	8.5	11.0	18.0	
3	2.0	4.0	5.5	6.5	8.5	10.5	18.0	
4	2.5	4.0	5.5	6.5	8.5	11.0	19.0	
5	3.0	4.5	6.0	6.0	10.0	12.0	19.5	
6	6.0	14.0	16.0	17.0	17.0	21.0	29.0	
7	7.0	13.0	16.5	18.0	19.0	22.0	29.0	
8	7.0	12.0	15.0	18.0	18.0	20.0	22.0	
9	5.0	10.5	13.5	15.0	15.0	16.0	19.0	
10	4.0	9.5	12.0	14.0	14.0	15.0	16.0	
11	1.5	3.5	4.5	5.5	5.5	5.5	5.5	
12	1.0	3.5	4.5	5.5	5.5	5.5	6.5	
13	1.0	3.0	4.5	5.5	5.5	5.5	5.5	
14	1.0	4.0	4.5	5.5	5.5	5.5	6.0	
15	2.0	5.0	5.5	7.0	8.0	9.0	11.0	
TOTAL:	49.5	99.5	113.5	132.0	153.0	180.0	243.0	

APPENDIX -C.12

Particle size = 6.0 mm. Initial bed height: 8 cm. Temp.: 22°C

Flow rate: 7.0 Lit/min. Voidage: 0.674

Applied volt.,mV	100	200	250	300	350	400	500	600
Cathode section	Current, mA							
1	2.0	3.5	4.5	7.5	9.5	13.0	21.0	26.0
2	1.0	2.5	3.5	5.5	8.5	11.0	18.5	24.0
3	1.0	2.0	3.5	5.5	8.5	11.0	19.0	24.0
4	1.0	2.0	3.5	5.5	8.5	11.0	18.0	24.0
5	1.0	2.5	3.5	5.5	9.0	11.0	18.0	24.0
6	2.5	6.0	8.5	11.0	14.0	24.0	20.0	44.0
7	3.5	7.0	9.5	12.5	16.0	22.0	25.0	40.0
8	4.0	9.0	12.0	13.0	15.0	20.0	25.0	30.0
9	4.0	9.0	10.0	11.0	14.5	19.0	24.0	26.0
10	4.0	9.0	10.0	11.0	14.0	17.0	21.0	24.0
11	1.0	2.5	3.5	4.0	5.0	5.5	4.0	7.5
12	1.0	2.5	3.5	4.0	5.5	6.0	7.5	9.0
13	1.0	3.0	3.5	4.0	5.0	5.5	7.0	7.5
14	1.0	3.0	3.5	4.0	5.0	5.5	8.0	8.5
15	1.5	4.0	5.0	5.5	7.0	9.0	10.5	12.0
TOTAL:	29.5	67.5	91.0	108.5	145.5	190.5	264.5	307.5

APPENDIX -C. 13

Particle size = 6.0 mm. Initial bed height: 8 cm. Temp.: 24°C

Flow rate: 8.2 Lit/min. Voidage: 0.724

Applied volt.,mV	100	200	250	300	350	400	450	500
Cathode section	Current, mA							
1	2.0	4.5	5.5	7.0	10.0	13.5	18.0	22.0
2	1.5	3.5	4.5	5.5	8.0	11.0	15.0	19.0
3	1.0	3.5	4.0	5.5	8.0	11.0	15.0	19.0
4	1.0	3.5	4.0	5.5	8.5	11.0	16.5	19.0
5	1.0	3.5	4.5	5.5	8.5	11.5	16.5	19.5
6	2.5	6.5	8.0	11.0	14.5	19.5	22.0	34.0
7	3.0	7.0	9.5	13.0	16.0	21.5	26.0	34.0
8	4.0	7.5	10.0	12.0	15.5	20.0	24.0	25.0
9	3.5	7.0	9.5	11.0	14.0	18.0	20.0	24.0
10	3.5	7.0	9.0	11.0	15.0	17.0	19.0	22.0
11	1.0	3.0	3.5	4.0	5.5	7.0	7.5	8.0
12	1.0	3.0	4.0	4.5	5.5	7.0	8.5	9.0
13	1.0	3.0	3.5	4.0	5.0	6.5	7.5	8.5
14	1.0	3.0	3.5	4.5	5.5	7.0	8.0	8.5
15	1.5	4.0	5.0	5.5	6.5	9.5	10.0	11.0
TOTAL:	28.5	69.5	88.0	109.5	145.0	190.0	231.0	281.5

APPENDIX -C.14

Particle size = 6.0 mm. Initial bed height: 8 cm. Temp.: 30°C

Flow rate: 9.5 Lit/min. Voidage: 0.76

Applied volt.,mV	100	200	250	300	350	400	450	500
Cathode section	Current, mA							
1	2.0	5.0	6.5	8.5	12.0	13.5	16.0	20.0
2	1.0	4.5	5.5	7.0	9.5	11.0	12.5	16.0
3	1.0	4.5	5.5	7.0	9.5	11.0	13.5	16.0
4	1.0	4.5	5.5	5.5	9.5	11.0	13.5	17.0
5	1.0	5.0	6.0	7.5	10.5	11.5	14.0	18.0
6	2.5	7.0	9.5	11.0	15.0	18.0	20.0	30.0
7	3.0	8.5	10.5	13.0	17.0	20.5	22.0	35.0
8	3.0	8.5	10.5	12.0	15.5	18.0	21.0	25.5
9	3.0	7.5	9.5	12.0	14.5	15.5	18.0	24.5
10	3.0	7.5	9.5	12.0	14.5	15.0	17.5	21.0
11	1.0	3.0	4.0	5.5	6.0	7.5	8.5	10.0
12	1.0	3.5	4.5	5.5	6.5	8.0	9.0	10.0
13	1.0	3.0	4.0	5.5	6.5	7.5	8.5	9.5
14	1.0	3.0	4.5	5.5	6.5	7.5	8.5	10.0
15	1.5	4.0	5.0	5.5	7.5	8.5	10.0	12.0
TOTAL;	26.0	79.0	100.5	120.0	159.5	184.0	212.5	273.5

APPENDIX -C.15

Particle size = 6.0 mm. Initial bed height: 8 cm. Temp.: 32°C

Flow rate:10.8 Lit/min. Voidage: 0.792

Applied volt.,mV	100	200	250	300	350	400	500	600
Cathode section	Current, mA							
1	2.5	5.0	6.0	7.5	9.0	12.0	20.0	30.0
2	1.5	4.0	5.0	6.0	7.5	9.5	18.0	25.0
3	1.0	4.0	5.0	6.0	7.5	9.5	16.0	24.0
4	1.0	4.0	5.0	6.0	7.0	9.5	16.0	24.0
5	1.0	4.5	5.5	6.5	7.5	10.0	17.0	25.0
6	3.0	6.0	7.5	10.0	12.5	16.0	32.0	42.0
7	3.5	7.0	8.5	11.0	14.0	19.0	33.0	38.0
8	3.5	7.0	8.5	11.0	14.0	19.0	34.0	38.0
9	3.5	6.5	8.5	10.5	12.5	16.0	28.0	30.0
10	3.5	6.5	8.5	10.0	12.5	16.0	28.0	30.0
11	1.0	3.0	4.0	4.5	5.5	8.0	12.0	14.0
12	1.0	3.5	4.5	5.5	6.0	8.0	13.0	14.5
13	1.0	3.0	4.0	5.0	6.5	7.0	10.0	12.0
14	1.0	3.5	4.5	5.5	6.5	7.0	11.0	12.0
15	1.5	4.0	4.5	6.5	7.0	8.5	12.5	15.0
TOTAL:	29.5	71.5	89.5	110.0	132.0	175.0	300.5	378.5

APPENDIX -C.16

Particle size = 4.5 mm. Initial bed height: 16 cm. Temp.: 24°C

Flow rate: 4.3 Lit/min. Voidage: 0.557

Applied volt.,mV	100	200	250	300	350	400	450	500
Cathode section	Current, mA							
1	2.5	4.5	5.0	7.0	10.0	14.0	18.0	22.0
2	2.0	4.0	4.5	6.0	8.5	12.0	17.0	20.0
3	2.0	4.0	4.5	6.0	8.5	12.0	16.0	20.0
4	2.0	4.0	4.5	6.0	8.5	12.0	16.0	20.0
5	2.0	4.0	4.5	6.0	8.5	12.0	16.0	20.0
6	3.0	8.0	11.0	13.0	16.0	22.0	25.0	32.0
7	3.0	7.5	10.0	12.0	17.0	22.0	26.0	35.0
8	3.0	7.5	7.0	12.0	17.0	23.0	28.0	34.0
9	3.0	7.0	10.0	12.0	16.0	20.0	23.0	28.0
10	3.5	8.5	10.5	12.0	15.0	18.0	20.0	22.0
11	1.0	4.0	4.0	4.5	5.5	6.0	6.5	7.0
12	1.0	4.0	4.5	4.5	5.5	6.0	7.0	7.5
13	1.0	4.0	4.0	4.5	5.0	6.0	6.5	7.0
14	1.0	4.0	4.0	4.5	5.5	6.0	6.5	7.0
15	1.0	4.5	4.5	5.0	6.0	7.0	8.0	9.0
TOTAL:	31.0	79.5	95.5	115.0	152.5	200.0	238.0	290.5

APPENDIX -C.17

Particle size = 4.5 mm. Initial bed height: 16 cm. Temp.: 20°C

Flow rate: 5.0 Lit/min. Voidage: 0.594

Applied volt.,mV	100	200	250	300	350	400	450	500
Cathode section	Current, mA							
1	2.5	4.5	5.5	7.0	10.0	14.0	17.0	20.0
2	1.5	4.0	4.5	6.0	9.0	12.0	15.5	18.0
3	1.5	4.0	4.5	6.0	9.0	12.0	15.0	18.0
4	1.0	4.0	4.5	6.0	9.5	12.0	15.5	18.0
5	1.0	4.0	4.5	6.0	8.5	10.0	15.5	18.0
6	3.5	7.0	9.0	12.0	17.0	22.0	22.5	35.0
7	3.5	7.5	10.0	14.0	18.0	22.0	22.5	38.0
8	3.0	7.5	9.5	13.0	18.0	24.0	28.0	35.0
9	3.5	7.0	10.0	13.0	16.0	22.0	28.0	36.0
10	3.5	7.5	10.0	13.0	17.0	21.0	22.0	30.0
11	1.0	3.5	4.5	5.0	6.0	6.5	7.0	7.5
12	1.0	4.0	4.5	5.5	6.5	7.0	7.5	8.0
13	1.0	4.0	4.5	5.0	5.5	6.0	6.5	7.0
14	1.0	3.5	4.5	5.0	5.5	6.0	7.0	7.5
15	1.5	4.5	5.0	5.5	7.0	8.5	9.0	9.5
TOTAL;	30.0	76.5	95.0	122.0	162.5	205.0	233.0	304.0

APPENDIX -C.18

Particle size = 4.5 mm. Initial bed height: 16 cm. Temp.: 24°C

Flow rate: 5.7 Lit/min. Voidage: 0.628

Applied volt.,mV	100	200	250	300	350	400	450	500
Cathode section	Current, mA							
1	5.0	7.5	8.5	9.0	11.0	14.0	19.02	25.0
2	5.0	7.0	8.0	8.5	10.0	12.0	17.0	23.0
3	4.0	7.0	7.5	8.0	10.0	12.0	17.0	23.0
4	4.0	5.0	6.0	7.5	10.0	13.0	18.0	24.0
5	4.0	6.0	7.0	8.0	11.0	13.0	20.0	24.0
6	7.0	11.0	14.0	17.0	20.0	23.0	27.0	37.0
7	11.0	14.0	16.0	19.0	22.0	27.0	37.0	43.0
8	11.0	14.0	17.0	19.0	21.0	27.0	37.0	44.0
9	6.0	11.0	14.0	16.0	19.0	27.0	37.0	44.0
10	6.0	11.0	14.0	17.0	21.0	27.0	33.0	41.0
11	3.0	5.0	5.0	7.0	7.5	9.0	9.5	10.0
12	3.0	5.0	6.0	7.0	8.0	10.0	11.0	13.0
13	3.0	5.0	6.0	6.0	6.5	8.0	9.0	10.0
14.	3.0	6.0	6.0	7.0	8.0	9.0	10.0	11.0
15	3.0	6.0	7.0	7.0	8.0	10.0	11.0	12.0
TOTAL:	78.0	120.0	142.0	162.0	192.9	241.0	312.0	384.

APPENDIX -C.19

Particle size = 4.5 mm. Initial bed height: 16 cm. Temp.: 26°C

Flow rate: 6.3 Lit/min. Voidage: 0.666

Applied volt.,mV	100	200	250	300	350	400	450	500
Cathode section	Current, mA							
1 4.0	8.0	9.0	10.5	12.5	15.0	20.0	26.0	2.0
1	4.0	8.0	9.0	10.5	12.5	15.0	20.0	26.0
2	4.0	8.0	9.0	10.0	11.0	13.0	18.0	23.0
3	5.0	9.0	10.0	11.0	12.0	15.0	20.0	24.0
4	5.5	9.5	11.0	12.0	13.0	16.0	21.0	25.0
5	6.0	10.0	12.0	12.0	14.0	18.0	21.0	25.0
6	7.0	15.0	18.0	22.0	23.0	24.0	27.0	30.0
7	9.0	16.0	18.0	22.0	24.0	30.0	35.0	40.0
8	8.0	15.0	18.0	21.0	23.0	28.0	32.0	36.0
9	9.0	19.0	22.0	24.0	26.0	30.0	35.0	39.0
10	9.0	20.0	22.0	24.0	27.0	32.0	35.0	39.0
11	4.0	8.0	9.0	11.0	12.0	13.0	14.0	17.0
12	6.0	10.0	11.0	12.0	13.0	14.0	15.0	18.0
13	5.0	10.0	10.0	10.0	11.0	8.0	10.0	11.0
14	5.0	8.0	10.0	10.0	11.0	12.0	13.0	14.0
15	4.0	8.0	9.0	9.0	9.0	9.0	9.0	10.0
TOTAL;	90.5	177.5	202.0	224.5	247.5	273.0	327.0	379.0

APPENDIX -C.20

Particle size = 4.5 mm. Initial bed height: 16 cm. Temp.: 26°C

Flow rate: 17.0 Lit/min. Voidage: 0.705

Applied volt.,mV	100	200	250	300	350	400	450	500
Cathode section	Current, mA							
1	4.0	7.0	8.0	12.0	14.0	17.0	22.0	24.0
2	3.0	6.0	6.5	9.0	11.0	15.0	18.0	22.0
3	4.0	7.0	7.5	10.0	12.5	16.0	21.0	24.0
4	4.0	7.5	9.0	12.0	14.0	17.0	21.0	28.0
5	5.0	9.0	11.0	12.0	14.0	18.0	22.0	28.0
6	4.0	9.0	12.0	16.0	17.0	23.0	26.0	28.0
7	5.0	10.0	12.0	18.0	23.0	30.0	35.0	40.0
8	4.0	8.0	12.0	18.0	21.0	27.0	34.0	35.0
9	6.0	11.0	15.0	20.0	23.0	30.0	36.0	38.0
10	6.0	12.0	16.0	22.0	24.0	29.0	36.0	38.0
11	3.0	4.5	6.0	7.0	8.0	11.0	19.0	20.0
12	4.0	7.0	9.0	10.0	12.0	14.0	18.0	23.0
13	4.0	7.0	8.0	9.0	11.0	13.0	15.0	17.0
14	4.0	6.0	7.0	9.0	10.0	12.0	13.0	14.0
15	4.0	5.0	6.0	8.5	9.5	11.0	13.0	14.0
TOTAL;	64.0	116.0	144.0	192.0	228.0	285.0	350.0	391.0

APPENDIX -C.21

Particle size = 4.5 mm. Initial bed height: 12 cm. Temp.: 22°C

Flow rate: 5.7 Lit/min. Voidage: 0.66

Applied volt.,mV	100	200	250	300	350	400	450	500
Cathode section	Current, mA							
1	3.5	5.0	6.0	7.0	15.0	20.0	25.0	30.0
2	2.5	4.0	5.0	6.0	11.0	18.0	22.0	33.0
3	2.0	4.5	5.0	6.0	11.0	18.0	22.0	32.0
4	1.0	4.0	4.5	5.0	10.0	11.0	21.0	32.0
5	1.0	4.0	5.0	5.5	10.5	18.0	21.0	32.0
6	4.5	12.0	14.0	15.0	22.0	35.0	45.0	62.0
7	4.0	13.0	16.0	17.0	24.0	35.0	46.0	63.0
8	4.0	12.0	16.0	17.0	25.0	40.0	45.0	63.0
9	4.0	11.0	13.0	15.0	21.0	33.0	38.0	45.0
10	4.0	11.0	12.5	13.0	17.0	23.0	28.0	38.0
11	1.0	2.5	3.0	4.0	4.5	5.0	6.0	7.0
12	1.0	3.0	3.5	4.0	5.0	5.5	6.5	7.5
13	1.0	3.0	4.0	5.0	5.5	6.0	7.0	8.5
14	1.0	3.0	4.0	5.0	5.5	6.0	7.5	8.5
15	1.0	4.0	5.0	6.0	6.5	7.5	9.0	10.0
TOTAL;	35.5	96.0	115.5	131.0	192.5	288.0	349.0	445.0

APPENDIX -C.22

Particle size = 4.5 mm. Initial bed height: 12 cm. Temp.: 22°C

Flow rate: 6.3 Lit/min. Voidage: 0.685

Applied volt.,mV	100	200	250	300	350	400	450	500
Cathode section	Current, mA							
1	3.5	4.5	5.0	6.0	8.5	10.5	14.5	18.0
2	2.0	2.5	3.5	5.5	8.0	8.0	14.0	17.0
3	1.5	2.5	3.5	5.5	7.5	9.5	13.5	16.5
4	1.0	2.5	3.5	5.5	7.5	9.5	13.5	16.5
5	1.0	2.0	3.5	5.5	7.5	9.5	13.5	16.5
6	4.0	6.0	7.5	11.5	13.0	15.5	21.0	30.0
7	4.5	7.0	8.5	13.0	15.0	18.0	22.0	31.0
8	4.5	7.0	8.5	13.0	15.0	19.0	23.0	32.0
9	4.0	6.5	8.5	11.5	14.5	17.5	20.5	26.0
10	3.5	5.5	8.0	10.5	13.0	15.0	18.0	22.0
11	1.0	2.0	3.0	4.0	5.0	5.5	6.5	7.5
12	1.0	2.0	3.0	4.5	5.5	5.5	6.5	8.0
13	1.0	2.5	3.5	4.5	5.0	5.0	6.0	7.0
14	2.0	3.0	4.0	5.0	5.5	6.0	7.0	7.5
15	2.5	3.5	4.5	5.5	6.0	7.5	9.5	10.5
TOTAL:	37.0	59.0	78.5	111.0	136.5	162.5	208.5	288.5

APPENDIX -C 23

Particle size = 4.5 mm. Initial bed height: 12 cm. Temp.: 22°C

Flow rate: 7.0 Lit/min. Voidage: 0.717

Applied volt.,mV	100	200	250	300	350	400	450	500
Cathode section	Current, mA							
1	2.5	4.5	5.5	6.5	9.0	12.0	16.0	22.0
2	1.0	3.5	4.5	5.5	8.5	11.0	15.0	20.0
3	1.0	3.5	4.5	5.5	8.5	10.5	15.0	19.0
4	1.0	3.5	4.5	5.5	8.5	11.0	15.0	20.0
5	1.0	3.5	4.5	5.5	8.5	10.5	14.5	19.0
6	3.0	6.5	8.5	12.0	15.0	17.0	25.0	34.0
7	3.0	7.0	8.5	13.0	18.0	20.0	26.0	35.0
8	3.0	7.0	8.5	12.0	15.5	22.0	27.0	36.0
9	3.0	7.0	8.0	12.0	15.5	21.0	24.5	32.0
10	3.0	7.0	8.5	12.5	15.5	18.0	22.0	25.0
11	1.0	3.5	4.0	5.0	6.0	7.0	7.5	9.0
12	1.0	3.5	4.0	5.0	6.0	7.5	8.0	9.0
13	1.0	3.0	3.5	4.5	5.5	7.0	7.5	9.0
14	1.0	3.5	4.0	4.5	5.5	7.0	7.5	9.0
15	2.0	4.0	4.5	5.5	7.0	9.0	10.0	12.0
TOTAL;	27.5	70.5	86.0	111.0	152.5	190.5	226.5	310.0

APPENDIX -C.24

Particle size = 4.5 mm. Initial bed height: 12 cm. Temp.: 26°C

Flow rate: 7.6 Lit/min. Voidage: 0.742

Applied volt.,mV	100	200	250	300	350	400	450	500	
Cathode section	Current, mA								
1	2.0	4.0	5.0	7.0	10.0	14.0	17.0	22.0	
2	1.0	3.5	4.5	6.0	9.0	12.0	15.0	21.0	
3	1.0	3.0	4.5	6.0	9.0	12.0	15.0	20.0	
4	1.0	3.0	4.5	5.5	9.0	12.0	15.0	20.0	
5	1.0	3.0	4.5	5.5	9.0	12.5	15.0	20.0	
6	2.5	7.0	8.5	12.0	17.0	20.0	26.0	32.0	
7	3.0	7.0	8.5	12.0	18.0	21.0	26.0	32.0	
8	3.0	7.0	8.5	13.0	17.5	32.0	27.0	34.0	
9	3.0	6.5	8.5	13.0	17.5	22.0	26.0	33.0	
10	3.0	7.0	9.0	13.0	17.5	21.0	26.0	32.0	
11	1.0	2.5	3.5	5.0	6.0	8.0	9.5	10.5	
12	1.0	3.0	4.0	5.0	7.0	8.5	9.5	10.5	
13	1.0	3.0	4.0	5.0	6.0	7.0	8.5	9.5	14.0
14	1.0	3.0	4.0	5.0	6.0	7.0	8.5	9.5	
15	1.0	4.0	4.5	4.5	7.0	8.5	9.0	12.0	
TOTAL;	25.4	66.5	86.0	117.5	165.5	207.5	253.0	318.0	

--

APPENDIX -C.25

Particle size = 4.5 mm. Initial bed height: 12 cm. Temp.: 28°C

Flow rate: 8.9 Lit/min. Voidage: 0.792

Applied volt.,mV	100	200	250	300	350	400	450	500
Cathode section	Current, mA							
1	3.0	5.0	8.0	10.0	11.0	13.0	17.0	25.0
2	2.0	4.5	7.5	9.0	10.0	12.0	15.0	15.0	23.0
3	1.5	4.0	7.0	9.0	10.0	12.0	15.0	23.0
4	1.5	4.0	7.0	8.0	10.0	11.5	15.0	23.0
5	1.5	4.0	7.0	8.0	10.5	12.0	15.0	23.0
6	4.5	9.5	15.0	20.0	22.0	24.0	30.0	40.0
7	5.0	11.0	16.0	22.0	23.0	26.0	32.0	40.0
8	5.0	10.5	15.0	19.0	21.0	23.0	31.0	42.0
9	5.0	10.0	14.0	17.0	19.0	21.0	28.0	37.0
10	4.5	10.0	14.0	17.0	19.0	21.0	27.0	34.0
11	1.0	3.5	5.0	6.0	7.0	8.0	9.0	10.0
12	1.0	4.0	6.0	7.0	8.0	9.0	10.0	11.0
13	1.0	3.5	5.5	6.0	7.0	8.0	9.0	11.0
14	1.0	4.0	5.5	7.0	8.0	9.0	10.0	12.0
15	1.0	4.5	7.0	8.0	9.5	11.0	12.0	15.0
TOTAL:	38.5	91.5	139.5	173.0	195.0	220.5	275.0	368.0

APPENDIX -C. 26

Particle size = 4.50 mm. Initial bed height: 8 cm. Temp.: 25°C

Flow rate: 7.0 Lit/min. Voidage: 0.738

Applied volt.,mV	100	200	300	350	400	450	500
Cathode section	Current, mA						
1	4.0	7.5	12.0	13.5	16.0	22.0	27.0
2	5.0	7.0	11.0	12.0	15.0	18.0	23.0
3	3.0	6.0	10.0	12.0	15.0	18.0	23.0
4	2.5	6.0	9.0	12.0	15.0	18.0	24.0
5	4.0	7.0	10.0	13.0	15.0	18.0	26.0
6	7.0	13.0	19.0	21.0	32.0	37.0	42.0
7	9.0	18.0	24.0	26.0	30.0	40.0	42.0
8	8.0	17.0	23.0	25.0	30.0	32.0	35.0
9	7.0	15.0	20.0	22.0	25.0	27.0	28.0
10	6.0	12.0	18.0	20.0	22.0	24.0	25.0
11	3.0	4.0	6.0	7.0	7.0	7.5	8.0
12	4.0	5.0	7.0	7.5	8.0	8.0	8.5
13	5.5	7.0	7.0	7.0	7.0	7.5	8.5
14	4.0	6.0	8.0	8.0	9.0	9.5	9.5
15	4.0	9.0	9.0	11.0	12.0	15.0	17.0
TOTAL;	76.0	139.5	193.0	195.0	256.0	299.5	348.0

APPENDIX -C. 27

Particle size = 4.5 mm. Initial bed height: 8 cm. Temp.: 27°c

Flow rate: 8.2 Lit/min. Voidage: 0.795

Applied volt.,mV	100	200	300	350	400	450	500	600
Cathode section	Current, mA							
1	3.0	7.0	11.0	15.0	22.0	26.0	32.0	
2	2.0	6.0	9.0	13.0	18.0	22.0	27.5	
3	2.0	5.5	9.0	13.0	19.0	23.0	26.0	
4	2.0	5.5	10.0	14.0	20.0	23.0	28.0	
5	2.0	6.0	10.0	15.0	20.5	24.0	28.0	
6	4.0	9.0	15.0	19.0	23.0	40.0	44.0	
7	4.0	10.5	21.0	29.0	34.0	47.0	58.0	
8	5.5	13.0	22.0	27.0	32.0	39.0	51.0	
9	6.0	14.0	20.0	24.0	28.0	32.0	40.0	1
10	5.0	13.0	20.0	22.0	24.5	27.0	31.0	
11	22.0	4.0	6.0	8.0	9.0	9.5	10.0	
12	2.0	5.0	8.0	9.0	10.0	11.0	12.0	
13	2.5	5.0	6.5	7.0	8.0	8.5	10.0	
14	2.5	5.0	7.0	8.0	9.0	11.0	12.0	
15	2.5	6.0	8.0	10.0	12.0	12.5	14.0	
TOTAL;	47.0	114.5	182.5	233.0	289.5	352.0	409.0	

APPENDIX -C. 28

Particle size = 4.5 mm. Initial bed height: 8 cm. Temp.: 29°C

Flow rate: 10.1 Lit/min. Voidage: 0.843

Applied volt.,mV	100	200	300	350	400	450	500	600
Cathode section	Current, mA							
1	4.0	8.0	12.0	17.0	22.0	30.0	33.0	
2	3.0	7.0	12.0	16.0	20.0	26.0	30.0	
3	3.0	7.0	11.0	14.0	19.0	26.0	28.0	
4	4.0	8.0	13.0	16.0	20.0	26.0	30.0	
5	5.0	10.0	15.0	17.0	19.0	27.0	30.0	
6	6.0	12.0	20.0	28.0	35.0	38.0	50.0	
7	6.0	13.0	20.0	30.0	40.0	45.0	55.0	
8	6.0	12.0	22.0	24.0	36.0	45.0	55.0	
9	7.0	14.0	25.0	28.0	37.0	38.0	54.0	
10	7.0	14.0	25.0	29.0	35.0	42.0	56.0	
11	3.0	5.0	9.0	11.0	12.0	13.0	22.0	
12	3.0	6.0	10.0	11.0	13.0	14.0	20.0	
13	3.0	6.0	9.0	9.0	10.0	11.0	15.0	
14	3.0	5.0	9.0	9.0	10.0	11.0	14.0	
15	3.0	5.0	7.0	10.0	13.0	14.0	16.0	
TOTAL;	66.0	131.0	21.9	269.0	341.0	406.0	508.0	

APPENDIX -C.29

Particle size = 3.0 mm. Initial bed height: 16 cm. Temp.: 22°C

Flow rate:5.7 Lit/min. Voidage: 0.596

Applied volt.,mV	100	200	250	300	350	400	500	600
Cathode section	Current, mA							
1	3.0	5.5	7.0	8.0	11.0	15.0	22.0	
2	2.5	5.0	6.0	7.5	10.0	13.5	21.0	
3	2.5	5.0	7.0	7.5	10.0	14.0	22.5	
4	2.0	4.0	5.0	5.0	5.0	6.0	10.0	
5	2.5	4.0	5.0	7.0	10.0	14.0	22.0	
6	5.5	10.0	12.0	13.0	21.0	23.0	30.0	
7	7.5	13.0	14.0	16.0	20.0	25.0	40.0	
8	7.0	13.0	14.0	15.5	17.5	23.0	40.0	
9	7.0	12.0	13.0	16.0	21.0	26.0	39.0	
10	6.0	11.0	12.0	15.0	20.0	22.0	30.0	
11	2.0	4.0	4.5	5.5	7.0	8.0	10.0	
12	2.5	4.5	5.0	6.0	7.5	8.0	10.0	
13	2.5	4.5	5.0	5.5	6.0	7.0	8.0	
14	3.0	5.0	5.0	5.5	6.0	8.0	9.0	
15	4.0	6.0	7.0	7.0	9.5	11.0	12.0	
TOTAL;	59.5	106.5	121.5	139.5	181.5	223.5	325.5	

--

APPENDIX -C. 30

Particle size = 3.0 mm. Initial bed height: 16 cm. Temp.: 23°C

Flow rate: 6.65 Lit/min. Voidage: o.664

Applied volt.,mV	100	200	250	300	350	400	500	600
Cathode section	Current, mA							
1	2.5	8.0	10.0	11.0	15.0	17.0	27.0	
2	2.0	6.0	8.0	9.0	10.0	12.0	21.0	
3	2.0	8.0	10.0	11.0	14.0	15.5	24.0	
4	1.0	5.0	6.0	7.0	11.0	13.0	24.0	
5	2.0	8.0	9.0	10.0	15.0	18.0	28.0	
6	3.0	10.0	14.0	16.0	17.0	22.0	30.0	
7	4.0	14.5	17.0	19.0	22.0	27.0	42.0	
8	4.5	13.0	16.0	18.0	20.5	26.0	41.0	
9	4.5	15.0	18.0	20.5	22.0	28.0	44.0	
10	5.0	14.0	18.0	19.0	21.0	26.0	40.0	
11	2.0	6.0	7.0	8.0	9.0	12.0	17.0	
12	2.0	7.0	9.0	10.0	10.5	13.0	17.0	
13	2.0	6.0	6.5	7.0	8.5	19.5	12.0	
14.	2.0	6.0	7.0	8.0	8.5	9.5	12.5	
15	3.0	6.0	8.0	9.0	9.5	10.5	14.0	
TOTAL:	42.0	131.5	168.0	186.5	213.5	259.0	393.5	

APPENDIX -C.31

Particle size = 3.0 mm. Initial bed height: 16 cm. Temp.: 32°C

Flow rate: 7.6 Lit/min. Voidage: 0.717

Applied volt.,mV	100	200	250	300	350	400	500	600
Cathode section	Current, mA							
1	5.0	10.5	15.5	18.0	20.0	25.0	27.0	
2	2.0	5.0	8.0	10.0	12.0	17.0	20.0	
3	3.0	9.0	14.0	16.0	18.0	22.0	25.0	
4	3.0	9.0	13.0	15.0	18.0	23.0	25.0	
5	5.0	10.0	15.0	17.0	19.0	24.0	26.0	
6	3.0	8.0	16.0	23.0	24.0	25.0	34.0	
7	4.0	11.0	18.0	24.0	30.0	36.0	48.0	
8	4.0	12.0	20.0	25.0	29.0	35.0	38.0	
9	5.0	12.0	21.5	25.0	31.0	42.0	45.0	
10	4.5	11.0	19.0	23.0	27.0	35.0	41.0	
11	2.0	4.5	8.0	9.0	11.0	19.0	23.0	
12	3.0	8.0	12.0	15.0	18.0	22.0	26.0	
13	3.0	6.0	9.0	12.0	14.0	18.0	22.0	
14	3.0	5.5	8.0	10.0	12.0	14.0	18.0	
15	23.0	5.5	8.0	9.0	11.0	13.0	14.0	
TOTAL;	52.5	127.0	205.0	251.0	293.0	368.0	431.0	

APPENDIX -C. 32

Particle size = 3.0 mm. Initial bed height: 12 cm. Temp.: 21°C

Flow rate: 5.7 Lit/min. Voidage: 0.621

Applied volt.,mV	100	200	250	300	350	400	450	600
Cathode section	Current, mA							
1	3.0	3.0	3.0	4.5	5.5	6.5	9.0	
2	2.0	3.0	3.0	4.0	5.0	6.0	8.5	
3	1.5	3.0	3.0	4.0	5.0	6.0	8.5	
4	2.0	2.5	2.5	3.5	4.5	5.5	8.5	
5	2.0	2.5	3.0	4.0	5.0	6.0	8.5	
6	3.0	5.0	5.5	7.5	10.0	12.0	18.0	
7	4.0	5.5	5.5	8.0	9.0	12.0	19.0	
8	4.0	5.0	5.0	8.0	10.0	14.0	19.0	
9	3.5	5.0	5.0	8.0	10.0	13.0	16.0	
10	3.0	5.0	5.0	8.0	9.5	12.0	15.0	
11	1.5	2.0	2.0	3.0	3.5	4.5	5.0	
12	1.0	2.0	2.5	3.5	4.0	4.0	4.5	
13	2.0	2.5	2.5	3.0	4.0	4.5	5.0	
14	2.0	2.5	2.5	3.5	3.5	5.0	5.0	
15	2.0	3.0	3.0	4.0	4.0	5.5	6.0	
TOTAL;	37.0	51.0	53.0	77.0	92.5	117.5	157.0	

APPENDIX -C.33

Particle size = 3.0 mm. Initial bed height: 12 cm. Temp.: 22°C

Flow rate: 6.3 Lit/min. Voidage: 0.657

Applied volt.,mV	100	200	250	300	350	400	500	600
Cathode section	Current, mA							
1.	2.0	3.5	4.5	5.0	6.5	9.0	12.0	
2	1.5	3.0	4.0	4.5	5.5	7.5	10.0	
3	1.5	3.0	4.0	4.0	5.5	7.0	10.0	
4	1.5	2.5	3.5	4.0	5.0	7.0	10.0	
5	1.0	2.5	3.5	4.0	5.0	7.0	10.0	
6	3.0	6.0	8.0	10.0-	11.0	12.0	17.0	
7	3.0	6.0	7.5	8.0	12.0	16.0	20.0	
8	3.0	6.0	7.5	8.5	13.5	16.0	20.0	
9	3.0	6.0	8.0	9.0	12.5	14.0	17.0	
10	3.0	6.0	8.0	9.0	12.0	13.0	15.0	
11	1.0	2.0	3.0	3.0	5.0	5.5	7.0	
12	1.0	2.5	3.5	3.5	5.0	5.5	7.0	
13	1.0	2.5	3.5	4.0	4.5	5.0	6.0	
14	1.0	2.5	3.5	4.0	4.5	5.0	6.0	
15	1.0	3.0	4.0	4.0	5.0	6.0	7.0	
TOTAL:	27.5	57.0	76.0	84.5	112.5	136.0	174.0	

--

APPENDIX -C. 34

Particle size = 3.0 mm. Initial bed height: 12 cm. Temp.: 22°C

Flow rate: 7.0 Lit/min. Voidage: 0.700

Applied volt.,mV	100	200	250	300	350	400	500	600
Cathode section	Current, mA							
1	2.0	4.0	4.5	5.5	10.0	12.5	19.0	
2	1.0	3.0	3.5	4.5	8.0	11.0	17.0	
3	1.0	2.5	3.0	4.5	8.0	11.0	19.0	
4	1.0	2.5	3.0	4.0	8.0	11.0	19.0	
5	1.0	2.0	3.0	4.0	8.5	12.0	19.0	
6	2.5	6.0	7.0	9.0	13.0	14.0	35.0	
7	2.5	5.5	7.0	9.5	17.5	20.0	37.0	
8	2.5	5.5	7.0	10.0	16.0	20.5	37.0	
9	2.0	5.5	8.0	10.5	16.0	20.5	28.0	
10	2.0	5.5	7.0	10.0	14.0	17.0	28.0	
11	1.0	2.0	2.5	3.5	5.0	6.0	9.0	
12	0.9	2.5	3.5	4.5	6.0	7.0	10.0	
13	1.0	2.0	2.5	4.0	5.0	5.5	8.0	
14	1.0	2.0	3.0	4.0	5.0	6.0	9.0	
15	1.0	2.5	5.0	5.0	6.0	6.0	12.0	
TOTAL:	21.5	53.0	69.5	92.5	145.5	180.0	306.0	

APPENDIX -C: 35

Particle size = 3.0 mm. Initial bed height: 12 cm. Temp.: 25°C

Flow rate: 7.6 Lit/min. Voidage: 0.723

Applied volt.,mV	100	200	250	300	350	400	500	600
Cathode section	Current, mA							
1	2.0	4.0	5.0	5.5	7.5	12.0	23.0	
2	1.5	3.5	4.0	4.5	6.0	11.0	22.0	
3	1.0	3.5	4.0	4.5	5.5	10.0	20.0	
4	1.0	3.5	4.0	4.5	6.0	11.0	23.0	
5	1.0	3.5	4.0	5.0	6.0	11.0	25.0	
6	3.5	8.0	9.0	10.0	12.0	16.0	32.0	
7	3.5	7.5	9.0	10.5	13.0	20.0	50.0	
8	3.0	7.5	9.0	10.5	13.0	21.0	42.0	
9	3.0	7.5	9.0	10.5	13.0	21.0	43.0	
10	3.5	7.5	90.0	11.0	14.0	20.0	41.0	
11	1.5	3.0	3.5	4.0	5.0	8.0	14.0	
12	1.5	3.5	4.0	5.0	5.5	8.0	14.0	
13	1.0	3.0	3.5	4.5	5.0	7.5	11.0	
14	1.0	3.0	3.5	4.5	5.0	7.5	11.0	
15	1.5	4.0	4.5	4.5	5.5	7.5	12.0	
TOTAL;	29.5	72.8	85.0	99.0	122.0	191.5	383.0	

APPENDIX -C. 36

Particle size = 3.0 mm. Initial bed height: 12 cm. Temp.: 31°C

Flow rate: 8.9 Lit/min. Voidage: 0.782

Applied volt.,mV	100	200	250	300	350	400	500	600
Cathode section	Current, mA							
1	2.0	4.5	6.0	7.0	10.0	14.0	19.0	
2	1.5	4.0	5.0	6.0	8.0	12.0	17.0	
3	1.0	4.0	5.0	6.0	8.0	10.5	17.0	
4	1.0	4.0	5.0	6.0	8.0	12.0	17.0	
5	1.0	4.0	5.0	6.0	9.0	13.0	17.0	
6	2.5	7.5	9.5	10.0	12.0	17.0	28.0	
7	3.0	8.0	10.0	12.0	16.0	23.0	31.0	
8	3.0	8.0	10.0	12.0	16.5	26.0	31.0	
9	3.0	8.0	10.5	12.0	16.5	17.0	31.0	
10	3.0	8.0	10.5	12.0	17.5	23.0	33.0	
11	1.0	3.0	4.5	4.5	6.0	8.0	17.0	
12	1.0	3.5	5.0	5.0	8.0	10.0	17.0	
13	1.0	3.5	4.5	5.0	6.5	8.0	14.0	
14	1.0	3.5	4.5	5.0	6.0	8.0	11.0	
15	1.0	4.0	5.0	5.0	6.0	8.0	12.0	
TOTAL;	26.0	77.5	100.0	114.0	153.5	193.5	312.0	

APPENDIX -C.37

Particle size = 3.0 mm. Initial bed height: 8 cm. Temp.: 25°C

Flow rate: 5.7 Lit/min. Voidage: 0.657

Applied volt.,mV	100	200	250	300	350	400	500	600
Cathode section	Current, mA							
1	2.0	4.0	4.0	5.5	8.0	12.0		
2	1.5	3.5	3.5	5.0	7.5	10.0		
3	1.0	3.5	3.5	4.5	7.5	10.0		
4	1.0	3.0	3.5	4.5	7.0	11.0		
5	1.0	3.0	3.0	4.5	8.0	12.0		
6	3.0	7.0	7.0	8.0	12.0	14.5		
7	3.0	7.5	8.0	12.0	15.0	18.0		
8	3.5	8.5	9.0	12.0	15.0	17.5		
9	3.0	8.0	9.0	12.0	15.0	17.0		
10	2.5	7.5	8.0	11.0	13.0	15.0		
11	1.0	3.0	3.0	4.0	4.5	5.5		
12	1.0	3.0	4.0	4.5	5.0	6.0		
13	1.0	2.5	4.0	4.5	5.0	5.5		
14	1.0	2.5	4.0	4.5	5.5	6.5		
15	1.0	3.0	5.0	7.0	8.0	9.5		
TOTAL:	25.8	69.5	78.5	103.5	136.5	169.5		

APPENDIX -C.38

Particle size = 3.0 mm. Initial bed height: 8 cm. Temp.: 25°C

Flow rate: 6.3 Lit/min. Voidage: 0.718

Applied volt.,mV	100	200	250	300	350	400	500	600
Cathode section	Current, mA							
1	1.5	3.5	5.0	6.0	9.0	13.0		
2	1.0	2.5	4.0	5.5	8.0	11.0		
3	1.0	2.5	4.0	5.5	8.0	10.5		
4	1.0	2.5	4.0	5.5	8.5	11.0		
5	1.0	3.0	4.5	6.0	8.5	11.5		
6	2.0	6.0	8.5	10.0	10.5	20.0		
7	2.5	6.0	8.0	12.0	15.0	22.0		
8	4.0	7.5	9.5	11.5	14.0	17.0		
9	5.0	8.5	9.5	11.5	14.0	17.0		
10	4.5	8.0	9.0	10.5	13.0	16.0		
11	1.0	3.0	3.5	4.5	6.0	6.5		
12	1.0	3.0	4.0	4.5	6.0	6.5		
13	1.0	3.5	4.0	4.5	6.0	6.5		
14	1.0	3.5	4.0	5.5	6.5	7.5		
15	2.0	5.0	5.5	6.0	8.0	10.0		
TOTAL;	27.3	68.0	85.5	108.5	138.0	186.5		

APPENDIX -C.39

Particle size = 3.0 mm. Initial bed height: 8 cm. Temp.: 29°C

Flow rate: 7.0 Lit/min. Voidage: 0.753

Applied volt.,mV	100	200	250	300	350	400	500	600
Cathode section	Current, mA							
1	1.5	4.0	5.0	7.0	9.0	14.0		
2	1.0	3.5	4.5	5.5	8.0	12.0		
3	1.0	3.0	4.5	5.5	8.0	12.0		
4	11.0	3.0	4.5	5.5	8.0	12.0		
5	1.0	3.5	4.5	6.0	8.0	12.5		
6	2.0	6.0	8.0	10.0	15.5	21.0		
7	2.0	7.0	9.0	11.5	16.5	23.0		
8	2.0	7.5	8.5	10.5	15.0	18.0		
9	2.5	7.5	8.0	10.0	14.0	17.0		
10	3.0	7.0	8.5	10.0	13.0	16.0		
11	1.0	3.0	3.5	4.5	6.0	7.0		
12	1.0	3.0	3.5	5.0	5.0	7.5		
13	1.0	3.0	3.5	4.5	6.0	7.0		
14	1.0	3.0	4.0	4.5	5.5	7.0		
15	1.5	4.5	5.0	6.0	7.0	9.0		
TOTAL:	21.2	68.5	84.5	106.5	144.5	195.0		

APPENDIX -C. 40

Particle size = 3.0 mm. Initial bed height: 8 cm. Temp.: 27°C

Flow rate: 8.2 Lit/min. Voidage: 0.782

Applied volt.,mV	100	200	250	300	350	400	500	600
Cathode section	Current, mA							
1				6.0	8.0	9.5	14.0	
2				5.0	7.0	8.0	12.0	
3				5.0	7.0	7.5	12.0	
4				5.0	7.0	7.5	12.5	
5				5.0	8.0	8.0	13.0	
6				7.5	9.0	14.0	15.0	
7				19.0	12.0	13.0	22.0	
8				9.0	10.5	13.0	22.0	
9				9.0	11.0	13.0	18.0	
10				9.0	9.0	11.0	14.0	
11				4.0	4.5	6.0	8.0	
12				4.5	5.0	7.0	8.5	
13				4.0	4.5	7.0	8.0	
14				4.0	4.5	6.0	8.0	
15				5.0	5.5	7.0	9.5	
TOTAL:				92.0	112.5	137.5	196.5	

APPENDIX -C. 41

Particle size = 3.0 mm. Initial bed height: 8 cm. Temp.: 32°C

Flow rate: 9.5 Lit/min. Voidage: 0.828

Applied volt.,mV	100	200	250	300	350	400	500	600
Cathode section			Current, mA					
1			6.0	7.0	10.0	13.0	23.0	
2			5.0	6.0	8.5	12.0	22.0	
3			5.0	6.0	8.5	12.0	21.0	
4			5.0	6.0	8.5	12.0	22.0	
5			5.0	6.0	19.0	13.0	23.0	
6			10.0	10.5	12.0	15.5	22.0	
7			10.0	12.0	16.0	22.0	35.0	
8			10.0	12.0	15.5	21.0	34.0	
9			10.0	11.5	15.5	22.0	34.0	
10			10.0	12.0	15.5	20.0	31.0	
11			4.5	5.5	7.5	9.0	14.0	
12			5.0	5.5	8.0	9.0	14.0	
13			4.5	5.0	7.0	8.0	12.0	
14			4.5	5.0	7.0	8.0	12.5	
15			5.0	5.5	8.0	9.0	14.0	
TOTAL:			99.5	115.5	156.5	205.5	333.5	

APPENDIX-C. 42 : Calculation of sectional limiting current densities (i_L amps/m²) and local average mass transfer coefficients (K_{lav}, m/s), Initial bed height= 16 cm. Particle size = 6.0 mm.

Flowrate lit/min	5.7		6.3		7.0		8.2		9.5	
Cathode sections	i_L amps/m²	K_{lav} X 10^6 m/s	i_L amps/m²	K_{lav}X10^6 m/s	i_L amps/m²	K_{lav}X10^6 m/s	i_L amps/m²	K_{lav}X10^6 m/s	i_L amps/m²	K_{lav}X10^6 m/s
1	10.0	3.45	13.0	4.49	18.0	6.22	19.0	6.56	28.0	9.67
2	9.0	3.11	12.0	4.15	16.0	5.53	18.0	6.22	25.0	8.64
3	9.0	3.11	12.0	4.15	16.0	5.53	18.0	6.22	25.0	8.64
4	11.0	3.80	12.0	4.15	16.0	5.53	18.0	6.22	26.0	8.98
5	8.0	3.76	13.0	4.49	17.0	5.87	19.0	6.56	28.0	9.67
6	4.0	1.38	5.25	1.81	7.75	2.68	9.25	3.20	12.0	3.11
7	4.5	1.55	6.0	2.07	8.0	2.76	9.0	3.11	12.5	4.32
8	4.5	1.55	6.0	2.07	8.0	2.76	9.0	3.11	12.5	4.32
9	4.75	1.64	6.25	2.16	8.5	2.95	9.5	3.28	12.5	4.32
10	4.75	1.64	5.50	1.90	7.50	2.59	8.0	2.76	10.5	3.63
11	8.0	2.76	10.0	3.45	14.0	4.84	18.0	6.22	26.0	8.98
12	9.0	3.11	11.0	3.80	14.0	4.84	18.0	6.22	26.0	8.98
13	8.0	2.76	10.0	3.45	12.0	4.15	16.0	5.53	22.0	7.60
14	8.0	2.76	10.0	3.45	12.0	4.15	15.0	5.18	20.0	6.91
15	11.0	3.80	13.0	4.49	14.0	4.84	16.0	5.53	22.0	7.60

APPENDIX-C.43 : Calculation of sectional limiting current densities (i_L amps/m²) and local average mass transfer coefficients(K_{lav},m/s), Initial bed height=12.0cm. Particle size = 6.0 mm.

Flowrate lit/min	5.7		6.3		7.0		8.2		9.5	
Cathode sections	i_L amps/m²	K_{lav} X 10^6 m/s	i_L amps/m²	K_{lav}X10^6 m/s	i_L amps/m²	K_{lav}X10^6 m/s	i_L amps/m²	K_{lav}X10^6 m/s	i_L amps/m²	K_{lav}X10^6 m/s
1	12.0	4.95	13.0	4.49	20.0	6.91	21.0	7.25	30.0	10.36
2	11.0	3.80	11.0	3.80	17.0	5.87	19.0	6.56	24.0	8.29
3	11.0	3.80	11.0	3.80	17.0	5.87	19.0	6.56	24.0	8.29
4	11.0	3.80	11.0	3.80	17.0	5.87	19.0	6.56	25.0	8.64
5	12.0	4.15	12.0	4.15	16.0	6.56	19.0	6.56	26.0	8.98
6	6.5	2.25	5.5	1.90	6.75	2.33	8.25	2.85	10.0	3.45
7	8.0	2.76	6.25	2.16	7.0	2.42	9.0	3.11	11.0	3.80
8	6.0	2.07	5.0	1.77	6.75	2.25	8.0	2.76	10.0	3.45
9	7.0	2.42	6.0	2.07	7.25	2.50	9.0	3.11	10.75	3.71
10	6.5	2.25	5.5	1.90	7.25	2.50	8.0	2.76	10.5	3.63
11	8.0	2.76	8.0	2.76	11.0	2.80	13.0	4.49	20.0	6.91
12	9.0	3.11	9.0	3.11	11.0	3.80	13.0	4.49	20.0	6.91
13	9.0	3.11	9.0	3.11	11.0	3.80	12.0	4.15	18.0	6.22
14	9.5	3.32	9.0	3.11	12.0	4.15	12.0	4.15	18.0	6.22
15	15.0	5.18	14.0	4.83	15.0	5.18	16.0	4.49	20.0	6.91

APPENDIX-C.44 : Calculation of sectional limiting current densities (i_L amps/m²) and local average mass transfer coefficients(K_{lav},m/s), Initial bed height=8.0 cm. Particle size = 6.0 mm.

Flowrate lit/min	5.7		7.0		8.2		9.5		10.0	
Cathode sections	i_L amps/m²	K_{lav} X 10^6 m/s	i_L amps/m²	K_{lav}X10^6 m/s	i_L amps/m²	K_{lav}X10^6 m/s	i_L amps/m²	K_{lav}X10^6 m/s	i_L amps/m²	K_{lav}X10^6 m/s
1	15.0	5.18	19.0	6.56	36.0	12.43	32.0	11.05	24.0	8.29
2	13.0	4.49	17.0	5.87	30.0	10.36	25.0	8.63	19.0	6.03
3	13.0	4.49	17.0	5.87	30.0	10.36	27.0	9.32	19.0	6.03
4	13.0	4.49	17.0	5.87	31.0	10.71	27.0	9.32	19.0	6.03
5	12.0	4.15	18.0	6.22	33.0	11.48	28.0	9.67	20.0	4.16
6	8.25	2.85	7.0	2.42	11.0	3.80	10.0	3.45	8.0	2.76
7	9.0	3.11	8.0	2.76	13.0	4.49	11.0	3.80	9.5	3.28
8	8.5	2.94	7.75	2.68	12.0	4.14	10.5	3.63	9.5	3.28
9	7.5	2.59	7.25	2.50	10.0	3.45	9.0	3.11	8.0	2.76
10	7.0	2.42	7.0	2.42	9.5	3.28	8.75	3.02	8.0	2.76
11	11.0	3.80	10.0	3.45	15.0	5.18	17.0	5.87	16.0	5.53
12	11.0	3.80	11.0	3.80	17.0	5.87	18.0	6.22	16.0	5.53
13	11.0	3.80	10.0	3.45	15.0	5.18	17.0	5.87	14.0	4.84
14	11.0	3.80	10.0	3.45	16.0	5.52	17.0	5.87	14.0	4.84
15	14.0	4.84	14.0	4.84	20.0	6.91	20.0	6.91	17.0	5.87

APPENDIX-C.45 : Calculation of sectional limiting current densities (i_L amps/m²) and local average mass transfer coefficients(K_{lav},m/s), Initial bed height=16.0cm. Particle size = 4.5 mm.

Flowrate lit/min	4.3		5.0		5.7		6.3		7.0	
Cathode sections	i_L amps/m²	K_{lav} X 10^6 m/s	i_L amps/m²	K_{lav}X10^6 m/s	i_L amps/m²	K_{lav}X10^6 m/s	i_L amps/m²	K_{lav}X10^6 m/s	i_L amps/m²	K_{lav}X10^6 m/s
1	10.0	3.45	11.0	3.80	17.0	5.87	21.0	7.25	24.0	8.29
2	9.0	3.11	9.0	3.11	16.0	5.53	20.0	6.91	18.0	6.22
3	9.0	3.11	9.0	3.11	18.0	5.18	22.0	7.60	20.0	6.91
4	9.0	3.11	9.0	3.11	12.0	4.15	24.0	8.29	24.0	8.29
5	9.0	3.11	9.0	3.11	14.0	4.84	24.0	8.29	24.0	8.29
6	6.5	2.25	4.5	1.55	7.0	2.42	11.0	3.81	8.0	2.76
7	6.0	2.07	5.0	1.73	8.0	2.76	11.0	3.84	9.0	3.11
8	6.0	2.07	4.75	1.64	8.5	2.94	10.5	3.63	9.0	3.11
9	6.0	2.07	5.0	1.73	7.0	2.42	12.0	4.17	10.0	3.45
10	6.0	2.07	5.0	1.73	7.0	2.42	12.0	4.15	11.0	3.80
11	8.0	2.76	9.0	3.11	10.0	3.45	22.0	7.60	14.0	4.84
12	9.0	3.11	9.0	3.11	12.0	4.15	24.0	8.29	20.0	6.91
13	8.0	2.76	9.0	3.11	12.0	4.15	20.0	6.91	18.0	6.22
14	8.0	2.76	9.0	3.11	12.0	4.15	20.0	6.91	18.0	6.22
15	9.0	3.11	10.0	3.45	14.0	4.84	18.0	6.22	17.0	5.87

APPENDIX-C.46 : Calculation of sectional limiting current densities (i_L amps/m²) and local average mass transfer coefficients(K_{lav},m/s), Initial bed height=12.0cm. Particle size = 4.5 mm.

Flowrate lit/min										
Cathode sections	i_L amps/m²	K_{lav} X 10^6 m/s	i_L amps/m²	K_{lav}X10^6 m/s	i_L amps/m²	K_{lav}X10^6 m/s	i_L amps/m²	K_{lav}X10^6 m/s	i_L amps/m²	K_{lav}X10^6 m/s
1	14.0	4.84	12.0	4.15	18.0	6.22	28.0	9.67	26.0	8.98
2	12.0	4.15	11.0	3.80	17.0	5.87	24.0	8.29	24.0	8.29
3	12.0	4.15	11.0	3.80	17.0	5.87	24.0	8.29	24.0	8.29
4	10.0	3.45	11.0	3.80	17.0	5.87	24.0	8.29	23.0	7.95
5	11.0	3.80	11.0	3.80	17.0	5.87	25.0	8.64	24.0	8.29
6	7.5	2.59	5.75	1.99	7.0	2.42	10.0	3.45	12.0	4.15
7	8.5	2.94	6.5	2.25	8.0	2.76	10.5	3.63	13.0	4.49
8	8.5	2.94	6.5	2.25	7.25	2.51	11.0	3.80	11.5	3.97
9	7.5	2.59	5.75	1.99	7.75	2.68	11.0	3.80	10.5	3.63
10	6.5	2.25	5.25	1.81	7.25	2.50	10.5	3.63	10.5	3.63
11	8.0	2.76	8.0	2.76	12.0	4.15	16.0	5.53	16.0	5.53
12	9.0	3.11	9.0	3.11	12.0	4.15	17.0	8.87	18.0	6.22
13	10.0	3.45	9.0	3.11	11.0	3.80	14.0	4.84	16.0	5.53
14	10.0	3.45	10.0	3.45	11.0	3.80	14.0	4.84	18.0	6.22
15	12.0	4.15	11.0	3.80	14.0	4.84	17.0	5.87	22.0	7.60

APPENDIX-C.47 : Calculation of sectional limiting current densities (i_L amps/m²) and local average mass transfer coefficients(K_{lav},m/s), Initial bed height= 8.0cm. Particle size = 4.5mm.

Flowrate lit/min	7.0		8.2		10.1	
Cathode sections	i_L amps/m²	K_{lav} X 10^6 m/s	i_L amps/m²	K_{lav}X10^6 m/s	i_L amps/m²	K_{lav}X10^6 m/s
1	24.0	8.29	30.0	10.36	24.0	8.29
2	22.0	7.60	26.0	8.98	24.0	8.29
3	20.0	6.91	26.0	8.98	22.0	7.60
4	18.0	6.22	28.0	9.67	26.0	8.98
5	20.0	6.91	30.0	10.36	30.0	10.36
6	9.5	3.28	9.5	3.28	10.0	3.45
7	12.0	4.15	14.5	5.01	10.0	3.45
8	11.5	3.97	13.5	4.66	11.0	3.80
9	10.0	3.45	12.0	4.15	12.5	4.32
10	9.0	3.11	11.0	3.80	12.5	4.32
11	12.0	4.15	16.0	5.53	18.0	6.22
12	14.0	4.83	18.0	6.22	20.0	6.91
13	14.0	4.83	14.0	4.84	18.0	6.22
14	16.0	5.53	18.0	5.53	18.0	6.22
15	18.0	6.22	20.0	6.91	14.0	4.84

APPENDIX-C.48 : Calculation of sectional limiting current densities (i_L amps/m²) and local average mass transfer coefficients(K_{lav},m/s), Initial bed height=16.0cm. Particle size = 3.0 mm.

Flowrate lit/min	5.7		6.65		7.6	
Cathode sections	i_L amps/m²	K_{lav} X 10^6 m/s	i_L amps/m²	K_{lav}X10^6 m/s	i_L amps/m²	K_{lav}X10^6 m/s
1	14.0	4.84	22.0	7.6	36.0	12.44
2	12.0	4.15	18.0	6.22	20.0	6.91
3	14.0	4.84	22.0	7.60	32.0	11.05
4	10.0	3.45	14.0	4.84	30.0	10.36
5	10.0	3.45	20.0	6.91	34.0	11.74
6	6.0	3.07	8.0	2.76	11.5	3.97
7	7.0	2.42	9.5	3.29	12.0	4.14
8	7.0	2.42	9.5	3.11	12.5	4.32
9	6.5	2.25	10.25	3.54	12.5	4.32
10	6.0	2.07	9.5	3.28	11.5	3.97
11	9.0	3.11	16.0	5.53	18.0	6.22
12	10.0	3.45	20.0	6.91	30.0	10.36
13	10.0	3.45	14.0	4.84	24.0	8.29
14	10.0	3.45	16.0	5.53	20.0	6.91
15	14.0	4.84	8.0	6.22	18.0	6.22

APPENDIX-C.49 : Calculation of sectional limiting current densities (i_L amps/m²) and local average mass transfer coefficients(K_{lav},m/s), Initial bed height=12.0cm. Particle size = 3.0 mm.

Flowrate lit/min	5.7		6.3		7.0		7.6		8.9	
Cathode sections	i_L amps/m²	K_{lav} X 10^6 m/s	i_L amps/m²	K_{lav}X10^6 m/s	i_L amps/m²	K_{lav}X10^6 m/s	i_L amps/m²	K_{lav}X10^6 m/s	i_L amps/m²	K_{lav}X10^6 m/s
1	6.0	2.07	10.0	3.45	10.0	3.80	14.0	5.18	20.0	6.91
2	6.0	2.07	9.0	3.11	9.0	3.11	12.0	4.15	16.0	5.53
3	6.0	2.07	8.0	2.76	9.0	3.11	11.0	3.80	16.0	5.53
4	5.0	1.73	8.0	2.76	8.0	2.76	12.0	4.15	16.0	5.53
5	5.0	1.73	8.0	2.76	8.0	2.76	12.0	4.15	18.0	6.22
6	3.0	0.95	5.0	1.73	4.5	1.55	6.0	2.07	6.0	2.07
7	3.0	0.95	4.0	1.38	4.75	1.64	6.5	2.25	8.0	2.76
8	2.5	0.86	4.25	1.47	5.0	1.73	6.5	2.25	8.25	2.85
9	3.0	0.95	4.50	1.55	5.25	1.81	6.5	2.25	8.25	2.85
10	2.5	0.86	4.5	1.55	5.0	1.73	7.0	2.42	8.50	2.93
11	4.0	1.38	6.0	2.07	7.0	2.42	10.0	3.45	12.0	4.15
12	5.0	1.73	7.0	2.42	9.0	3.11	11.0	3.80	16.0	5.53
13	5.0	1.73	8.0	2.76	8.0	2.76	10.0	3.45	13.0	4.49
14	5.0	1.73	8.0	2.76	8.0	2.76	10.0	3.45	12.0	4.42
15	6.0	2.07	8.0	2.76	10.0	3.45	11.0	3.80	12.0	4.42

APPENDIX-C.50 : Calculation of sectional limiting current densities (i_L amps/m²) and local average mass transfer coefficients(K_{lav},m/s), Initial bed height=8.0 cm. Particle size = 3.0 mm.

Flowrate lit/min	5.7		6.3		7.0		8.2		9.5	
Cathode sections	i_L amps/m²	K_{lav} X 10^6 m/s	i_L amps/m²	$K_{lav}X10^6$ m/s	i_L amps/m²	$K_{lav}X10^6$ m/s	i_L amps/m²	$K_{lav}X10^6$ m/s	i_L amps/m²	$K_{lav}X10^6$ m/s
1	8.0	2.76	12.0	4.15	18.0	6.22	19.0	6.56	20.0	6.91
2	7.0	2.42	11.0	3.80	16.0	5.53	16.0	5.53	17.0	5.87
3	7.0	2.42	11.0	3.80	16.0	5.53	15.0	5.17	17.0	5.87
4	7.0	2.42	11.0	3.80	16.0	5.53	15.0	5.18	17.0	5.87
5	6.0	2.07	12.0	4.15	16.0	5.53	16.0	5.53	18.0	6.22
6	3.5	1.21	5.0	1.73	7.75	2.68	7.0	2.42	6.0	2.07
7	4.0	1.38	6.0	2.07	8.25	2.85	6.5	2.25	8.0	2.76
8	4.5	1.55	5.7	1.99	7.6	2.59	6.5	2.25	7.75	2.68
9	4.5	1.55	5.75	1.99	7.0	2.42	6.5	2.25	7.75	2.68
10	4.0	1.38	5.25	1.81	6.5	2.25	5.5	1.90	7.75	2.68
11	6.0	2.07	9.0	3.11	12.0	4.15	12.0	4.15	15.0	5.18
12	8.0	2.76	9.0	3.11	10.0	3.45	14.0	4.83	16.0	5.53
13	8.0	2.76	9.0	3.11	12.0	4.15	14.0	4.83	14.0	4.83
14	8.0	2.76	11.0	3.80	11.0	3.80	12.0	4.15	14.0	4.83
15	10.0	3.45	12.0	4.15	14.0	4.84	14.0	4.84	16.0	5.53

APPENDIX-C.51 : Calculation of necessary terms for the mass transfer correlations

Particle size = 6.0 mm.

Flow rate liter/min	Initial bed height	Limiting current i_L amp/m²	Average mass transfer coefficient $K_{av} X\ 10^6$ m/s	Superficial Velocity U m/s	Voidage ε	$St_I Sc^{2/3} X10^3$ $=K_{av}\ \varepsilon\ Sc^{2/3}/U$	$Re_I = \frac{Ud_p}{\nu(1-\varepsilon)}$
5.7		6.03	2.08	0.095	0.585	1.80	1333
6.3		7.73	2.67	0.105	0.620	2.21	1669
7.0	16.0	10.27	3.55	0.117	0.649	2.53	2078
8.2		11.8	4.08	0.137	0.685	3.25	2815
9.5		15.87	5.48	0.158	0.739	2.98	4087
5.7		8.10	2.81	0.095	0.577	2.39	1308
6.3		7.33	2.53	0.105	0.610	2.11	1632
7.0	12.0	9.63	3.33	0.117	0.638	2.34	2015
8.2		10.93	3.78	0.137	0.678	2.30	2653
9.5		14.46	4.98	0.158	0.74	2.63	4014
5.7							
5.7		8.80	3.10	0.095	0.62	3.01	1415
7.0		9.7	3.35	0.117	0.674	2.87	2055
8.2	8.0	15.4	5.33	0.137	0.724	3.79	2885
9.5		14.17	4.89	0.158	0.76	2.73	4122
10.8		11.67	4.03	0.180	0.79	1.89	5934

APPENDIX-C.52 : Calculation of necessary terms for the mass transfer correlations

Particle size = 4.5 mm.

Flow rate liter/min	Initial bed height	Limiting current i_L amp/m²	Average mass transfer coefficient $K_{av} \times 10^6$ m/s	Superficial Velocity U m/s	Voidage ε	$St_I Sc^{2/3} \times 10^3 = K_{av}\, \varepsilon\, Sc^{2/3}/U$	$Re_I = \frac{U d_p}{\nu(1-\varepsilon)}$
4.3		7.0	2.42	0.072	0.557	2.527	707
5.0		6.3	2.19	0.083	0.594	2.273	871
5.7	16.0	9.47	3.27	0.095	0.628	2.907	1161
6.3		14.67	5.08	0.105	0.667	4.34	1473
7.0		12.83	4.43	0.117	0.705	4.01	1924
5.7		8.73	3.02	0.095	0.660	2.95	1220
6.3		7.40	2.56	0.105	0.685	4.46	1415
7.0	12.0	9.83	3.40	0.117	0.717	3.33	1802
7.6		13.83	4.77	0.127	0.74	3.60	2302
8.9		14.67	5.08	0.148	0.792	3.33	3468
7.0		12.87	4.45	0.117	0.738	3.73	2056
8.2	8.0	15.57	5.37	0.137	0.795	3.92	3192
10.1		14.6	5.04	0.168	0.843	3.00	5302

APPENDIX-C.53 : Calculation of necessary terms for the mass transfer correlations

Particle size = 3.0 mm.

Flow rate liter/min	Initial bed height	Limiting current i_L amp/m²	Average mass transfer coefficient $K_{av} X\ 10^6$ m/s	Superficial Velocity U m/s	Voidage ε	$St_I Sc^{2/3} X10^3 = K_{av}\, \varepsilon\, Sc^{2/3}/U$	$Re_I = \frac{Ud_p}{\nu(1-\varepsilon)}$
5.7		8.10	2.798	0.095	0.596	2.51	675
6.65	16.0	12.43	3.75	0.111	0.664	3.08	979
7.6		16.73	5.78	0.127	0.717	3.71	1304
5.7		3.53	1.22	0.095	0.621	1.16	709
6.3		5.63	1.94	0.105	0.657	1.74	909
7.0	12.0	6.17	2.13	0.117	0.700	1.79	1190
7.6		8.13	2.81	0.127	0.723	2.10	1494
8.9		10.23	3.54	0.148	0.782	2.12	2345
5.7		5.23	1.81	0.095	0.657	1.65	852
6.3		7.23	2.54	0.105	0.718	2.30	1188
7.0	8.0	9.63	3.33	0.117	0.753	2.57	1557
8.2		9.17	3.18	0.137	0.782	1.88	2114
9.5		10.43	3.60	0.158	0.828	2.07	3229

APPENDIX-C.54: Mass Transfer Correlations

Mass transfer correlations have been found for different particle sizes by regressional analysis done by a computer program and the correlations are as follows:

For 30 mm particle size

$$St_I Sc^{2/3} = 0.0494\ Re_I^{-0.40}$$

(Standard deviation = 15.48%)

For 4.5 mm particles

$$St_I (Sc)^{2/3} = 0.0383\ Re_I^{-0.3}$$

(Standard deviation = 11.30%)

For 6.0 mm particles

$$St_I (Sc)^{2/3} = 0.0195\ Re_I^{-025}$$

(Standard deviation = 12.66%)

APPENDIX D

Computer program listings

```
*****************************************************************************
*    This program fits a sets of data using the methode of least squares.*
*   -The following provisions are included to extends its generality:      *
*                    - Power function                                       *
*                    - Exponential function                                 *
*                    - A polynomial of upto ninth (10 terms) degree         *
*****************************************************************************
*************** Variable Identification  ********************************** *
*      NDATA= Number of pairs of input data                                 *
*      X     = NDATA-element vector                                         *
*      Y     = NDATA-element vector                                         *
*      N     = Input quantity indicating the type of curve to be used       *
*            N=0  indicates the power function                              *
*            N=1  indicates the exponential function                        *
*            N=2,3...10 indicates the polynomial of gegree (N-1)            *
*****************************************************************************
      PARAMETER(NDATA=7)
      DIMENSION X(NDATA),Y(NDATA),A(2,3),D(2),C(2)
      OPEN(UNIT=5,FILE='SQD2',STATUS='OLD')
      OPEN(UNIT=6,FILE='RESULT2',STATUS='NEW')
      READ(5,8) N
      DO 400 I=1,NDATA
         READ(5,9) Y(I),X(I)
  400 CONTINUE
    8 FORMAT(I1)
    9 FORMAT(E12.3,F6.0)
*      WRITE(6,3001) N
 3001 FORMAT(/10X,'INPUT N=0 FOR A POWER FUNCTION'//10X,'INPUT N=1 FOR
     ?AN EXPONENTIAL FUNCTION'//10X,'INPUT N=2,3..10 FOR A POLYNOMIAL OF
     ? DEGREE (N-1)'///10X,'INPUT N=',I2///10X,'X-VALUES',10X,'Y-VALUES'
     ?/10X,8(1H-),10X,8(1H-)/)
      IF(N.GE.2) GOTO 110
      DO 430 I=1,NDATA
         Y(I)=ALOG(Y(I))
  430 CONTINUE
      IF(N.EQ.1) GOTO 110
      DO 435 I=1,NDATA
         X(I)=ALOG(X(I))
  435 CONTINUE
  110 N1=N
      IF(N1.GE.2) GOTO 120
      N1=2
  120 DO 440 I=1,N1
      DO 440 J=1,N1
         A(I,J)=0.0
         D(I)=0.0
  440 CONTINUE
      DO 450 I=1,N1
         DO 460 J=1,N1
            IF((I+J).GT.2) GOTO 130
            A(I,J)=NDATA
            GOTO 460
  130       DO 470 K=1,NDATA
               A(I,J)=A(I,J)+X(K)**(I+J-2)
  470       CONTINUE
  460    CONTINUE
         DO 480 K=1,NDATA
            IF(I.GT.1) GOTO 140
            D(I)=D(I)+Y(K)
            GOTO 480
  140       D(I)=D(I)+Y(K)*X(K)**(I-1)
  480    CONTINUE
  450 CONTINUE
      N2=N1+1
      DO 490 I=1,N1
         A(I,N2)=D(I)
```

```
  490 CONTINUE
*
*    Call subroutine SIMUL to solve simultaneous linear equations
*
       CALL SIMUL(A,C,N1,N2)
       IF(N.GT.1) GOTO 150
       C1=EXP(C(1))
       IF(N.EQ.1) GOTO 160
       WRITE(6,3003) C1,C(2)
 3003 FORMAT(/10X,'POWER FUNCTION: Y=',F10.5,'X**',F10.5/)
       GOTO 170
  160 WRITE(6,3004) C1,C(2)
 3004 FORMAT(/10X,'EXPONENTIAL FUNCTION: Y=',F10.5,'EXP('F10.5,
     ?'X)'//)
       GOTO 170
  150 IF(C(2).GE.0.0) GOTO 180
       WRITE(6,3005) C(1),C(2)
 3005 FORMAT(/10X,'POLYNOMIAL FUNCTION: Y=',F10.3,F10.3,'X'//)
       GOTO 190
  180 WRITE(6,3006) C(1),C(2)
 3006 FORMAT(/10X,'POLYNOMIAL FUNCTION: Y=',F10.3,'+',F10.3,'X'//)
  190 IF(N.EQ.2) GOTO 170
       DO 500 I=3,N
          L=I-1
          IF(C(I).GE.0.0) GOTO 200
          WRITE(3,3007) C(I),L
          GOTO 500
  200     WRITE(6,3008) C(I),L
  500 CONTINUE
 3007 FORMAT(40X,F10.3,'X**',I3)
 3008 FORMAT(40X,'+',F10.3,'X**',I3)
*
* Print input values of x and y and calculated values of y
*
  170 IF(N.GE.2) GOTO 210
       DO 510 I=1,NDATA
          Y(I)=EXP(Y(I))
  510 CONTINUE
       IF(N.EQ.1) GOTO 210
       DO 520 I=1,NDATA
          X(I)=EXP(X(I))
  520 CONTINUE
  210 WRITE(6,3009)
 3009 FORMAT(/10X,'X',10X,'Y(Actual)',3X,'Y(Calc)'/10X,
     ?3(9(1H-),2X)/)
       S=0.0
       DO 530 I=1,NDATA
          IF(N.GE.2) GOTO 220
          IF(N.EQ.1) GOTO 230
          Y1=C1*X(I)**C(2)
          GOTO 240
  230     Y1=C1*EXP(C(2)*X(I))
          GOTO 240
  220     Y1=C(1)
          DO 540 J=2,N
             Y1=Y1+C(J)*X(I)**(J-1)
  540     CONTINUE
  240     S=S+((Y(I)-Y1)/Y(I)*100.)**2
          WRITE(6,3010) X(I),Y(I),Y1
  530 CONTINUE
 3010 FORMAT(10X,F10.3,2E12.3,1X))
       S=SQRT(S/NDATA)
       WRITE(6,3011) S
 3011 FORMAT(//10X,'% Standard deviation=',E10.5/)
       STOP
       END
```

```
      SUBROUTINE SIMUL(A,C,M,N)
      DIMENSION A(M,N),C(M)
      DO 411 K=1,M
         PIVOT=A(K,K)
         IF(ABS(PIVOT).LE.0.0001) GOTO 20
         DO 412 J=K,N
            A(K,J)=A(K,J)/PIVOT
  412    CONTINUE
         DO 413 I=1,M
            IF(I.EQ.K) GOTO 413
            PIVI=A(I,K)
            DO 414 J=K,N
               A(I,J)=A(I,J)-PIVI*A(K,J)
  414       CONTINUE
  413    CONTINUE
  411 CONTINUE
      DO 415 J=1,M
         C(J)=A(J,N)
  415 CONTINUE
      RETURN
   20 WRITE(6,3000) K
 3000 FORMAT(10X,'Pivot element',I2,'is close to zero'/)
      RETURN
      END
```